# Oxovanadium Complex-Catalyzed Aerobic C-C Bond Cleavage of Biomass-derived Scaffolds

**Christopher Godwin**

Thesis submitted

in partial fulfillment of the requirements for the degree of the

Master of Science, Chemistry

Department of Chemistry and Biomolecular Sciences

Faculty of Science

University of Ottawa

## Abstract

The non-sustainable nature of fossil fuels as feedstocks for valuable chemicals, combined with the environmental damage caused by their extraction and combustion, increases the need for the development of a bio-based economy. While industry and public opinion are slowly shifting towards acceptance of this change, efficient technologies for the depolymerization and subsequent separation of lignocellulosic biomass fall short of the ever-increasing demand. In particular, there are currently no efficient, sustainable mass scale methods to convert lignin, the most abundant source of aromatic molecules on Earth. The use of oxovanadium(V) catalyst complexes to aerobically cleave C–C bonds has been demonstrated previously and remains an attractive option for incorporation into a sustainable bio-based economy.

Two new triphenoxyamine oxovanadium(V) catalysts with reduced steric bulk and electron density at the metal center (vs. previously reported complexes) have been synthesized for aerobic oxidative diol C–C bond cleavage. These complexes were found to cleave less activated and more complex substrates than previous generations, including cyclic diols and polyalcohols. Several insights into the reaction pathways of this class of complex were elucidated through a series of kinetic studies. Experimentally, the rate of C–C bond cleavage of both pinacol and hydrobenzoin was determined to be unaffected by substitution of the O–H bonds with deuterium, suggesting that currently proposed mechanisms need to be revised. Multiple catalytic regimes were observed during anaerobic reaction, which were not altered significantly by the brief addition of $O_2$. A series of density functional theory calculations revealed a plausible mechanism for the trialkoxy complex that did not involve a proton transfer in the rate determining step, instead suggesting that ligand-arm dissociation-reassociation play a significant role in the reaction.

In a second project, new bisphenoxyamine-*N*-appended base ligand with less steric hindrance and electron density at the metal center, has been synthesized utilizing similar design principles gained from work with triphenoxyamine catalysts. When reacting with lignin model compound 1,2-diphenyl-2-methoxyethanol, this new complex displays a higher selectivity towards aldehydes and esters (relative to previous bisphenoxyamine-*N*-appended ligands), leading to a higher rate of C–C bond cleavage. Investigations into the mechanism of bisphenoxy complexes, as well as the role of the *N*-appended base in reactivity, were performed using

substrate pre-complexed bisphenoxy compounds. Thermolysis at 60 and 100 °C produced almost exclusively oxidative C–H bond cleavage product benzyl methyl ether, with evidence for overoxidation product benzoic acid observed. Thermolysis of labelled substrate pre-complexed revealed that *N*-appended base may impede C–C cleavage of 1,2-diphenyl-2-methoxyethanol by forcing the methyl ether away from the oxovanadium(V) center.

Through the use of these multidentate phenoxyamine ligands, advances have been made towards sustainable oxovanadium catalysis in the pursuit of efficient and selective lignocellulosic disassembly for a sustainable bio-based economy.

## Acknowledgements

A lot of people contributed to my survival of this process, probably more than they know. First and foremost, I'd like to thank Dr. R. T. Baker; not only was he a fantastic mentor, but his patience with me was invaluable and more appreciated than I think I can really put into words. In particular, I have to mention how understanding he was when it came to my desire to be a better teacher than researcher; while I know that I wasn't necessarily his ideal graduate student, he helped to nurture my talents. I can honestly say I have never met another professor quite like him, and cannot imagine I would have been able to have an experience like this in any other research group. Having someone with actual musical taste to talk with was also a blessing.

Of course, much appreciation also goes out to the Baker group, who were supportive and ever-ready to have lengthy discussions about chemistry, despite my role as the black sheep of the group. In particular, I have to thank Alexandra Rochon, who gave me perspective on a lot more than just my research, and Matt Elsby, who had perfect timing on multiple occasions. My former students, Therese and Ahmed, also have my appreciation for all their hard work over the year and a half I had the pleasure of mentoring them. Therese, I know you'll be a fantastic researcher if that is the path you choose. Ahmed, you'll be a great doctor if you just remember a few simple words from our man K.W.

While at uOttawa, I had the pleasure of working with and learning from Dr. Focsaneanu; without a doubt, she is one of the finest and most organized instructors I have ever met. Speaking of highly organized women, I have to give thanks to Jeanne Mason-Makdisi; you were incredibly supportive and thoughtful, and our talks helped get me through some rough patches in my research.

Of course, I would not be where I am without those that helped me on my way here. To Dr. Brzezowski, thank you for being a fantastic example to follow and for taking a personal interest and giving me some very helpful advice. Dr. West, thank you for even considering me as a potential student for your group and for helping to push me even farther down the path of organic chemistry. Dr. Lundgren, thank you for teaching me almost everything I know about working in a research lab. Morgan aka Little M, I can honestly say that I would not be where I am today without you; not just for your guidance during my undergraduate research, but also

your advice when applying to graduate school. From the bottom of my heart, thank you. As both a student and a TA in your labs, Dr. Hayley Wan, you have been and continue to be an inspiration to me. I hope that I can one day attain your prowess as a lab instructor. Finally, I have to thank Con Ferris and Dr. Brian Stackhouse, both of whom greatly sharpened my ability to solve problems in and out of the classroom.

Finally, on a personal note, I'd like to thank my family and friends for all their support. Both my mother and grandmother have been a constant source of support throughout my life and these past three years were no exception. My surrogate parents, Jacqueline, Donna, and Dale were also incredibly supportive and I would not be the person I am today without all of you. My closest "chem friends" Marissa, Derek, and Nathan have been fantastic friends and great role models. I've missed chatting with each of you daily (in particular your advice), but I know you're all well on your way to successful and fulfilling careers in chemistry. To my weekly DnD group, thank you for providing me with something to ward off the madness of grad school. Gerry, while I didn't follow your advice on preparing to write a thesis as closely as I probably should have, at least I managed to pass it on to others so they might actually do it properly. Dakota, I honestly can't express how happy I am to have met you. You truly helped me sort through some dark times for which I am eternally grateful; I promise to repay you as best I can with dank memes. To Kyle, Happy Birthday (as of writing this)! Your help in proofreading my work throughout my career so far in chemistry has been invaluable, and I appreciate having you as a friend. Aaron, thank you for everything; while I probably stayed up far later than I should have to chat with you, I think it was worth destroying my sleep schedule from time to time. Hajime, I appreciate your thoughtfulness over the past several months. I hope everything works out for you in the end. And finally, I'd like to thank my body; I know I put you through a lot of punishment these past few years (especially the past two months) and I promise to make it up to you very, very soon.

## Table of Contents

**List of Figures**

**List of Schemes**

**List of Tables**

**List of Abbreviations**

BME - Benzoin Methyl Ether

Cat. - Catalyst

CCS - Carbon Capture and Storage

Conv. - Conversion

DCM - Dichloromethane

Dipic - Dipicolinate

DFT - Density Functional Theory

DMF - *N*,*N*-Dimethylformamide

DMSO - Dimethylsulfoxide

Equiv. - Equivalents

GHG - Greenhouse Gas

GVL - γ-Valerolactone

HBO - Hydrobenzoin

HMF - Hydroxymethyfurfural

HMTA - Hexamethylenetetraamine

Hz - Hertz

IL - Ionic Liquid

KIE - Kinetic Isotope Effect

Mes - Mesitylene

MeTHF - 2-Methyltetrahydrofuran

NMP - *N*-Methyl-2-pyrrolidinone

NMR - Nuclear Magnetic Resonance

ppm - Parts per million

PTSA - *para*-Toluenesulfonic acid

Pyr - Pyridine

r.t. - Room temperature

Temp. - Temperature

THF - Tetrahydrofuran

Tol - Toluene

TS - Transition state

v/v - volume/volume ratio

VHPO - Vanadium haloperoxidase

## List of Compounds

*Cellulose Model compounds*

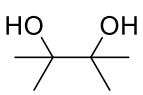


pinacol

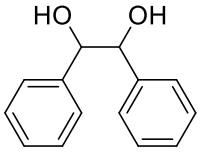


hydrobenzoin (HBO)

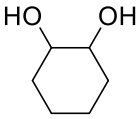


1,2-cyclohexanediol (CHD)

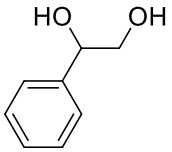


1-phenyl-1,2-ethanediol

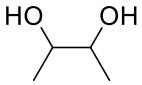


2,3-butanediol

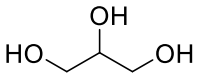


glycerol

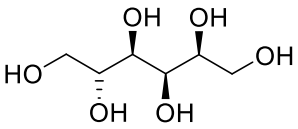


mannitol

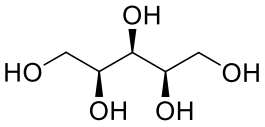


xylitol

*Miscellaneous oxovanadium(V) complexes*

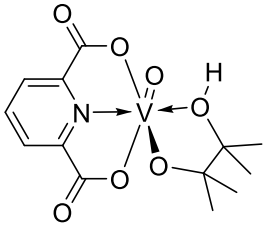

**DP1**

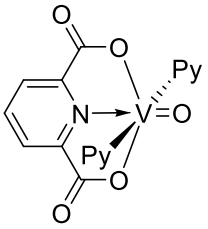

**DP2**

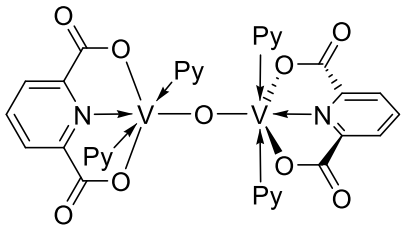

**DP3**

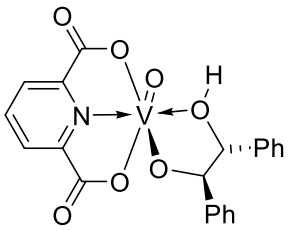

**DP4**

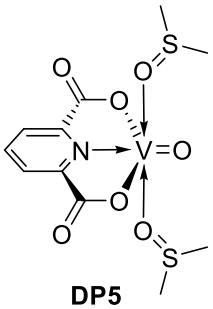

**DP5**

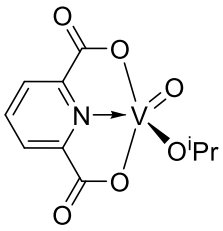

**DP6**

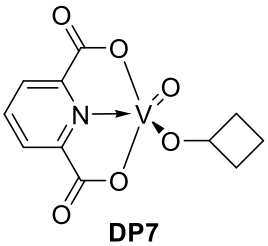

**DP7**

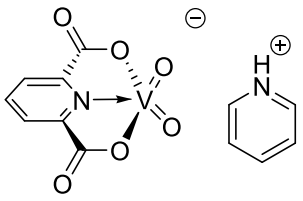

**DP8**

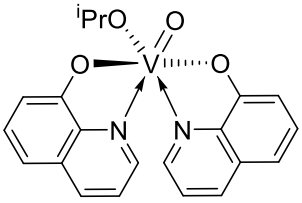

**OQ**

*Trialkoxyamine and triphenoxyamine Ligands (TL)*

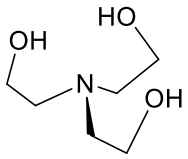


triethanolamine

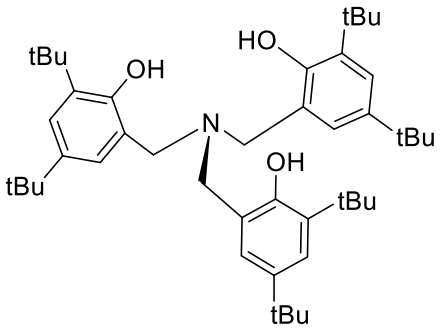


**TL1**

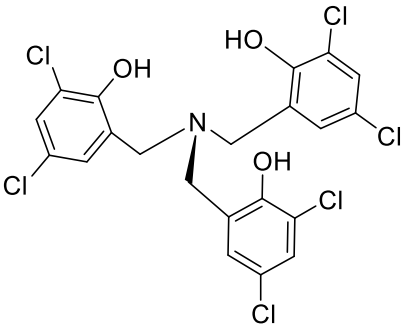


**TL2**

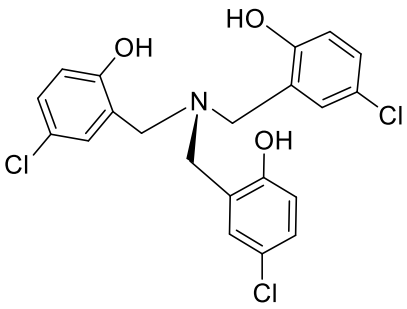


**TL3**

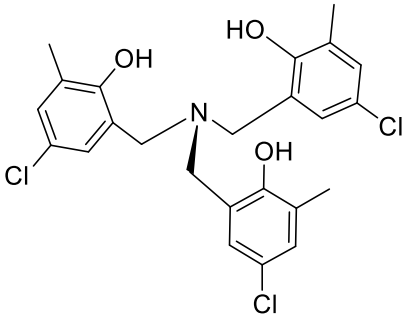


**TL4**

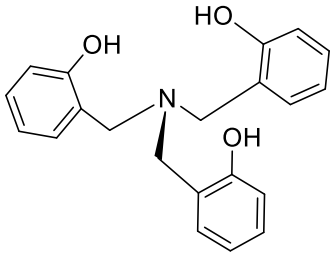


**TL5**

*Trialkoxyamine (TA) and triphenoxyamine complexes (TP)*

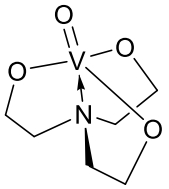

**TA**

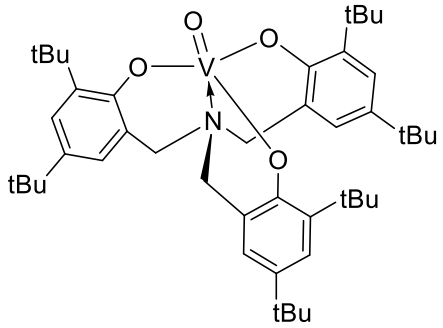

**TP1**

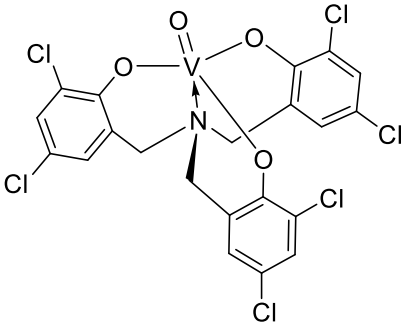

**TP2**

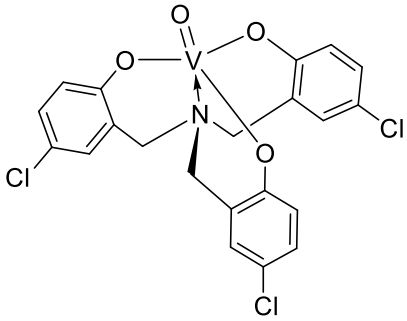

**TP3**

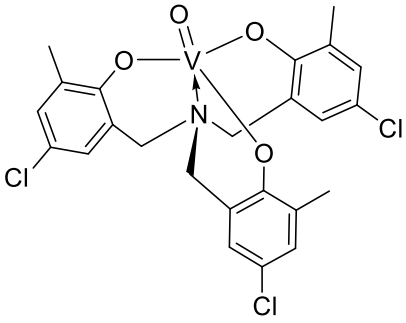

**TP4**

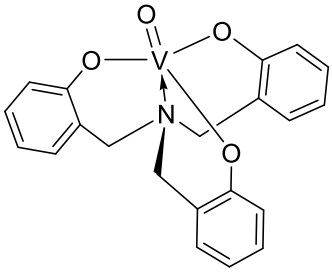

**TP5**

*Lignin Model compounds (LM)*

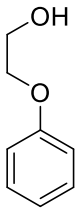

2-phenoxyethanol
**LM1**

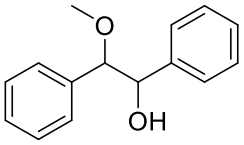

1,2-diphenyl-2-methoxyethanol
**LM2**

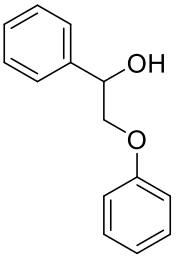

1-phenyl-2-phenoxyethanol
**LM3**

*Bisphenoxyamine Ligands (BL)*

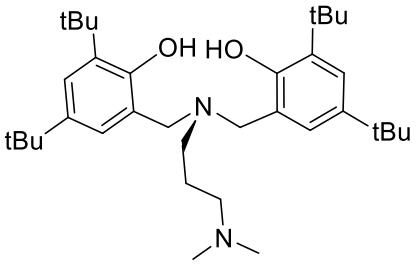


**BL1**

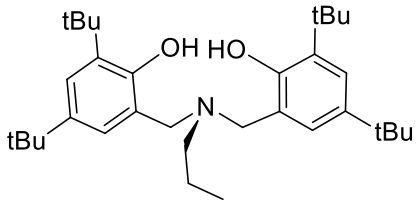


**BL2**

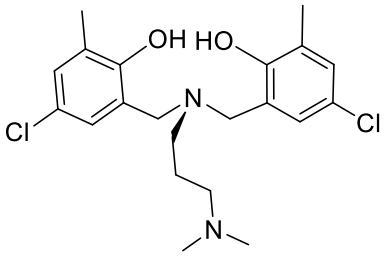


**BL3**

*Bisphenoxyamine complexes (BP)*

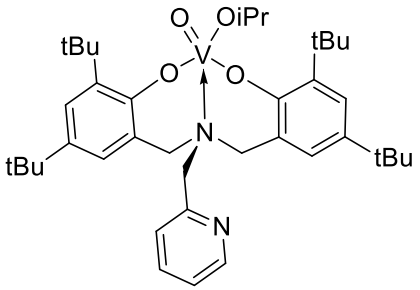


**BP-pyr**

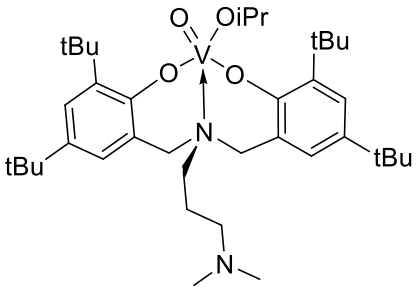


**BP1**

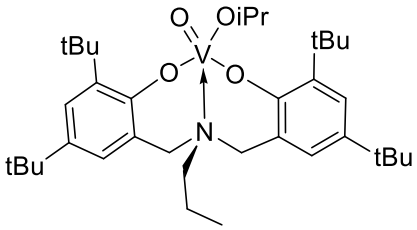


**BP2**

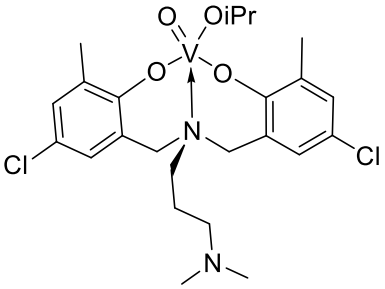


**BP3**

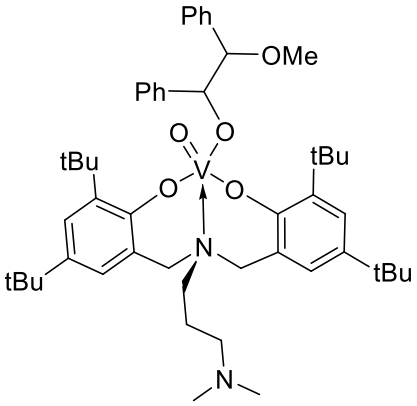


**BP4**

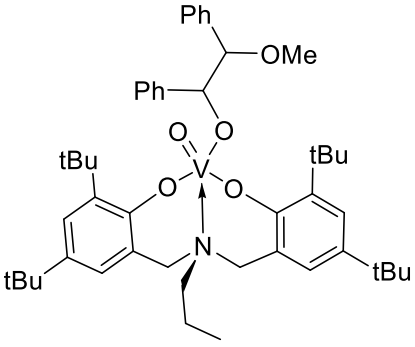


**BP5**

**List of Contributions**

*Publication resulting from this thesis:*

Godwin, C.; McCauley-Walden, D. W.; Diaz-Urrutia, C.; Chan, T.; Musa, A.; Korobkov, I.; Michel, C.; Fleurat-Lessard, P.; Baker, R. T. **2019**, *submitted for publication.*

*Publication resulting from the work not presented in this thesis:*

Castillo-Contreras, E. B.; Lauzon, J. M.; James, B. R.; Godwin, C.; Baker, R. T. **2019**, *manuscript in preparation.*

*Presentations given on the work in this thesis:*

Godwin, C.; Chan, T.; Musa, A.; Fleurat-Lessard, P.; Baker, R. T.; CSC 2018 (poster)

*Other contributions:*

Mentoring over a period of 17 months given to undergraduate students Therese Chan and Ahmed Musa (May 2017-Sept 2018).

Technical assistance provided to the following workers in the Baker lab: Torsten Rinesch (PhD student visitor from Aachen, Germany; May-Aug 2017), Prof. Organ students and postdocs Philip Eckert, Michael Lazarus, Dr. Colin Diner, Dr. Pierre Alexander Champagne (Sept 2017-Jan 2018), Siham Abouhadjar, Frédéric Vachon, Alec Macdermott (La Cité student researchers; May 2018-June 2019) and Antonio Hernandez (PhD student visitor from Lyon, France; Nov-Dec 2018).

# Chapter 1: Introduction

*1.1 Climate and Energy*

Over the past several decades, climate change has emerged as one of the most significant challenges that society and the planet as a whole currently face. Recent research and projections have shown that the effects of greenhouse gas (GHG) emissions from the burning of fossil fuels will continue to have negative impacts for decades to come, even if an immediate cessation of all fossil fuel combustion were to take place.[1] As the potentially catastrophic changes set to occur become an increasingly pressing and necessary issue to address, the need for less environmentally damaging sources of energy has increased dramatically. Green feedstocks are required not only for the various types of fuels, but also for pharmaceuticals and polymers. The only widely available, mass-produced, and sustainable chemical feedstock that currently exists is biomass.[2] In the United States alone, approximately 1.3 billion dry tons of lignocellulosic biomass could be harvested each year;[3] this would only require minor changes and would have little to no impact on production of food, in the case of agricultural biomass, or on textile production, in the case of forestry biomass.[3] Significantly, this relatively small change would supplant 30% of the current petroleum demand within the U.S. In conjunction with the reduced GHG emissions of current biofuels, implementation of these changes could result in upwards of a 15% reduction in GHG production within the U.S.,[4] resulting in an approximate 2.3% reduction globally.[5]

Several steps have been taken in recent years to move towards more sustainable and environmentally friendly alternatives to currently employed methods of energy generation.[6] However, significant drawbacks exist for each form of energy generation available. The most significant source of energy currently used is fossil fuels, which generated almost two thirds of the world's energy in 2018.[7] More specifically, these encompass coal, natural gas, and petroleum, all of which contribute to GHGs and climate change via combustion to $CO_2$. Alternative sources of energy include nuclear fission (which currently generates dangerous waste and can cause massive environmental damage, as evidenced by recent disasters),[8,9] hydroelectric power (which interferes with the ecosystems in and around the rivers used to power the turbines),[10] and wind power (which can interfere with aerial species and tends to have low efficiency).[11] Geothermal power is very efficient and can generate tremendous amounts of "free"

energy; however, it tends to be regionally specific, which drastically reduces its potential as a global energy solution.[12] Solar power is currently the most promising alternative source of energy to fossil fuels, though it is plagued by similar issues as wind power, given the sun may not always be able to provide energy.[13] Use of solar energy may prove even more difficult to overcome if potentially proposed geoengineering projects such as artificial cloud formation move forward.[14] Adding to the difficulties faced by solar energy is the need for far more efficient energy storage than currently exists. Currently, the state of the art requires extensive mining, which itself causes further environmental harm;[15] in addition, many of the solar panels currently in use are made from toxic and environmentally hazardous chemicals, making them far less sustainable than they might appear.[13] Nuclear fusion is a potentially safe and sustainable option, but remains to be safely achieved.[16] Biofuels, while still a form of combustion like fossil fuels, have reduced GHG emissions, making them attractive; despite these positive qualities, biofuels are merely a small piece of the energy puzzle, and must be combined with other technologies to act as a truly sustainable replacement for fossil fuels. Recent advances in carbon capture and storage (CCS) could further reduce the environmental impact of both bio- and fossil fuels, allowing more time to develop greener technologies or develop this particular combination further.[17,18]

Currently, fossil fuels are the most widely used feedstock, not only for organic fuels, but also for pharmaceuticals and polymers. However, fossil fuels are becoming increasingly difficult to obtain, with more environmentally damaging methods, such as fracking[19] and deep-sea drilling,[20] being used to meet the ever-increasing demand. Given the increasingly limited nature of fossil fuels and the damage being done to the planet in order to obtain, produce, and utilize them, lignocellulosic biomass represents the most attractive option currently attainable; due to the long-term non-viability of fossil fuels, this field has seen renewed research interest in recent years. Due to the complex chemical makeup of biomass, it can also be used as a feedstock for both polymers and pharmaceuticals, making it an ideal replacement for fossil fuels.[21] By using CCS to sequester $CO_2$, GHG emissions could potentially be harnessed as further feedstocks via $CO_2$ activation chemistry.[18]

Attempts have been made in recent years to utilize biomass in a more significant role within the global economy. Biodiesel, which utilizes leftover fats from vegetables or animals to

produce esters for combustion, has been the most successful to date.[22] Despite reduced GHG emissions, it remains a partial solution as it only addresses the need for energy. The proposed methanol economy put forth by the late George A. Olah represents a more rounded iteration, allowing production of fuels, and nearly any chemical due to the small size of methanol and myriad reactions it can undergo; the simple structure and versatility make methanol an ideal building block for making nearly anything.[23] However, starting with a small molecule for every synthesis is not always viable or efficient, especially for larger molecules and polymeric materials. Lignocellulosic biomass has a diverse set of chemical moieties embedded within its polymeric structures, which could allow for larger molecules to be used as starting points for syntheses of desired chemicals and materials.[24]

### *1.2 Lignocellulosic Biomass*

Biomass consists primarily of three distinct polymers: lignin, cellulose, and hemicellulose. The ratio of each material varies, but softwoods tend to contain a significantly higher cellulose percentage, up to 50% in some cases; hemicellulose generally accounts for 20-35% of biomass structure while lignin accounts for 15-30%.[24] Other minor constituents include oils and terpenes, which are in small enough abundance to have little use as large scale chemical feedstocks, despite desirable structures for use as starting materials in fine chemical synthesis, in addition to higher energy content than lignocellulosic biomass. Cellulose and hemicellulose are carbohydrate-based polymers, with cellulose existing as a straight chain polymer of glucose units; it acts as the primary backbone within plants. Hemicellulose, however, is a heteropolysaccharide, formed from a wide variety of monomers including both C5 (xylose, arabinose) and C6 (glucose, galactose, mannose) sugars.[21] The branched structure of hemicellulose helps to link individual strands of cellulose, increasing structural integrity (**Figure 1.1**). Both have β–1–4 linkages, making them relatively easy to break down with acids. Currently, methods to isolate, break down, and utilize cellulosic biomass already exist as industrial processes.[25]

In contrast, lignin is formed through a radical polymerization of three monomers known as monolignols: p-coumaryl alcohol, coniferyl alcohol, and sinapyl alcohol (**Figure 1.2**).[26] Each

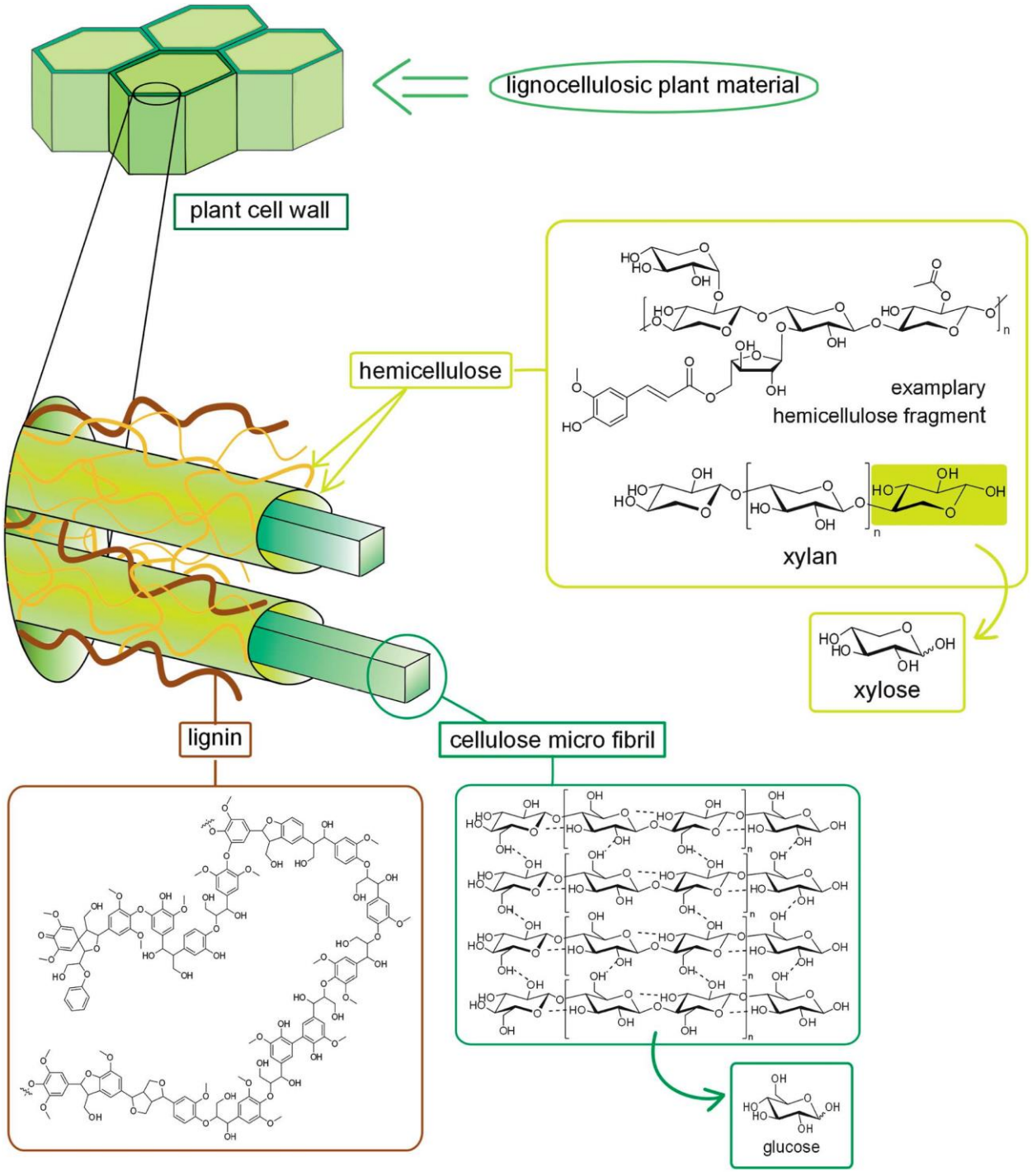


**Figure 1.1.** Chemical and macro structures of lignocellulosic biomass (reprinted from ref. 27).

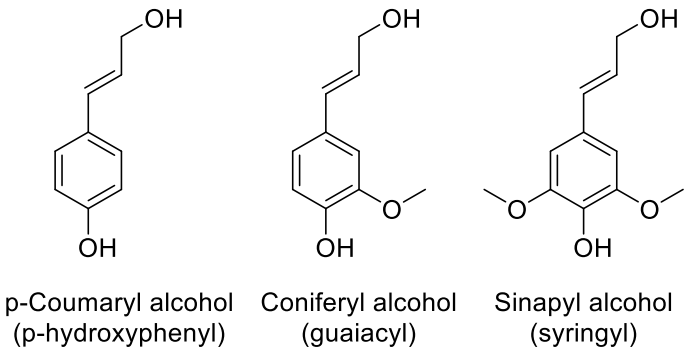


**Figure 1.2.** Monolignol monomers. Names in parentheses refer to the aromatic substituents in the lignin macromolecules.

plant species has a different ratio of monolignols, further adding complexity to individual lignin polymers; the structure can further be affected by the soil and weather conditions that each individual plant experiences during growth. The process of radical polymerization leads to a myriad of bond types including 5–5, β–β, β–O–4, β–5, β–1, α–O–4, and 4–O–5 (**Figure 1.3**).[27] The randomly cross-linked structure of lignin grants woody biomass its hardness; generally, harder woods have greater lignin content (**Figure 1.1**). The diversity of bonds present within lignin, along with the randomly cross-linked nature of lignin, makes it difficult to break down at all, let alone into reproducible products.[27]

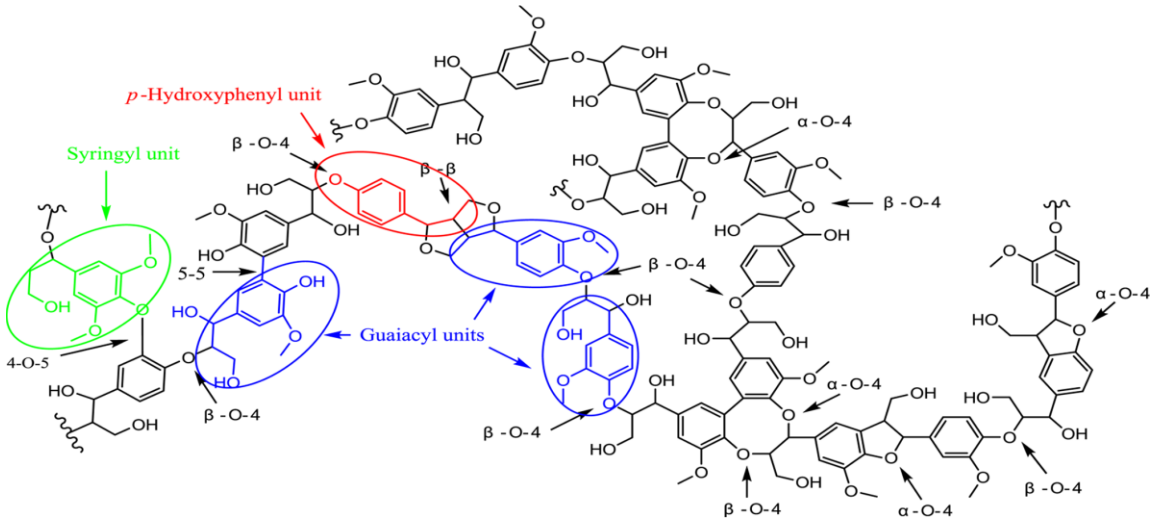


**Figure 1.3.** Example of possible lignin polymer. Monolignols and specific linkages are highlighted (reprinted from ref. 29).

The high degree of biomass variability ensures that no two samples, even from the same species of plant, will produce the same mixture of products unless they can be transformed to simpler components, such as methanol or aromatic monomers. This variability presents an issue when trying to break down whole samples of plants, but even with available techniques to separate cellulosic and hemicellulosic biomass from lignin, the lignin is generally burned as fuel at pulp mills.[28] Given the abundance of lignin within biomass, this practice effectively wastes a potentially valuable source of aromatic molecules that could be used to synthesize fine chemicals or polymers.

### *1.3 Lignocellulosic Biomass Refinement*

Lignocellulosic biomass is regularly separated into its individual components on megaton scales; annually, over 50 million tons are processed in pulp mills and bioethanol plants worldwide.[30] Several different fractionation processes are used, with the goal of obtaining cheap and pure cellulose for production of paper and textiles. The most popular form of chemical pulping is the Kraft process, which utilizes an aqueous solution of $Na_2S$ and NaOH at 170 °C for several hours (**Figure 1.4**). This process is able to break the lignin and hemicellulose into water-soluble molecules while leaving the cellulose intact and mostly pure.[31] This process yields an aqueous solution containing lignin with α–O–5 and β–O–5 linkages mostly cleaved and approximately 1-3% incorporation of sulfur in the form of thiol groups, in addition to fragments of hemicellulose. Sulfite lignin, which utilizes sulfites or bisulfites, yields a lignin containing 4-8% sulfur as sulfonate groups (**Figure 1.4**).[30] Despite the highly pure cellulose obtained using these methods, they are less than ideal in terms of sustainable usage of the biomass stream due to the presence of sulfur within the lignin; both thiol and sulfonate groups can act as poisons for transition metal catalysts, inhibiting their breakdown into monolignols and other small molecules.[30] Soda pulping, which utilizes the same conditions as Kraft without $Na_2S$, yields a non-thiol lignin but weaker pulp, and is seen as undesirable due to the current low value of lignin and hemicellulose (**Figure 1.4**).[32] Klason lignin is obtained via use of 72% $H_2SO_4$, but is mainly used as a method of assay for lignin content rather than a fractionation method (**Figure 1.4**).[33] All of these methods involve either modifications that are detrimental to further functionalization

and/or the use of non-catalytic reagents, cutting potential resource streams while consuming potentially unnecessary reagents.

Less destructive methods have been developed in recent years for the fractionation of lignocellulosic biomass. Organosolv lignin results from lignocellulose treated with protic organic solvents (MeOH, EtOH, or AcOH) or aprotic organic solvents (THF, MeTHF, glycerol, or GVL) mixed with catalysts (HCl, oxalic acid, $NH_4^+X^-$, $MCl_x$, or various Lewis acids) at 140-220 °C; this yields few, if any monomer units, as β–O–4 bonds are not cleaved consistently (**Figure 1.4**).[30] Due to the low pH, repolymerization via C–C bond formation is also possible during this process;[34] Luterbacher et al. were able to counteract this with addition of approximately 0.05 M formaldehyde.[35]

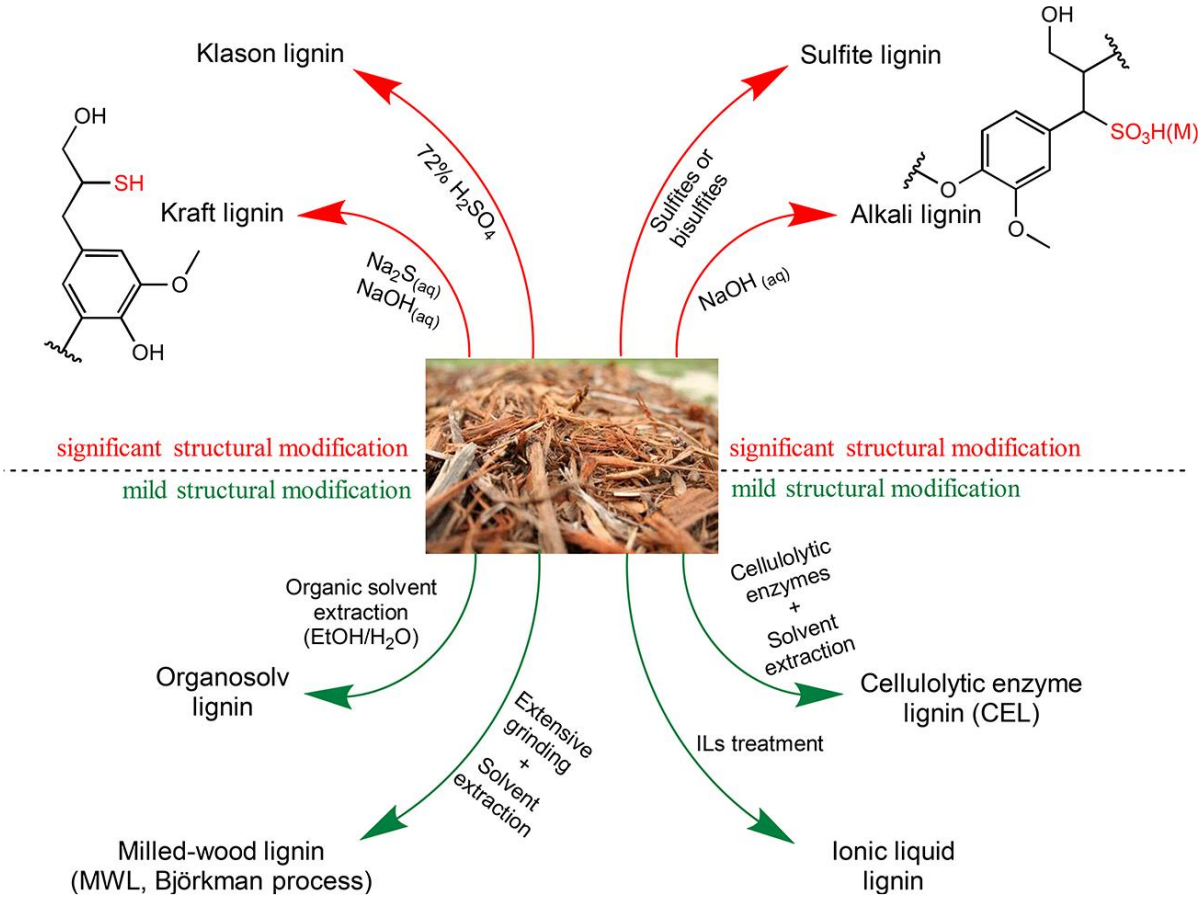


**Figure 1.4.** Common methods of lignocellulose fractionation. Cellulose is a left as a solid pulp while hemicellulose and lignin are made to be water-soluble (Reprinted from ref. 30).

Milled wood lignin is formed by milling a lignin sample in a mixture of 96% v/v aqueous dioxane for 24 hours; Fujimoto and coworkers reported that this process can cause additional carbonyl and hydroxyl groups to form, however (**Figure 1.4**).[36] Ionic liquids (ILs) have also been used for lignin disassembly, with a large variety of ILs able to depolymerize lignin effectively while leaving cellulose intact.[24] Despite these advantages, ILs tend to be cost prohibitive and potentially environmentally hazardous (**Figure 1.4**). George et al. demonstrated that ethylammonium sulfate ILs could be cost effective while performing delignification at 75% of the efficiency of the state of the art ILs.[37] Cellulolytic enzyme lignin is another mild path of delignification, utilizing enzymes which partially hydrolyze lignin; however, this method yields very large fragments and is not ideal for obtaining monomers (**Figure 1.4**).[38] This is a common theme for the milder methods; the lignin is not modified, but molecular weights are generally higher than what would be obtained via the more structurally modifying methods. However, these methods also produce less hazardous waste streams. It has been suggested that combinations of these methods may yield properly depolymerized lignin, at the cost of the time to use multiple methods in sequence.[35]

To simulate the disassembly of these bonds on newer catalysts, lignin model compounds are employed. A wide variety of model complexes exist; three of the more simplistic compounds are 2-phenoxy ethanol (**LM1**), 1,2-diphenyl-2-methoxyethanol (**LM2**), and 1-phenyl-2-phenoxy-ethanol (**LM3**) (**Figure 1.5**).[39] **LM1** and **LM3** afford access to the β–O–4 linkage while **LM2** and **LM3** afford access to the β–1 linkage, two common linkages found throughout the structure of lignin (**Figure 1.3**). While more complex lignin models exist,[39] they are not utilized in this thesis.

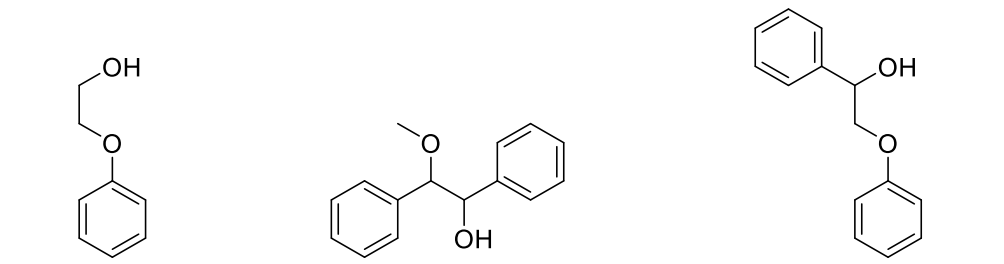


2-phenoxyethanol **LM1** | 1,2-diphenyl-2-methoxyethanol **LM2** | 1-phenyl-2-phenoxyethanol **LM3**

**Figure 1.5.** Simple lignin models used to develop new lignin depolymerization catalysts.

*1.4 Valuable Feedstocks*

Relative to fossil fuels, biomass offers the opportunity to potentially skip one or more steps on the way to synthesizing particular molecules of interest; this is due to the high oxygen content found within lignocellulosic biomass (**Figure 1.1**). Alcohols, ketones, aldehydes, and carboxylic acids can all be obtained through various processes when utilizing lignin or cellulose.[24] Of particular interest is the aldehyde moiety, which is incredibly versatile due to its relatively high reactivity. Aldehydes can undergo nucleophilic addition by a wide variety of nucleophiles, yielding functional groups such as alcohols,[40] acetals,[41] and aldols.[42]

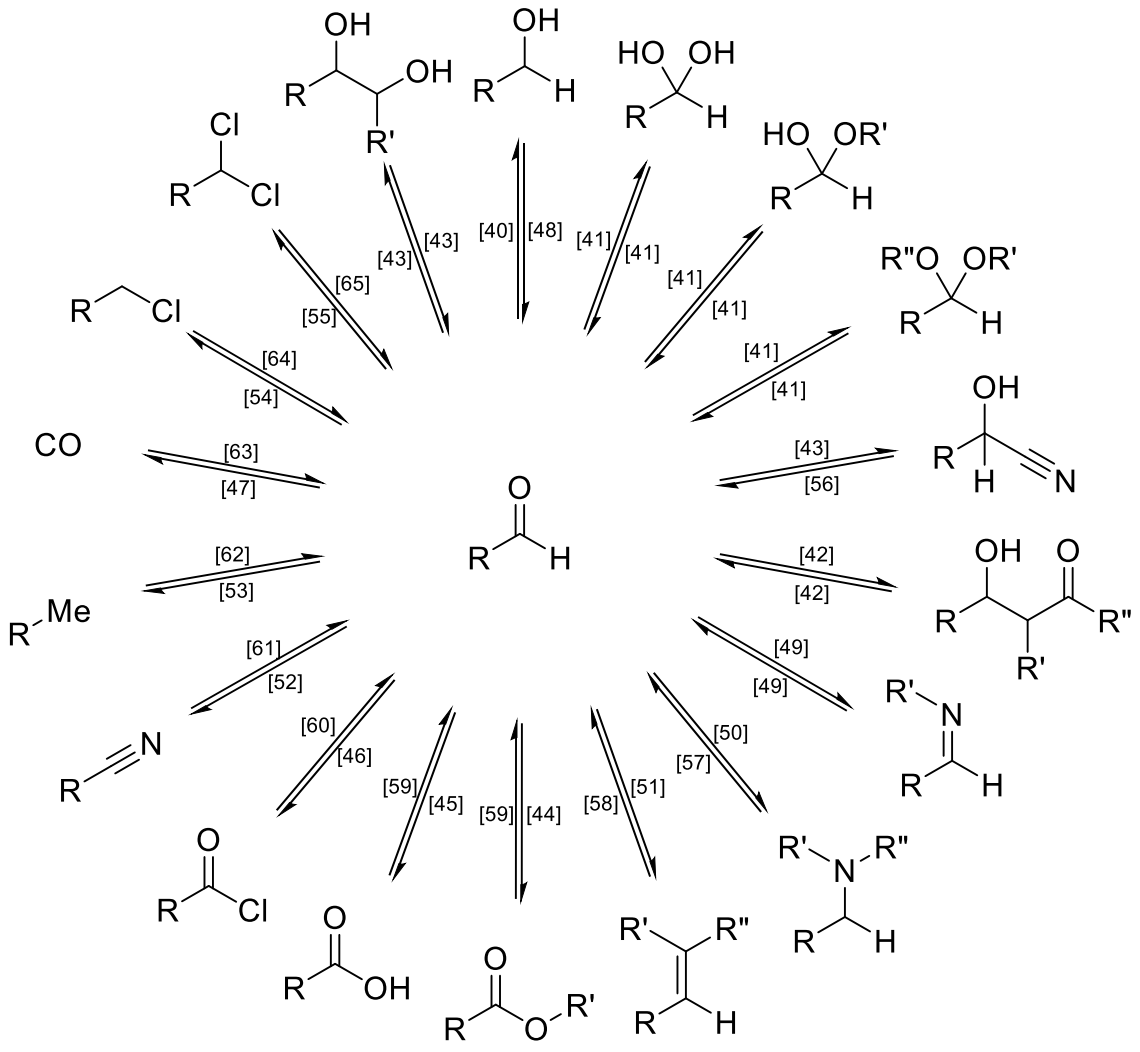


**Figure 1.6.** A selection of possible transformations to and from aldehydes.

Of particular note are cyanohydrins, synthesized via insertion of cyanide; this reaction can create an additional carbon scaffold from which to make further modifications, or in some cases, can create an umpolung effect to allow for C–C bond formation.[43] Synthesis of benzoin via benzaldehyde demonstrates the potential of this reaction. Aldehydes can also be readily converted into other carbonyl functional groups such as esters,[44] carboxylic acids,[45] and acid chlorides.[46] Through high pressure and/or heat, it is even possible to cleave an aldehyde group off and form CO gas.[47] While these reactions do not represent the entire scope of aldehyde conversion and functionalization, they demonstrate the versatility of this functional group. Most significantly, these transformations can be used to obtain aldehydes[41, 42, 48, 49, 56-65] or with aldehydes as the starting material (**Figure 1.6**).[40-47, 50-55] Many of these reactions apply to the synthesis of ketones, as few of these reactions require the hydrogen of the aldehyde group.

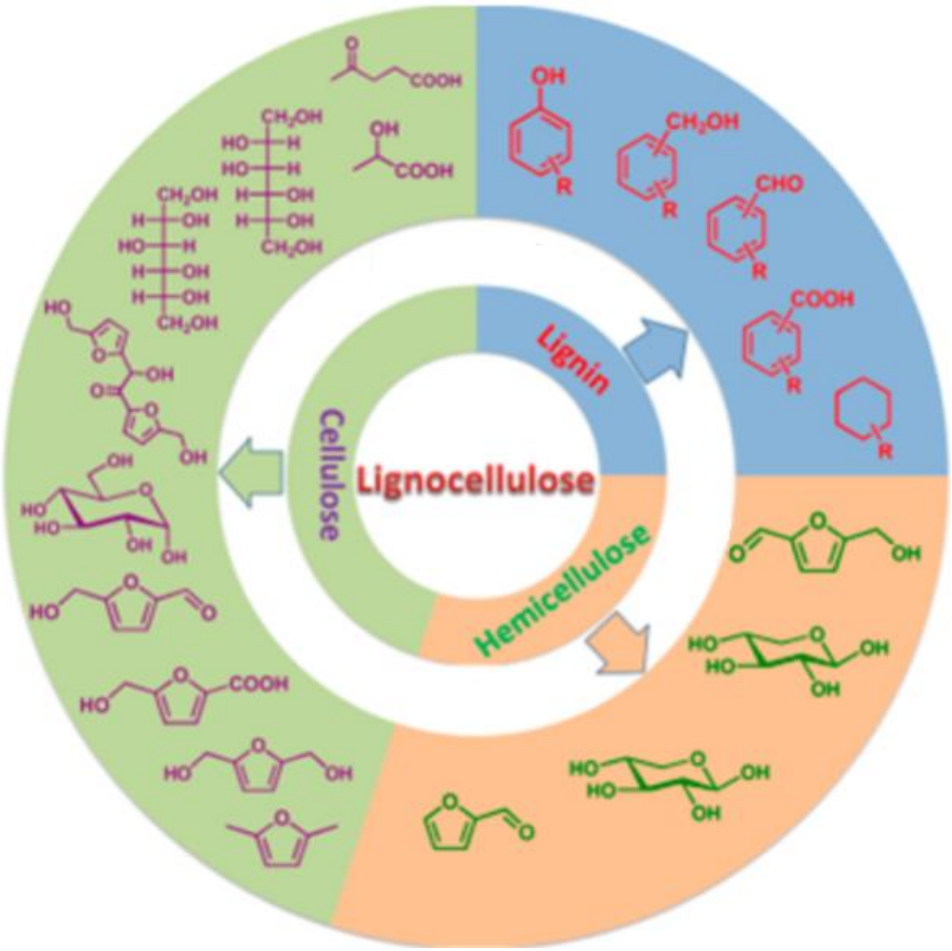


**Figure 1.7.** A selection of valuable chemicals that can be derived from lignocellulosic biomass (adapted from ref 24).

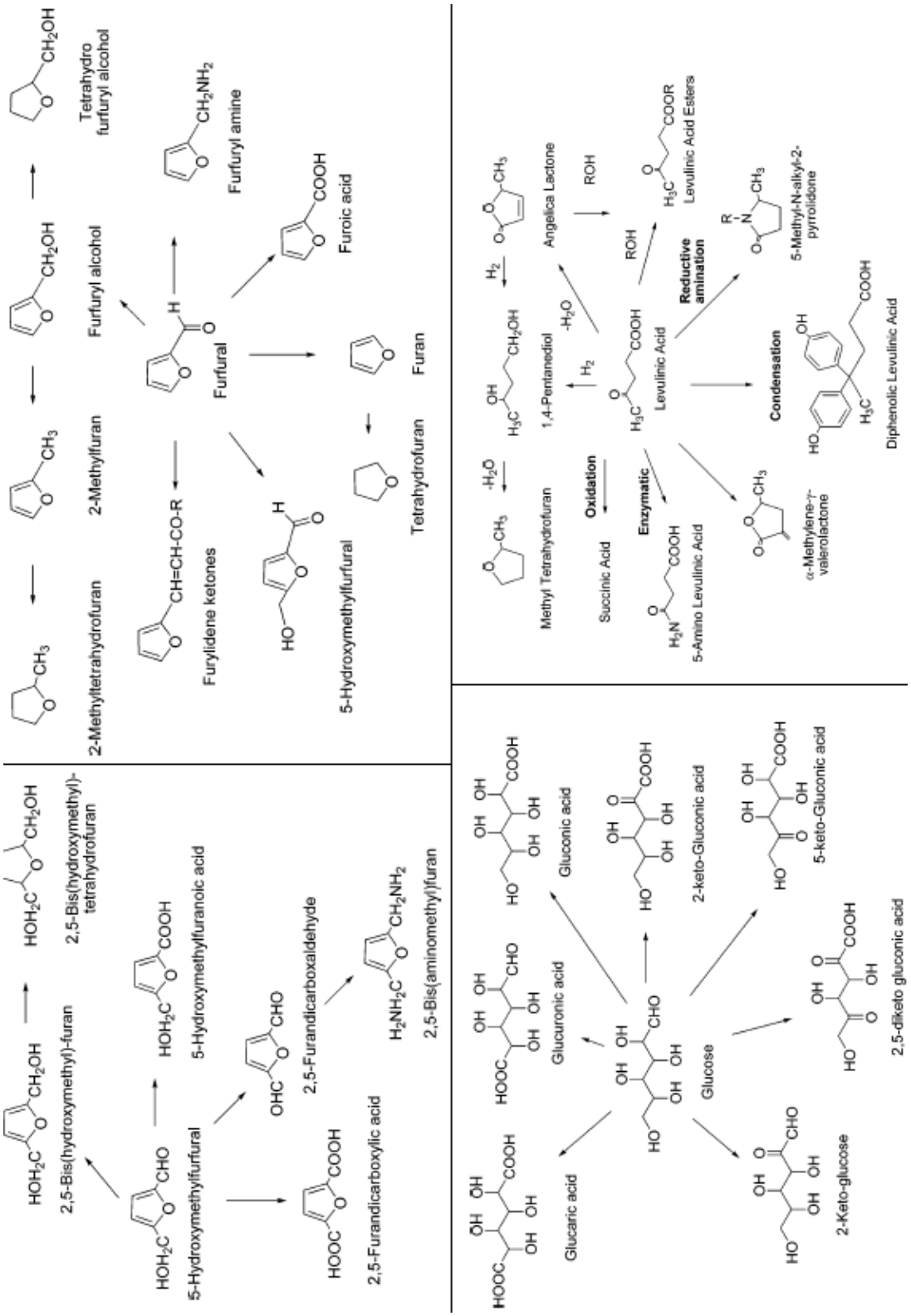


**Figure 1.8.** Various examples of chemicals derived from cellulose and hemicellulose feedstocks (adapted from ref. 2).

Carboxylic acids can also be formed from biomass but are seen as less desirable given their higher degree of stability and ease of formation. Powerful oxidants to form carboxylic acids have been available for decades, but selectively forming aldehydes through controlled oxidation remains more challenging without the use of exotic reagents. [65]

A key advantage of lignin as a feedstock is the pre-existence of aromatic rings. While these can be found through some natural sources, lignin is by far the most abundant and likely represents the most sustainable source of aromatic molecules. This structure enables access to various phenols, benzylic acids, benzaldehydes, and benzoic acids; through hydrogenation, cyclohexanes are also accessible (**Figure 1.7**).[2] These can act as starting materials for a wide variety of valuable chemicals, including pharmaceuticals, industrial solvents, polymers, pigments, and dyes.[66]

Hemicellulose affords access to sugars, as previously mentioned, as well as furfural and 5-hydroxymethylfurfural (HMF) (**Figure 1.7**). The sugars have value as starting materials for biofuels, as well as furfural and HMF themselves. HMF is primarily used a starting material to form monomer units for polyesters, polyurethanes, and polyamides.[67,68] Furfural is used to synthesize a wide variety of chemical feedstocks; these are used in the production of fragrances, vitamins, resins, pharmaceuticals, pesticides, and medicines (**Figure 1.8**).[2]

Cellulose can be disassembled into a wide variety of chemical feedstocks; similar to hemicellulose, it can yield furfural and HMF, as well as monosaccharide units (**Figure 1.7**). The most significant chemical it can produce is levulinic acid, which can be used as a gateway to numerous valuable chemicals. These include solvents, plasticizers, biofuels, polymers, herbicides, and pesticides.[2] Glucose, the most common monomer unit within biomass, can also be used to synthesize chemicals which have uses in the food, cosmetic, detergent, pharmaceutical, and medical industries (**Figure 1.8**).[2]

### *1.5 Oxovanadium Catalysis*

The use of catalysis to aid in depolymerization of lignocellulosic biomass represents a necessary step forward towards a sustainable carbon economy. Many second and third row

transition metals have been found effective at depolymerizing lignin; however, more robust and sustainable catalysts are needed given the low abundance of these metals, coupled with their susceptibility to poisoning via sulfur-based functional groups found in Kraft, Klason, and sulfite lignins.[29], has created a demand for. Vanadium is been used extensively within nature and exists as one of the most abundant transition metals in the ocean.[69] Specifically, $V^V$ is used in vanadium haloperoxidase (VHPO) enzymes to oxidatively cleave organohalide bonds within fungi, bacteria, and algae (**Figure 1.9**).

Using the trigonal bipyramidal structure as inspiration, efforts were put forth to create similar catalysts for oxidative cleavage. Early efforts came from Mimoun, who demonstrated alkene epoxidation with a vanadium(V) alkylperoxy complex,[70] and Thorn, who demonstrated lability of alkoxy groups with $V^V$ metal complexes.[71] While neither adhered strictly to the structure used within VHPOs, they clearly demonstrated the ability of oxovanadium complexes to interact meaningfully and catalytically with oxygenated substrates and their products.

With these findings in mind, Baker and Thorn applied oxovanadium(V) complexes to the oxidative cleavage of C–C bonds in diols, representative of cellulose and hemicellulose.[72] Pinacol was complexed to the dipicolinate (dipic) complex **DP1** before anaerobic reaction in pyridine to afford 1 equiv. of acetone, 1/2 equiv. of pinacol, and $V^{IV}$ dipic complex **DP2**.

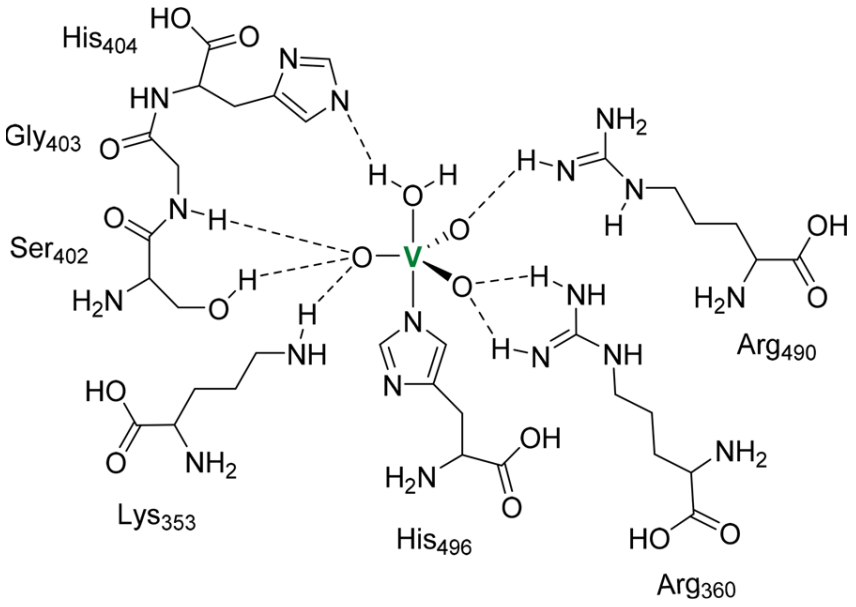


**Figure 1.9.** Example of a VHPO from *C. inaequalis*. (reprinted from ref. 72).

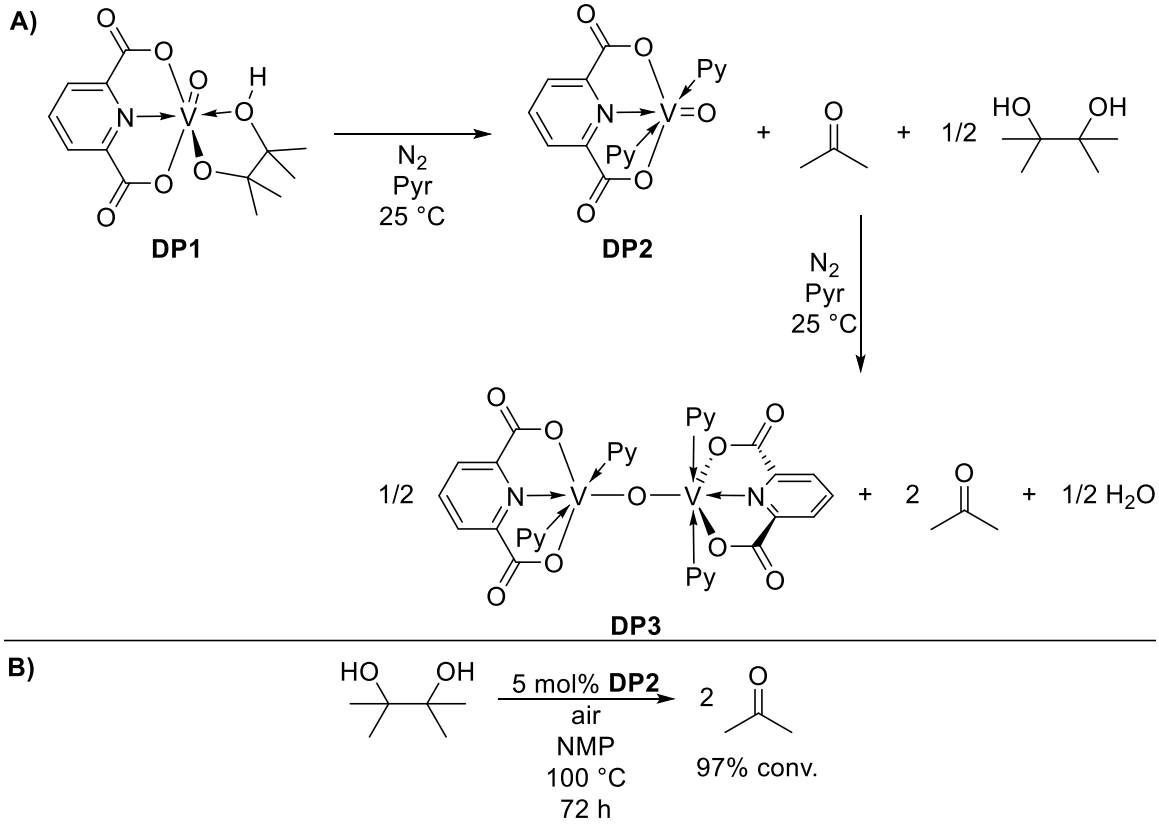


**Scheme 1.1.** Summary of Baker and Thorn's early work on oxovanadium C–C bond cleavage (adapted from ref. 74).

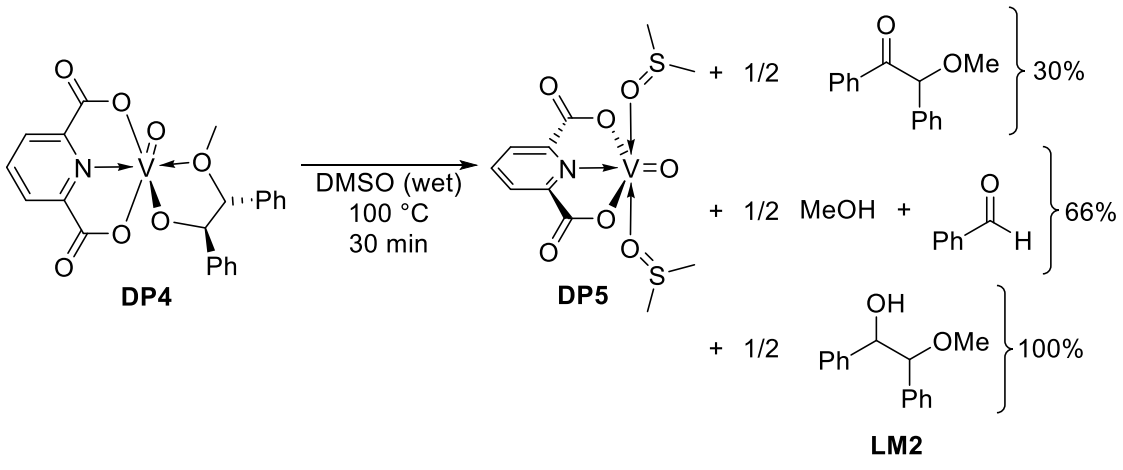


**Scheme 1.2.** Summary of Baker, Gordon, and Thorn's stoichiometric disassembly of hydrobenzoin with dipic complex **DP4** (adapted from ref. 75).

Moreover, this complex reacted further with pinacol at 100 °C to afford a second equiv. of acetone, 1/2 equiv. of water, and the μ-oxo $V^{III}$ complex dimer **DP3**. (**Scheme 1.1A**) A catalytic reaction was achieved under similar conditions, using 5 mol% **DP2,** *N*-methyl-2-pyrrolidinone (NMP) as the solvent, and air as the oxidant, yielding 2 equiv. of acetone (97% conv.) after 72 hours (**Scheme 1.1B**).

Dipic complex **DP1** was also used to make **DP4**, which was applied to the stoichiometric breakdown of **LM2**.[74] Use of pyridine as a solvent did not allow for the C–C cleavage of **LM2**; instead, C–H oxidative cleavage of the α-hydroxy hydrogen afforded benzoin methyl ether (BME). However, using wet DMSO at 100 °C over 30 minutes led to a mixture of BME (30%), MeOH and benzaldehyde (66%), and **LM2** (100%), in addition to the *trans*-DMSO-coordinated **DP5** (**Scheme 1.2**).

**Table 1.1.** Summary of Baker, Gordon, and Thorn's catalytic disassembly of **LM2** with dipic complex **DP6** (adapted from ref. 75).

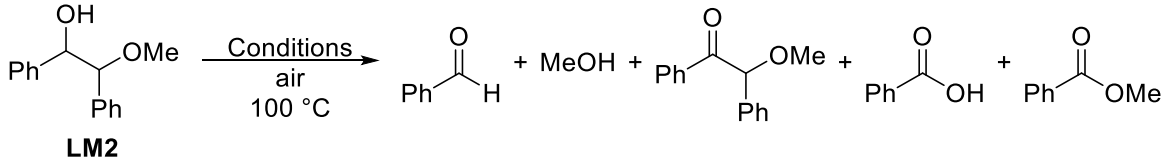


| | | | | | | |
|---|---|---|---|---|---|---|
| 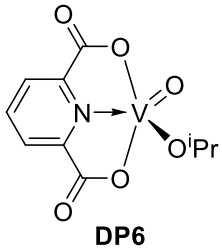 **DP6** | 5 mol% DMSO 20 h | 73% | 69% | 13% | 5% | 5% |
| | 10 mol% pyridine 6 days | 9% | 6% | 9% | 85% | 84% |

Catalytic oxidation of **LM2** was realized via the dipic complex **DP6** (**Table 1.1**).[74] The complex was shown to be capable of C–C, C–H, and C–O cleavage even when used catalytically, yielding the same products as the stoichiometric reaction, with a few key differences; no **LM2** remained, but benzoic acid and methyl benzoate were observed as products. This is likely due to overoxidation, caused by Cannizzaro[45] or Tishchenko[44] type chemistry,

which produce carboxylic acids and esters, respectively. DMSO was able to yield a much higher proportion of the desirable aldehyde significantly more quickly than pyridine.

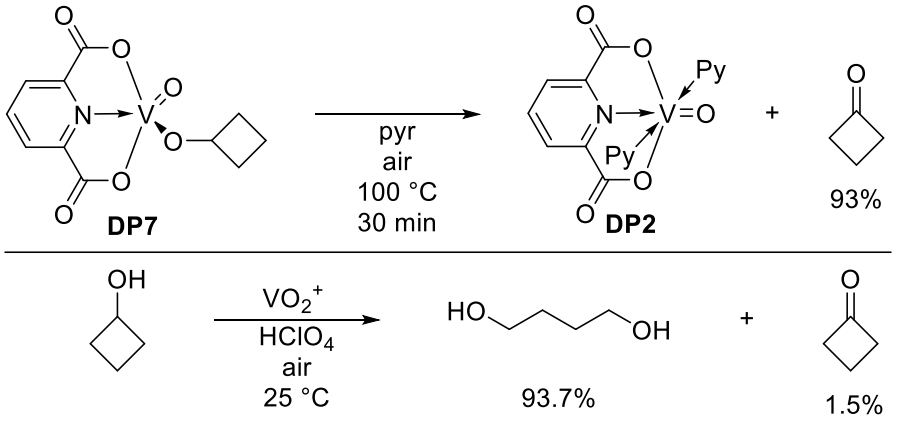


**Scheme 1.3.** Baker, Gordon, and Thorn's evidence of a two-electron oxidation pathway for dipic catalyst in pyridine.

The mechanism for the reaction of **DP6** and **LM2** in pyridine was suspected to proceed through a two-electron pathway as opposed to a radical pathway, due to an experiment with cyclobutanoxide (**Scheme 1.3**).[74] Using pyridine as the solvent, dipic complex **DP7** was heated at 100 °C for 30 minutes producing almost exclusively cyclobutanone (93%), which is consistent with a two-electron pathway. A radical pathway would likely include ring-opened products, as seen using $VO_2^+$ in $HClO_4$ with cyclobutanol from which 1,4-butanol (93.7%) was the primary product obtained (**Scheme 1.3**).

Given the earlier evidence that conversion from $V^{IV}$ **DP2** to $V^{III}$ **DP3** only requires one electron[73] and the evidence for a two-electron pathway given from the reaction of **DP7**,[74] Baker,

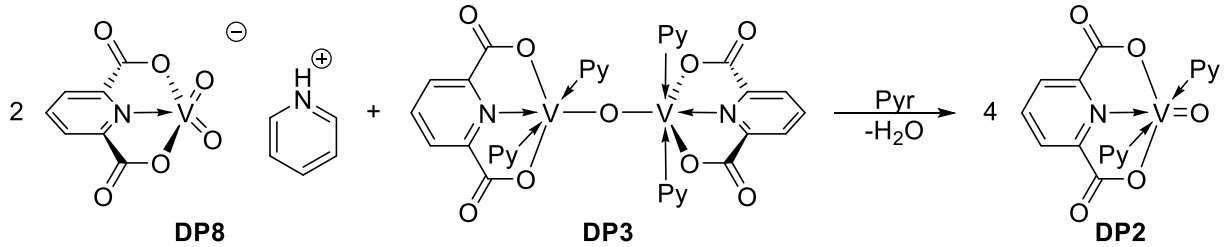


**Scheme 1.4.** Comproportionation of oxidized $V^V$ dipic complex with $V^{III}$ dimer to form $V^{IV}$ dipic complex (adapted from ref. 76).

Gordon, and Hanson further investigated the mechanism of these complexes under basic conditions.[76] Utilizing oxidized $V^V$ dipic complex **DP8** obtained via reacting with air or water in pyridine, and the aforementioned $V^{III}$ μ-oxo dimer **DP3**, a comproportionation was observed, yielding the $V^{IV}$ **DP2**. This strongly suggested that a two-electron reduction occurred before comproportionation yielded the $V^{IV}$ product that otherwise might have suggested a one-electron pathway.

While these reactions demonstrate the potential of these systems, there is a need for an improved version of these vanadium complexes; ideally with a wider scope and efficiency. In order to facilitate these advances, the mechanism for these complexes must be fully elucidated, through a combination of experimental and computational studies.

### *1.6 Conclusions*

Lignocellulosic biomass represents the only currently viable alternative to fossil fuels as a feedstock for biofuels, pharmaceuticals, and polymers. Given the current state of alternative energies and their drawbacks, in addition to the climate and environmental issues currently faced by the planet, biofuels represent an attractive and likely necessary goal. However, current methods of lignocellulose depolymerization and separation are lacking, despite renewed interest in recent years. Catalytic depolymerization of lignocellulosic biomass is a potentially sustainable method that would further lead to a sustainable carbon economy; vanadium, given its abundance and oxidative capabilities, represents an attractive option for achieving these goals.

Chapter 2 of this thesis will focus on investigations into the mechanism of triphenoxyamine oxovanadium(V) catalysts to cleave the C–C bond in selected diols as models for cellulose- and hemicellulose-derived sugars, as well as the synthesis and use of new catalysts in an effort to improve upon the state of the art. Chapter 3, on the other hand, focuses on elucidation of the mechanism of bisphenolate oxovanadium catalysts with pendant arms for C–C bond cleavage of simple lignin models. Additionally, using lessons learned from the work in Chapter 2, a new catalyst was synthesized and its reactivity was examined. Finally, in Chapter 4 the results in this thesis are summarized and used to propose potential future directions for this chemistry.

*1.7 References*

[1] IPCC, 2018: Summary for Policymakers. In: Global Warming of 1.5°C. An IPCC Special Report on the impacts of global warming of 1.5°C above pre-industrial levels and related global greenhouse gas emission pathways, in the context of strengthening the global response to the threat of climate change, sustainable development, and efforts to eradicate poverty [Masson-Delmotte, V., P. Zhai, H.-O. Pörtner, D. Roberts, J. Skea, P.R. Shukla, A. Pirani, W. Moufouma-Okia, C. Péan, R. Pidcock, S. Connors, J.B.R. Matthews, Y. Chen, X. Zhou, M.I. Gomis, E. Lonnoy, T. Maycock, M. Tignor, and T. Waterfield (eds.)]. World Meteorological Organization, Geneva, Switzerland, 32 pp.
[2] Corma, A.; Iborra, S.; Velty, A. *Chem. Rev.* **2007**,*107*, 2411−2502.
[3] Perlack, R. D.; Wright, L. L.; Turhollow, A. F.; Graham, R. L.; Stokes, B. J.; Erbach, D. C. U. S. Department of Energy, Biomass as Feedstock for a bioenergy and bioproducts industry: the technical feasibility of a billion-ton annual supply, 2005. https://www1.eere.energy.gov/bioenergy/pdfs/final_billionton_vision_report2.pdf.
[4] Renewable Fuel Standard Program (RFS2) Regulatory Impact Analysis https://web.archive.org/web/20110202202402/http:/www.epa.gov/otaq/renewablefuels/420r10006.pdf (accessed May 9, 2019).
[5] Global Greenhouse Gas Emissions Data https://www.epa.gov/ghgemissions/global-greenhouse-gas-emissions-data (accessed May 9, 2019).
[6] BP Statistical Review of World Energy 2018 https://www.bp.com/content/dam/bp/business-sites/en/global/corporate/pdfs/energy-economics/statistical-review/bp-stats-review-2018-full-report.pdf (accessed May 9, 2019).
[7] Global Energy & $CO_2$ Status Report https://www.iea.org/geco/electricity/ (accessed May 9, 2019).
[8] Ewing, R. C., *Nature Materials.* **2015**, *14*, 252–257.
[9] Mizuno, T.; Kubo, H. *Sci. Rep.* **2013**, *3*, 1742.
[10] Chen, S.; Chen, B.; Fath, B.D. *Renew. Sustain. Energy Rev.* **2015**, *42*, 78-92.
[11] Leung, D.Y.C.; Yang, Y. *Renew. Sustain. Energy Rev.* **2012**, *16*, 1031-1039.
[12] Rybach, L. *Geothermics* **2003**, *32*, 463–70.
[13] N. Kannan, D. Vakeesan *Renew. Sustain. Energy Rev.* **2016,** *62*, 1092–1105.
[14] a) Rasch, R. J.; Latham, J. ; Chen, C. J. *Environ. Res. Lett.* **2009**, *4*, 045112. b) Jones, A.; Haywood, J.; Boucher, O. *J. Geophys. Res.* **2009**, *114*, D10106.
[15] Zeng, X.; Li, J.; Sing, N. *Critical Rev. Environ. Sci. Technol.* **2014**, *44*, 1129-1165.
[16] Petrescu, F. I.; Apicella, A.; Petrescu, R. V.; Kozaitis, S.; Bucinell, R.; Aversa, R.; Abu-Lebdeh, T. *Amer. J. Appl. Sci.* **2016**, *13*, 941-946.
[17] Kemper, J. *Int. J. Greenhouse Gas Control* **2015**, *40*, 401-430.
[18] Dittmeyer, R.; Klumpp, M.; Kant, P. *Nature Comm.* **2019**, *10*, 1818.
[19] Jackson, R. B.; Vengosh, A.; Carey, J. W.; Davies, J. D.; Darrah, T. H.; O'Sullivan, F.; Pétron, G. *Ann. Rev. Environ. Res.* **2014**, *39*, 327-362.
[20] Cordes, E. E. ; Jones, D. O. B. ; Schlacher, T.; Witte, U. *Front. Environ. Sci.* **2016**, *4*, 58.
[21] Polysaccharides: Structural Diversity and Functional Versatility, ed. Dumitriu, S. Marcel Dekker, New York, 2nd ed., 2005.
[22] Ma, F.; Hanna, M. A. *Biores. Technol.* **1999**, *70*, 1-15.

[23] a) Olah, G. A. *Angew. Chem. Int. Ed.* **2005**, *44*, 2636-2639 b) Yang, C.; Jackson, R. B. *Energy Policy* **2012**, *41*, 878-884. c) Stephan, D. W. *Nature* **2013**, *495*, 54-55. d) Alberico, E.; Nielsen, M. *Chem. Commun.* **2015**, *51*, 6714-6725.
[24] Zhang, Z.; Song, J.; Han, B. *Chem. Rev.* **2017**,*117*, 6834−6880.
[25] Klemm, D.; Heublein, B.; Fink, H.; Bohn, A. *Angew. Chem. Int. Ed.* **2005**, *44*, 3358-3393
[26] Ralph, J.; Lundquist, K.; Brunow, G.; Lu, F.; Kim, H.; Schatz, P. F.; Marita, J. M.; Hatfield, R. D.; Ralph, S. A.; Christensen, J. H.; Boerjan, W. *Phytochem. Rev.* **2004**, *3*, 29.
[27] Möller, M.; Schröder, U. *RSC Adv.* **2013**, *3*, 22253-22260.
[28] Fang, Z., Jr.; Smith, R. L., Jr. Production of Biofuels and Chemicals from Lignin; Springer, 2016.
[29] Li, C.; Zhao, X.; Wang, A.; Huber, G. W.; Zhang, T. *Chem. Rev.* **2015**, *115*, 11559−11624.
[30] Sun, Z.; Fridrich, B.; De Santi, A.; Elangovan, S.; Barta, K. *Chem. Rev.* **2018**, *118*, 614−678.
[31] Chakar, F. S.; Ragauskas, A. J. *Ind. Crops Prod.* **2004**, *20* 131-141.
[32] González, M.; Cantón, L.; Rodríguez A.; Labidi, J. *Biores. Technol.* **2008**, *99*, 6621-6625
[33] Chen, H. Lignocellulose Biorefinery Engineering, Elsevier, 2015, 37-86.
[34] Freudenberg, K.; Neish, A. C. *Constitution and Biosynthesis of Lignin*; Springer-Verlag: New York; 1968; pp. 45-122.
[35] Shuai, L.; Amiri, M. T.; Questell-Santiago, Y. M.; Héroguel, F.;Li, Y.; Kim, H.; Meilan, R.; Chapple, C.; Ralph, J.; Luterbacher, J. S. *Science* **2016**, *354*, 329−333.
[36] Fujimoto, A.; Matsumoto, Y.; Chang, H. M.; Meshitsuka, G. *J. Wood Sci.* **2005**, *51*, 89−91.
[37] George, A.; Brandt, A.; Tran, K.; Zahari, S. M. S. N. S.; Klein-Marcuschamer, D.; Sun, N.; Sathitsuksanoh, N.; Shi, J.; Stavila, V.; Parthasarathi, R.; Singh, S.; Molmes, B. M.; Welton, T.; Simmons, B. A.; Hallett, J. P. *Green Chem.* **2015**, *17*, 1728−1734.
[38] Axelsson, L.; Franzén, M.; Ostwald, M.; Berndes, G.; Lakshmi, G.; Ravindranath, N. H. *Biofuels, Bioprod. Biorefin.* **2012**, *6*, 246−256.
[39] Zakzeski, J.; Bruijnincx, P. C. A.; Jongerius, A. L.; Weckhuysen, B. M. *Chem. Rev.* **2010**, *110*, 3552-3599.
[40] Gribble, G. W.; Ferguson, D. C. *J. Chem. Soc.* **1975**, *13*, 535-536.
[41] Clode, D. M. *Chem. Rev.* **1979,** 79, 491-513.
[42] Heathcock, C. H. *Comp. Org. Synth.*, **1991**, *2*, 133-179.
[43] Lapworth, A. J. *J. Chem. Soc.***1903**, *85*, 1222.
[44] Stapp, P. R. *J. Org. Chem.* **1973,** *38(7)*, 1433-1434.
[45] Cannizzaro, S. *Liebigs Ann. Chem. Pharm.* **1853**, *88*, 129-130.
[46] Mansueto, E. S.; Wight, C. A. *J. Phys. Chem.* **1992**, *96*, 1502-1504.
[47] Tsuji, J.; Ohno, K. *Tett. Let.* **1965,** *6*, 3969-3971.
[48] a) Corey, E. J.; Suggs, J. W. *Tett. Let.* **1975,** *16*, 2647-2650. b) Dess, D. B.; Martin, J. C. *J. Org. Chem.* **1983**, *48*, 4155. c) Omura, K.; Swern, D. *Tetrahedron* **1978**, *34*, 1651-1660.
[49] Morales, S.; Fernando, G.; Garcia Ruano, J. L.; Cid, M. B. *J. Am. Chem. Soc.* **2014**, 136, 1082-1089.
[50] Borch, R. F; Bernstein, M. D., Dupont Durst, H.; *J. Am. Chem. Soc.* **1971,** *93*, 2897-2904.
[51] Wittig, G.; Schöllkopf, U. *Chem. Be*r. **1954**, *87*, 1318.
[52] Coskun, N.; Arikan, N. *Tetrahedron*, **1999**, *55*, 11943-11948.
[53] Clemmensen, E. *Chem. Ber.*, **1913**, *46*, 1837-1843.
[54] Li, Z.; Sheng, C.; Qiu, H.; Zhang, Y. *New J. Org. Synth*. **2007**, *39*, 412-415.
[55] Seeger, D. E.; Lahti, P. M.; Angelo, R. R.; Berson, J. A. *J. Am. Chem. Soc.* **1986**, *108*, 1251-1265.

[56] Stork, G.; Worrall, W. S.; Pappas, J. J. *J. Am. Chem. Soc.* **1960**, *82*, 4315-4323.
[57] Carstanjen, E. *J. Prakt. Chem.* **1863,** *89*, 486-491.
[58] Veysoglu, T.; Mitsher, L. A.; Swayze, J. K. *Synthesis*, **1980**, 807-810.
[59] Webb, D.; Jamison, T. F *Org. Lett.* **2012**, *14*, 568-571.
[60] Hoffmann, R. W.; Eicken, K. R. *Chem. Ber.*, **1967**, *100*, 1465-1473.
[61] Stephen, H. *J. Chem. Soc. Trans.* **1925,** *127*, 1874-1877.
[62] Necsoiu, I.; Balaban, A. T. *Tetrahedron*, **1963**, *19*, 1133-1142.
[63] Evans, D.; Osborn, J. A.; Wilkinson, G. *J. Am. Chem. Soc.* **1968**, *33*, 3133-3142.
[64] Kornblum, N.; Jones, W. J.; Anderson, G. J. *J. Am. Chem. Soc.* **1959**, *81*, 4113-4114.
[65] Schemerling, L. *J. Am. Chem. Soc.* **1945**, *67*, 1438-1441.
[66] Holladay, J. E.; White, J. F.; Bozell, J. J.; Johnson, D. Top Value-Added Chemicals from Biomass. Vol. II: Results of Screening for Potential Candidates from Biorefinery Lignin; U.S. Department of Commerce: VA, 2007; p 1.
[67] Moreau, C.; Belgacem, M. N.; Gandini, A. *Top. Catal.* **2004**, *27*, 11.
[68] Pentz, W. J. GB Patent 2131014, 1984.
[69] Winter, J. M.; Moore, B. S. *J. Biol. Chem.* **2009**, *284*, 18577−18571.
[70] Mimoun, H.; Mignard, M.; Brechot, P.; Saussine, L. *J. Am. Chem. Soc.* **1986**, *108*, 3711–3718
[71] Thorn, D. L.; Harlow, R. L.; Herron, N. *Inorg. Chem.* **1996**, *35*, 547–548.
[72] Langeslay, R. R.; Kaphan, D. M.; Marshall, C. L.; Stair, P. C.; Sattelberger, A. P.; Delferro, M. *Chem. Rev.* **2019**, 119, 2128-2191.
[73] Hanson, S. K.; Baker, R. T.; Gordon, J. C.; Scott, B. L.; Sutton, A. D.; Thorn, D. L. *J. Am. Chem. Soc.* **2009**, *131*, 428−429.
[74] Hanson, S. K.; Baker, R. T.; Gordon, J. C.; Scott, B. L.; Thorn, D. L. *Inorg. Chem.* **2010**, *49*, 5611−5618.
[75] Rocek, J.; Aylward, D. E. *J. Am. Chem. Soc*. **1975**, *97*, 5452–5456.
[76] Hanson, S. K.; Baker, R. T.; Gordon, J. C.; Scott, B. L.; Silks, L. A. P.; Thorn, D. L. *J. Am. Chem. Soc.* **2010**, *132*, 17804–17816.

# Chapter 2: Kinetics and Mechanistic Studies of Oxovanadium Complex-Catalyzed Diol C-C Bond Cleavage

*This chapter will be partially contained in:* Godwin, C.; McCauley-Walden, D. W.; Diaz-Urrutia, C.; Korobkov, I.; Michel, C.; Fleurat-Lessard, P.; Baker, R. T. **2019**, *submitted for publication.*

## *2.1 Introduction*

Efficient conversion of biomass into valuable chemicals and materials presents a daunting challenge for catalysis science.[2,77] Methods for elaboration of cellulose-derived sugars have been focused either on catalyzed reduction to polyalcohols (sorbitol, mannitol)[78,79] or hydrolysis to the platform chemicals HMF, levulinic acid and γ-valerolactone (GVL).[80] Selective oxidation of sugars to carbonyl compounds remains a challenge for catalysis, considering that biological oxidation of glucose using phosphate requires ten different enzymes just to form two equiv. of pyruvate.[81] While base-catalyzed aldol condensation of biomass-derived aldehydes has been used to increase the carbon number of promising biofuel intermediates,[82,83] selective C–C bond cleavage of cellulose-derived sugars and polyalcohols using air as an oxidant could provide a complementary technique for biorefinery applications.[84]

Traditional methods for C–C bond cleavage of polyalcohols generally involve stoichiometric reagents, such as periodic acid or lead tetraacetate, that would be impractical for effective biomass conversion.[85] Alternatively, use of transition metal complexes often requires high catalyst loadings and co-additives.[86,87] More recent work using a layered sodium-manganese oxide catalyst under oxygen at 100 °C affords high yields of aldehydes, but is not active for aliphatic or cyclic diols;[88] a silver-catalyzed variant used 10 mol% catalyst in the presence of 3 equiv. of base to afford carboxylic acid products.[89]

Although oxovanadium(V) complexes such as **DP6** and **OQ** (**Figure 2.1**) can effect the aerobic C–C bond cleavage of pinacol and hydrobenzoin (HBO),[73,74,76,90,91] they proved too reactive with glucose, affording primarily formic acid and $CO_2$.[92] Although Hanson and coworkers previously surveyed a number of variously ligated oxovanadium complexes for aerobic alcohol oxidation to carbonyl compounds,[91a] previous work in the Baker group turned to

more electron-rich trialkoxy- and triphenoxyamine oxovanadium(V) complexes, **TA** and **TP1**,[93,94] that have been shown previously to serve as functional mimics for vanadium hydroperoxidase enzymes.[95]

Initial studies showed it was shown that complexes **TA** and **TP1** could effect the oxidation of activated diols, such as pinacol and HBO, via a 2-electron mechanism using air at 80 °C.[96] More recently Bo, Licini, and coworkers followed up on this work, reporting that Kol's 2,4-dichlorophenoxy-substituted **TP2** oxidized a variety of aromatic and aliphatic diols to predominantly aldehyde products using as little as 10 ppm of catalyst.[97] While this work proposed a reasonable reaction pathway involving pre-association of the substrate followed by a 2-electron oxidation mechanism, some details of their proposed mechanism seemed to be inconsistent with experimental results obtained during the course of this thesis. This chapter details a series of in depth kinetic and DFT studies that reveal a potential alternative reaction mechanism for this efficient metal-catalyzed C–C bond cleavage.

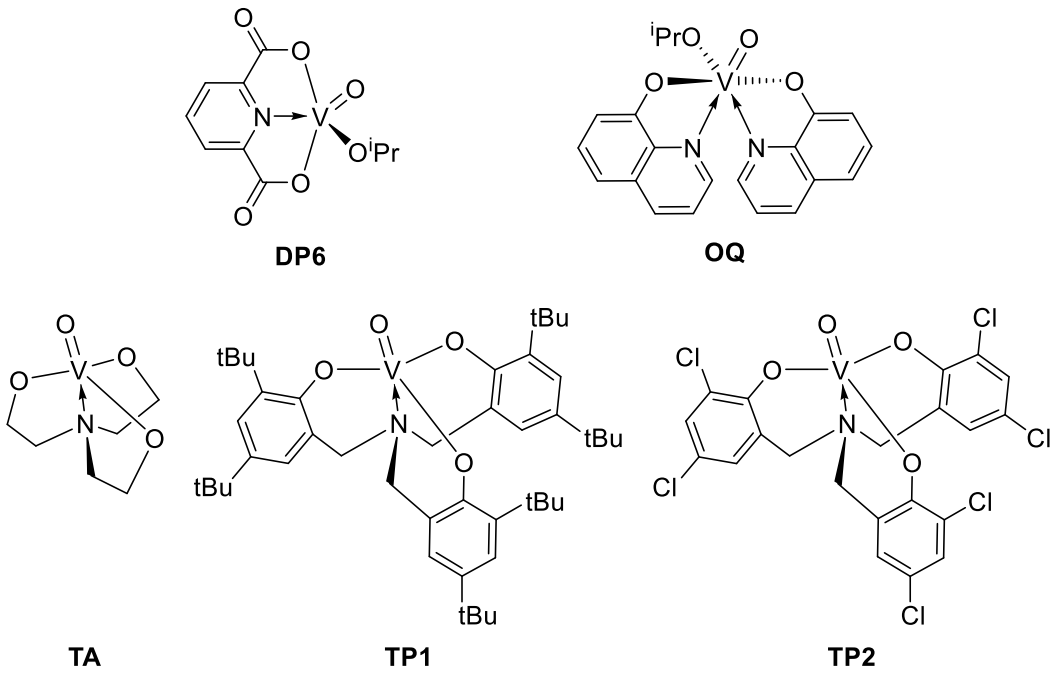


**Figure 2.1.** Oxovanadium(V) complexes with dipicolinate (**DP6**), 8-oxyquinoline (**OQ**), trialkoxyamine (**TA**), and triphenoxyamine (**TP1**, **TP2**) ancillary ligands.

*2.2 Materials and Methods*

### *2.2.1 General considerations*

Unless specified otherwise, all reactions were carried out under a dry nitrogen atmosphere using either glovebox or Schlenk techniques. Acetone, acetonitrile (MeCN), chloroform ($CHCl_3$), dichloromethane (DCM), diethyl ether ($Et_2O$), hexanes, methanol (MeOH), pentanes, tetrahydrofuran (THF), and toluene (Tol) were purchased from Alfa Aesar, Fisher Scientific, or Sigma-Aldrich. MeCN and DCM were dried via reflux over $CaH_2$. $Et_2O$, hexanes, THF, and Tol were dried on columns of activated alumina using a J. C. Meyer solvent purification system. All other solvents used in inert atmosphere were dried using activated 4 Å molecular sieves; all solvents used in air were used as obtained. Deuterated acetonitrile ($CD_3CN$), benzene ($C_6D_6$), chloroform ($CDCl_3$), dimethylsulfoxide (DMSO-$d_6$), and toluene (toluene-$d_8$) were purchased from Cambridge Isotope Laboratories and dried using activated 4 Å molecular sieves. Deuterated tetrahydrofuran (THF-$d_8$) was purchased from Sigma-Aldrich and used as obtained. All other reagents were used as obtained. $^1H$, $^{13}C\{^1H\}$, and $^{51}V$ NMR spectra were obtained on Bruker AVANCE 300 or 400 MHz spectrometers; chemical shifts were referenced to residual solvent signals ($^1H$ and $^{13}C\{^1H\}$) or externally to $VOCl_3$ (δ 0.00, $^{51}V$). The residual solvent peaks for $^1H$ NMR are: $CD_3CN$ (δ 1.94), $C_6D_6$ (δ 7.16), $CDCl_3$ (δ 7.26), DMSO-$d_6$ (δ 2.50), THF-$d_8$ (δ 3.58, 1.72), and toluene-$d_8$ (δ 7.09, 7.01, 6.97, and 2.08). The residual solvent peaks for $^{13}C\{^1H\}$ NMR are: $CD_3CN$ (δ 118.3, 1.3), $C_6D_6$ (δ 128.1), $CDCl_3$ (δ 77.2), DMSO-$d_6$ (δ 39.5), THF-$d_8$ (δ 67.2, 25.3), and toluene-$d_8$ (δ 137.5, 128.9, 128.0, 125.1, and 20.4). Tri-(2-hydroxybenzyl)amine (**TL5**),[98,99] oxovanadium complex **TP5**,[99] and hydrobenzoin-($CD_2$)[100] were prepared using literature techniques.

### *2.2.2 Synthesis of TL1 ligand*

**TL1** was synthesized according to a modified published procedure.[94a] 2,4-Di-*tert*-butylphenol (6.2 g, 30 mmol), HMTA (0.34 g, 2.5 mmol), and formaldehyde (0.29 mL, 11 mmol), were added to a 100 mL round bottom flask. The mixture was heated to 125 °C and stirred under air for 2 days. The solution was then cooled and the resulting solid was dissolved in 150 mL of $CHCl_3$. The solution was washed with 3 × 75 mL of $H_2O$ followed by 1 × 75 mL brine, then dried over $MgSO_4$. Solvent was removed *in vacuo* and the crude product was

recrystallized with $Et_2O$ and MeOH. Suction filtration and subsequent rinses with cold MeOH afforded 1.4 g of a white solid (83% yield). $^1$H NMR (300 MHz, $CDCl_3$): δ 7.23 (d, 3H, *J*=2.4 Hz), 6.97 (d, 3H, *J*=2.4 Hz), 3.63 (s, 6H), 1.39 (s, 27H), 1.27 (s, 27H). $^{13}C\{^1H\}$ NMR (100 MHz, $CDCl_3$): δ 151.4, 142.1, 125.6, 124.0, 121.8, 121.5, 56.5, 34.9, 34.2, 15.3.

### *2.2.3 Synthesis of TL2 ligand*

**TL2** was synthesized according to a modified published procedure.[101] 2,4-Dichlorophenol (3.2 g, 18 mmol), HMTA (0.32 g, 2.3 mmol), and PTSA (29 mg, 0.17 mmol), were added to a 100 mL round bottom flask. The mixture was heated to 125 °C and stirred under air for 2 days. The solution was then cooled and the resulting solid was dissolved in 80 mL of $CHCl_3$. The solution was washed with 3 × 40 mL of 1 M $H_2SO_4$ followed by 1x 40 mL of brine, then dried over $MgSO_4$. Solvent was removed *in vacuo* and the crude product was recrystallized with a 1:1 mixture of $Et_2O$:MeOH. Suction filtration and subsequent rinses with cold MeOH afforded 1.2 g of a white solid (96% yield). $^1$H NMR (300 MHz, DMSO-$d_6$): δ 7.39 (d, 3H, *J*=1.8 Hz), 7.19 (d, 3H, *J*=1.8 Hz), 3.84 (s, 6H). $^{13}C\{^1H\}$ NMR (100 MHz, DMSO-$d_6$): δ 152.3, 128.1, 128.0, 128.0, 122.7, 121.5, 48.5.

### *2.2.4 Synthesis of TL3 ligand*

4-Chlorophenol (7.0 g, 55 mmol), HMTA (0.96 g, 6.8 mmol), and PTSA (72 mg, 0.38 mmol), were added to a 250 mL round bottom flask. The solution was heated to 125 °C and stirred at under air for 2 hours. The solution was then cooled and the resulting solid was dissolved in 200 mL of boiling MeCN. Suction filtration and subsequent rinses with cold MeCN afforded 1.2 g of a white solid (64% yield). $^1$H NMR (400 MHz, DMSO-$d_6$): δ 7.19 (dd, 3H, *J*=2.6, 8.3 Hz), 7.10 (dd, 3H, *J*=2.6, 8.3 Hz), 6.75 (d, 3H, *J*=8.3 Hz), 3.71 (s, 6H). $^{13}C\{^1H\}$ NMR (100 MHz, DMSO-$d_6$): δ 155.3, 128.3, 127.4, 127.0, 122.1, 116.6, 47.68.

### *2.2.5 Synthesis of TL4 ligand*

4-Chloro-2-methylphenol (3.0 g, 21 mmol), HMTA (0.36 g, 2.6 mmol), and PTSA (30 mg, 0.16 mmol), were added to a 100 mL round bottom flask. The solution was heated to 125 °C and stirred under air for 5 days. The solution was then cooled and the resulting solid was dissolved in 100 mL of boiling MeCN. Suction filtration and subsequent rinses with cold MeCN

afforded 0.8 g of a white solid (67% yield). $^{1}$H NMR (400 MHz, DMSO-$d_6$): δ 9.46 (s, 3H), 7.15 (m, 6H), 4.33 (m, 6H), 2.16 (s, 9H).

### *2.2.6 Synthesis of TA complex*

**TA** was synthesized according to a modified published procedure.[93a] In a 50 mL round bottom flask, $N(CH_2CH_2OH)_3$ (134 mg, 0.9 mmol) was dissolved in 5 mL of MeOH. In a separate 50 mL round bottom flask, $V(O)(O^iPr)_3$ (253 μL, 1.0 mmol) was dissolved in 5 mL of MeOH. The $V(O)(O^iPr)_3$ solution was added dropwise to the $N(CH_2CH_2OH)_3$ solution over 5 minutes, yielding a cloudy yellow-white solution. This was stirred for 3 days before removing solvent *in vacuo*. Suction filtration and subsequent rinses with cold MeOH, followed by an additional 12 hours of drying *in vacuo*, afforded 100 mg of a yellow-olive powder (47% yield). $^{1}$H NMR (300 MHz, $CD_3CN$): δ 4.59 (s, 3H), 3.10 (m, 3H). $^{51}$V NMR (79 MHz, $CD_3CN$): δ −380.1.

### *2.2.7 Synthesis of TP1 complex*

**TP1** was synthesized according to a modified published procedure.[94a] In a 250 mL round bottom flask, **TL1** (2.7 g, 4 mmol) was dissolved in 40 mL of DCM. In a separate 250 mL round bottom flask, $V(O)(O^iPr)_3$ (944 μL, 4 mmol) was dissolved in 40 mL of DCM. The $V(O)(O^iPr)_3$ solution was added dropwise to the **TL1** solution over 5 minutes, yielding a dark red solution. This was stirred for 18 hours before removing solvent *in vacuo*. The crude solid was then recrystallized with Tol and stored at −35 °C for 5 hours. Suction filtration and subsequent rinses with cold toluene afforded 257 mg of a red solid (9% yield). $^{1}$H NMR (300 MHz, $C_6D_6$): δ 7.41 (d, 3H, *J*=2.7 Hz), 7.01 (d, 3H, *J*= 2.4Hz), 3.83 (d, 3H, *J*=13.5 Hz), 2.86 (d, 3H, *J*=13.5 Hz), 1.54 (s, 27H), 1.28 (s, 27H). $^{13}$C{$^{1}$H} NMR (75 MHz, $C_6D_6$): 145.2, 127.8, 127.5, 126.3, 124.4, 122.0, 57.8, 35.2, 34.3, 31.4, 29.7. $^{51}$V NMR (79 MHz, $C_6D_6$): δ −373.1.

### *2.2.8 Synthesis of TP2 complex*

**TP2** was synthesized according to a modified published procedure.[94a] In a 20 mL scintillation vial, **TL2** (268 mg, 0.5 mmol) was dissolved in 3 mL of MeCN. In a separate 20 mL scintillation vial, $V(O)(O^iPr)_3$ (150 μL, 0.6 mmol) was dissolved in 3 mL of MeCN. The $V(O)(O^iPr)_3$ solution was added dropwise to the **TL2** solution over 5 minutes, yielding an

opaque black solution. This was stirred for 5 days before removing solvent *in vacuo*. The crude solid was then recrystallized with MeCN and stored at −35 °C for 18 hours. Suction filtration and subsequent rinses with cold MeCN afforded 105 mg of a light purple solid (35% yield). $^{1}$H NMR (300 MHz, $CDCl_3$): δ 7.41 (m, 6H), 3.89 (m, 6H). $^{51}$V NMR (79 MHz, DMSO-$d_6$): δ −496.8, −530.2.

### *2.2.9 Synthesis of TP3 complex*

In a 20 mL scintillation vial, **TL3** (221 mg, 0.5 mmol) was dissolved in 3 mL of MeCN. In a separate 20 mL scintillation vial, V(O)($O^iPr$)$_3$ (150 μL, 0.6 mmol) was dissolved in 3 mL of MeCN. The V(O)($O^iPr$)$_3$ solution was added dropwise to the **TL3** solution over 5 minutes, yielding an opaque black solution. This was stirred for 5 days before removing solvent *in vacuo*. The crude solid was then recrystallized with MeCN and stored at −35 °C for 1 week. Suction filtration and subsequent rinses with cold MeCN afforded a black powder. A hot filtration with 5 mL of boiling MeCN was then performed, which afforded 127 mg of a dark purple powder (50% yield). $^{1}$H NMR (400 MHz, DMSO-$d_6$): δ 7.01 (m, 9H), 6.88 (s, 3H), 3.88 (m, 6H). $^{51}$V NMR (79 MHz, DMSO-$d_6$): δ −479.5.

### *2.2.10 Synthesis of TP4 complex*

In a 20 mL scintillation vial, **TL4** (247 mg, 0.5 mmol) was dissolved in 3 mL of MeCN. In a separate 20 mL scintillation vial, V(O)($O^iPr$)$_3$ (250 μL, 0.9 mmol) was dissolved in 3 mL of MeCN. The V(O)($O^iPr$)$_3$ solution was added dropwise to the **TL4** solution over 5 minutes, yielding an opaque blue solution. This was stirred for 2 days before removing solvent *in vacuo* for an additional 2 days. The solid was triturated with 15 mL of hexanes and dried *in vacuo* at 40 °C for 2 hours, which afforded 246 mg of a dark blue powder (88% yield). $^{1}$H NMR (300 MHz, DMSO-$d_6$): δ 7.01 (d, 3H, $J$ = 2.1 Hz), 6.88 (s, 3H), 2.19 (s, 9H). $^{51}$V NMR (79 MHz, DMSO-$d_6$): δ −399.3, −474.6.

### *2.2.11 Synthesis of (O-$^{2}$H)$_2$-Hydrobenzoin*

In a 50 mL round bottom flask, hydrobenzoin (214 mg, 1.0 mmol) was dissolved in 10 mL of THF. In a separate 50 mL round bottom flask, NaH (49 mg, 2.1 mmol) was combined with 10 mL of THF. The hydrobenzoin solution was added dropwise to the NaH mixture over 5

minutes. After 2 hours, $D_2O$ (100 μL, 5.6 mmol) was added dropwise over 5 minutes to the reaction mixture. Once the solution had become transparent with a white precipitate, a liquid-liquid extraction was used to isolate the organic layer. The organic layer was dried over $K_2CO_3$, filtered, and THF was removed *in vacuo*. The compound was dried for an additional 18 hours to afford 199 mg of an off-white solid (92% yield). $^1$H NMR (300 MHz, $CDCl_3$): δ 7.23 (m, 10H), 4.82 (s, 2H). $^{13}C\{^1H\}$ NMR (75 MHz, $CDCl_3$): 139.7, 128.2, 128.1, 127.0, 77.8.

### *2.2.12 Synthesis of (O-$^2$H)$_2$-Pinacol*

In a 50 mL round bottom flask, pinacol (236 mg, 2.0 mmol) was dissolved in 10 mL of THF. In a separate 50 mL round bottom flask, NaH (99 mg, 4.2 mmol) was combined with 10 mL of THF. The pinacol solution was added dropwise to the NaH mixture over 10 minutes. Once the solution had become yellow, a solution of DCl in $D_2O$ (100 μL, 4.4 mmol) was added dropwise to the pinacolate solution over 10 minutes. Once the solution had become transparent with a white precipitate, solvent was removed *in vacuo*. The compound was dried for an additional 10 days to afford an off-white solid. The crude product was then sublimed at 170 °C until a flaky white solid (42% yield) formed on the cold finger of the sublimator. $^1$H NMR (400 MHz, DMSO-$d_6$): δ 1.06 (s, 12H)

### *2.2.13 General procedure for of polyalcohols with TA or TP complexes*

In a 4 mL scintillation vial, the desired diol was dissolved in 0.5 mL of the desired deuterated solvent. In a separate 4 mL scintillation vial, the desired amount of oxovanadium catalyst was dissolved in 0.5 mL of the same solvent. The diol solution was then added to the oxovanadium solution. 5 μL of 1,3,5-trimethoxy benzene or mesitylene were added as an internal standard. A small sample was taken for an initial $^1$H NMR spectrum and a Teflon stir bar was added before sealing the vial and heating at the desired temperature for the desired reaction time. After completion of the allotted reaction time, another sample was taken to obtain $^1$H, $^{13}$C, and/or $^{51}$V NMR spectra. Blank reactions with no oxovanadium catalyst were performed using the same general procedure.

### *2.2.14 General procedure for kinetics*

In a 4 mL scintillation vial, the desired diol was dissolved in 0.4 mL of toluene-$d_8$. In a separate 4 mL scintillation vial, the desired amount of oxovanadium catalyst was dissolved in an additional 0.4 mL of toluene-$d_8$. 5 µL of 1,3,5-trimethoxy benzene or mesitylene were added as an internal standard. Both solutions were then transferred to an NMR tube and sealed. The reaction was monitored over 12 hours via NMR spectroscopy at the desired temperature.

## *2.3 Results and Discussion*

### *2.3.1 Aerobic Catalytic Oxidation of Activated 1,2-Diols*

Trialkoxyamine oxovanadium complex **TA** has been reported to bind alcohols, ROH, as alkoxides by reversible protonation of one alkoxy arm; it can even undergo conversion to $V(O)(OR)_3$ and free triethanolamine in neat alcohols.[93a] Conversely, no alcohol reactivity has been reported for complex **TP1**;[93a] heating stoichiometric mixtures of **TA** or **TP1** with 2-phenoxyethanol or 1,2- diphenylethanol in $CD_3CN$ under either aerobic or anaerobic conditions (80 °C, 48 h) did not afford any new vanadium complexes or oxidized products as evidenced by $^{51}V$ and $^{1}H$ NMR spectroscopy. In contrast, heating equimolar amounts of pinacol and **TA** ($CD_3CN$, 80 °C, 18 h) in air afforded 100% conversion to acetone (**Scheme 2.1; Table 2.1,** entry 1). Decreasing the catalyst loading of **TA** to 1 mol% afforded fair conversion in MeCN (52%, entry 3), which improved in DMSO and benzene, and was best in pyridine (87%, entry 6). Catalyst **TP1** was particularly poor in DMSO (9%, entry 8), only moderate in benzene and acetonitrile, and again best in pyridine (86%, entry 10). Surprisingly, under the same conditions, catalyst **TP2** was found to be less effective than **TA** or **TP1** in DMSO for this substrate, with a 10 mol% loading (10%, entry 11). A control experiment (no catalyst) in pyridine-$d_5$ showed no reaction upon heating pinacol under air at 100 °C for 14 days (entry 12).

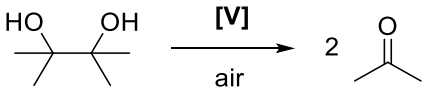


**Scheme 2.1.** Aerobic C–C bond cleavage of pinacol with oxovanadium complexes **TA**, **TP1**, and **TP2** (**Table 2.1**).

**Table 2.1.** Catalytic C–C bond cleavage of pinacol after 18 h at 80 °C (**Scheme 2.1**).

| Entry | Cat. (mol%) | Solvent | Conv. (%)[a] |
|---|---|---|---|
| 1 | **TA** (100) | $CD_3CN$ | 100 |
| 2 | **TA** (100) | dmso-$d_6$ | 7 |
| 3 | **TA** (1) | $CD_3CN$ | 52 |
| 4 | **TA** (1) | dmso-$d_6$ | 66 |
| 5 | **TA** (1) | $C_6D_6$ | 67 |
| 6 | **TA** (1) | pyr-$d_5$ | 87 |
| 7 | **TP1** (1) | $CD_3CN$ | 46 |
| 8 | **TP1** (1) | dmso-$d_6$ | 9 |
| 9 | **TP1** (1) | $C_6D_6$ | 31 |
| 10 | **TP1** (1) | pyr-$d_5$ | 86 |
| 11 | **TP2** (10) | dmso-$d_6$ | 10 |
| 12[b] | control | pyr-$d_5$ | 0 |

[a] $^1$H NMR integration against an internal standard. [b]14 days at 100 °C.

The aerobic oxidation of HBO (**Scheme 2.2**) to aldehydes was also studied using **OQ**, **TA**, **TP1**, and **TP2**. With 1 mol% of **TA**, total conversion of HBO was achieved in $CD_3CN$ at 80 °C over 18 hours with only fair selectivity for benzaldehyde (PhCHO; 24%, **Table 2.2**, entry 1). In contrast, use of DMSO as a solvent gave high conversion (99%) and selectivity (98%) even at 0.1 mol% catalyst loading (**Table 2.2**, entry 4). Higher selectivity relative to MeCN was also observed in benzene and pyridine, but the latter did not outperform DMSO for this substrate. In the case of catalyst **TP1**, DMSO was also the best solvent (**Table 2.1**, entry 12). Under these conditions, overoxidation to benzoic acid (PhCOOH) was not observed and high selectivity for aldehydes was obtained even with catalyst loadings as low as 0.1 mol% (**Table 2.2**, entries 7 and 12). A previous generation oxovanadium complex, **OQ**, was shown to have relatively fast reaction times at 0.1 mol% catalyst loading (**Table 2.2**, entries 16-18). Selectivity of this complex was high with modest yields after only several hours of reaction time (**Table 2.2**, entry 16); however, when the reaction was run for 18 hours, selectivity decreased dramatically despite complete conversion (**Table 2.2**, entry 18). The addition of base to the reaction using **OQ** (**Table 2.2**, entry 17) also had a negative effect on selectivity, decreasing it from 93% to 49%. Prior to the work published by Licini and coworkers, **TP2** was investigated as a potential improvement to **TP1** due to the decreased electron density at the metal center (**Table 2.2**, entry 19). At only 1 mol% catalyst loading, it was able to fully convert HBO with perfect selectivity, indicating that

triphenoxyamine ligands with weak electron withdrawing groups could enable greater catalyst activity.

### *2.3.2 Aerobic Catalytic Oxidation of Less Activated 1,2-Diols*

The lack of reactivity with 1,2-diphenylethanol points to the highly selective nature of complexes **TA** and **TP1** as aerobic C–C bond cleavage catalysts. In fact, even activated diols such as 1- phenyl-1,2-ethanediol were not readily oxidized by **TA** or **TP1**.[97] However, complex **TP2** was able to oxidize a racemic mixture of 1,2-cyclohexanediol (CHD) to hexanedial in trace amounts (**Scheme 2.3**).

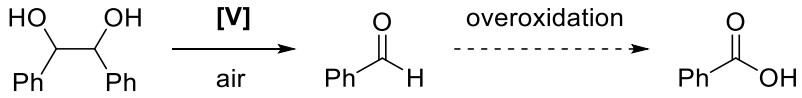


**Scheme 2.2.** Aerobic C–C bond cleavage of HBO with oxovanadium complexes **HQ**, **TA**, and **TP1-3** (**Table 2.2**).

Hypothesizing that decreased electron density at the vanadium center enabled access to new substrates in addition to the high selectivity observed with HBO, two new oxovanadium(V) complexes were synthesized. Ligands **TL3** and **TL4** were synthesized using commercially available reagents in Mannich condensations.[101] Complexes **TP3** and **TP4** were synthesized by using stoichiometric V(O)($O^iPr$)$_3$ in MeCN, similar to previous procedures (**Figure 2.2**).[94a] As no previous ligands had incorporated a "push-pull" system of one electron donating group coupled with one electron withdrawing group, **TP4** was favoured for study. Additionally, **TL4** did not undergo oligomerization during synthesis due to blocking methyl groups in the ortho position of the rings, making **TP4** more convenient to study.

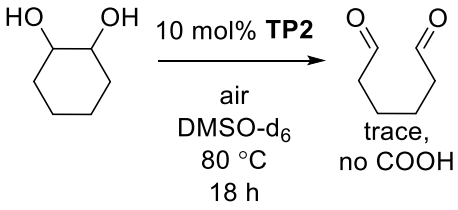


**Scheme 2.3.** Oxidation of CHD using with oxovanadium complex **TP2**.

**Table 2.2.** Catalytic C–C bond cleavage of HBO after 18 h at 80 °C (**Scheme 2.2**).

| Entry | Cat. (mol%) | Solvent | Conv. (%)[a] | PhCHO (%)[b] | PhCOOH (%)[b] | S (%)[c] |
|---|---|---|---|---|---|---|
| 1 | **TA** (1) | $CD_3CN$ | 100 | 56 | 34 | 24 |
| 2 | **TA** (0.1) | $CD_3CN$ | 45 | 12 | 1 | 85 |
| 3 | **TA** (1) | DMSO-$d_6$ | 100 | 83 | 1 | 98 |
| 4 | **TA** (0.1) | DMSO-$d_6$ | 100 | 84 | <1 | 100 |
| 5[d] | **TA** (0.1) | DMSO-$d_6$ | 70 | 52 | <1 | 100 |
| 6 | **TA** (1) | $C_6D_6$ | 84 | 78 | <1 | 97 |
| 7[e] | **TA** (0.1) | pyr-$d_5$ | 100 | 83 | 14 | 71 |
| 8 | **TP1** (1) | $CD_3CN$ | 100 | 92 | 10 | 80 |
| 9[e] | **TP1** (1) | $CD_3CN$ | 70 | 56 | 3 | 90 |
| 10 | **TP1** (0.1) | $CD_3CN$ | 16 | 5 | 0 | 100 |
| 11 | **TP1** (1) | DMSO-$d_6$ | 100 | 91 | <1 | 100 |
| 12 | **TP1** (0.1) | DMSO-$d_6$ | 83 | 62 | <1 | 100 |
| 13 | **TP1** (1) | $C_6D_6$ | 87 | 86 | <1 | 100 |
| 14 | **TP1** (1) | pyr-$d_5$ | 100 | 84 | 10 | 79 |
| 15 | **TP1** (0.1) | pyr-$d_5$ | 55 | 74 | 5 | 87 |
| 16[e] | **OQ** (0.1) | $CD_3CN$ | 60 | 53 | 2 | 93 |
| 17[e,f] | **OQ** (0.1) | $CD_3CN$ | 82 | 56 | 19 | 49 |
| 18 | **OQ** (0.1) | $CD_3CN$ | 100 | 44 | 40 | 5 |
| 19 | **TP2** (1) | DMSO-$d_6$ | 100 | 100 | 0 | 100 |
| 20 | **TP3** (10) | DMSO-$d_6$ | 100 | 100 | 0 | 100 |
| 21 | **TP3** (10) | dioxane | 10 | 10 | 0 | 100 |
| 22 | **TP3** (10) | DMF | 10 | 10 | 0 | 100 |
| 23 | **TP3** (10) | pyr | 3 | 3 | 0 | 100 |
| 24 | control | $CD_3CN$ | <1 | n/d | <1 | n/a |

[a] $^1$H NMR integration against an internal standard. [b] Yields are based on the maximum theoretical amount of moles produced with respect to the substrate. [c] Selectivity for PhCHO = (%PhCHO − %PhCOOH) / (%PhCHO + %PhCOOH) × 100. [d] After 1 hour. [e] After 7 hours. [f] With 100 equiv. $Et_3N$ per V.

The new oxovanadium complexes, **TP3-5**, were initially compared to the previously synthesized complexes, **TA**, **TP1**, and **TP2** (**Table 2.3**). Using a 10 mol% catalyst loading, **TP3** was shown to be significantly more active in DMSO vs other aprotic polar solvents (**Table 2.2**, entries 20-23); this was in line with results from both **TA** and **TP1**, implying that a highly polar

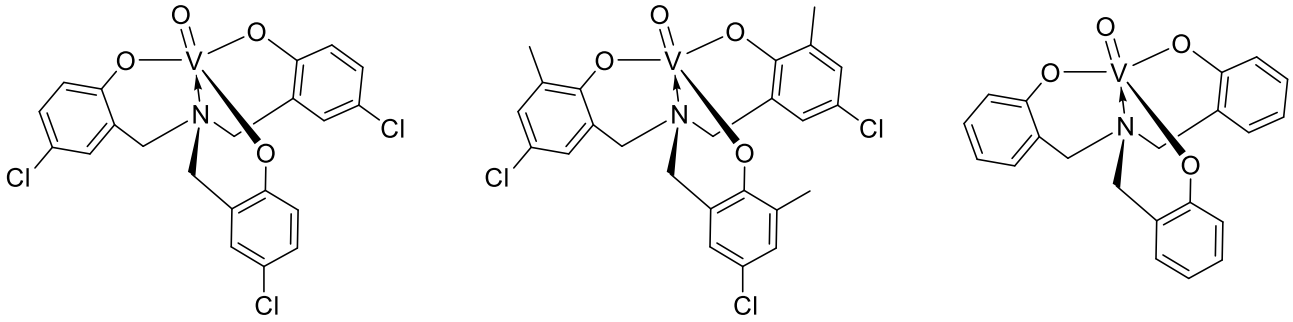


**Figure 2.2.** Triphenoxyamine oxovanadium(V) complexes with reduced electron donation from ligands and reduced steric bulk around the metal center.

environment facilitates greater reactivity. With HBO, each of the new catalysts could achieve 100% conversion with a loading of 1 mol%; selectivity for aldehydes was high, if not exclusive, in all cases. Curiously, after 10 days of reaction time at r.t., **TP4** was able to selectively convert 45% HBO to PhCHO (**Table 2.3**, entry 5), despite no previous catalyst having displayed reactivity at r.t. The C–C bond cleavage of pinacol to yield acetone was found to be of a significantly higher conversion using **TP3-5** relative to the previous catalysts at 10 mol% loading (**Table 2.3**, column 3). As the reactivity with HBO and pinacol had been examined exhaustively by the Baker group and others, no further effort was put into optimizing these reactions. Due to the apparent increased activity in these complexes, CHD was revisited as a benchmark using 10 mol% loading.

**Table 2.3.** Comparison of catalytic C–C bond cleavage using various trigonal bipyramidal oxovanadium complexes after 18 h in DMSO at 80 °C.

| Entry | Catalyst | HBO conv. 1% cat. (%)[a] | Pinacol conv. 10% cat. (%)[a] | CHD conv. 10% cat. (%)[a] |
|---|---|---|---|---|
| 1 | **TA** | 100 | 66 | 0 |
| 2 | **TP1** | 100 | 9 | 0 |
| 3 | **TP2** | 100 | 10 | trace |
| 4 | **TP3** | 100 | 90 | 8 |
| 5 | **TP4** | 100[b] | 100 | trace |
| 6 | **TP5** | 100 | 100 | 8 |

[a] $^1$H NMR integration against an internal standard. [b] After 10 days at r.t., 45% conversion to PhCHO.

Both **TP3** and **TP5** were able to achieve low, but significantly improved conversion (8%, **Table 2.3**, entries 4 and 6) relative to the strongly electron withdrawing **TP2** and the "push-pull" **TP4** (trace, **Table 2.3**, entries 3 and 5). Both complexes with reduced yields had blocking groups in the ortho position on the coordinated ligand, while the more successful complexes had hydrogen atoms in the ortho position of the coordinated ligand. This could imply a steric hindrance which slows coordination of the substrate to the metal center. However, it should also be noted that the lack of steric bulk relative to that of the *tert*-butyl group in the ortho position of the ligand present in **TP1** could contribute to the activation of CHD, as this could hinder the ability for substrates to coordinate to the metal center. The degree to which electron density and steric bulk contribute to the reactivity of these complexes is still unknown, though it does appear that both play an effect.

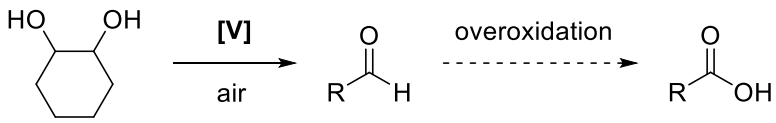


**Scheme 2.4.** General scheme for oxidation of CHD and potential overoxidation to carboxylic acid (**Table 2.4**).

Triphenoxyamine oxovanadium complexes **TP3-5** were examined more closely in an attempt to increase CHD conversion while maintaining aldehyde selectivity (**Scheme 2.4** and **Table 2.4**). First, the effects of temperature were examined; a positive correlation of increased CHD conversion with temperature was found (**Table 2.4**, entries 4-8). However, this increase in conversion coincided with a significant decrease in selectivity; at temperatures up to 60 °C (**Table 2.4**, entries 4 and 5), perfect aldehyde selectivity was maintained. At temperatures from 80-120 °C, selectivity shifted towards carboxylic acids, down to −60% selectivity at 120 °C (**Table 2.4**, entry 8). An atmosphere of $O_2$ was then examined as an alternative method to increase reactivity (**Table 2.4**, entry 9); similarly, a trend of overoxidation was noticed and selectivity dropped to 0% despite an increase in conversion from 8 to 26%. This pattern was also observed for **TP5** (**Table 2.4**, entry 14), with a decrease from −25% selectivity to −45%; however, **TP4** (**Table 2.4**, entry 12) saw a slight increase in selectivity, from 0 to 6% selectivity. This could imply that having a blocking group in the ortho position on the ligand plays a role in preventing overoxidation of substrates. However, this could also be an electronic effect as **TP3**

**Table 2.4.** Catalytic C–C bond cleavage of CHD using 10 mol% cat. after 18 h in DMSO at various temperatures (**Scheme 2.4**).

| Entry | Cat. | Temp. (°C) | Conv. (%)[a] | RCHO yield (%)[b] | RCOOH yield (%)[b] | S (%)[c] |
|---|---|---|---|---|---|---|
| 1 | **TA** | 80 | 0 | 0 | 0 | 0 |
| 2 | **TP1** | 80 | 0 | 0 | 0 | 0 |
| 3 | **TP2** | 80 | trace | trace | 0 | 100 |
| 4 | **TP3** | 25 | trace | trace | 0 | 100 |
| 5 | **TP3** | 60 | 2 | 2 | 0 | 100 |
| 6 | **TP3** | 80 | 8 | 7 | 1 | 75 |
| 7 | **TP3** | 100 | 25[f] | 12 | 13 | −4 |
| 8 | **TP3** | 120 | 40 | 8 | 32 | −60 |
| 9 | **TP3**[d] | 80 | 26 | 13 | 13 | 0 |
| 10 | **TP3**[e] | 80 | 0 | 0 | 0 | n/a |
| 11 | **TP4** | 80 | trace | trace | trace | 0 |
| 12 | **TP4**[d] | 80 | 17 | 9 | 8 | 6 |
| 13 | **TP5** | 80 | 8 | 3 | 5 | −25 |
| 14 | **TP5**[d] | 80 | 11 | 3 | 8 | −45 |
| 15 | control | 80 | 0 | 0 | 0 | n/a |

[a] $^1$H NMR integration against an internal standard. [b] Yields are based on the maximum theoretical amount of moles produced with respect to the substrate. [c] Selectivity for RCHO = (%RCHO − %RCOOH) / (%RCHO + %RCOOH) × 100. [d] Under 1 atm $O_2$. [e] Added 4 Å molecular sieves. [f] After 7 days, 100% conversion to RCOOH.

was able to achieve a high selectivity without an ortho group. Additionally, this result strongly suggests that the re-oxidation step is not limiting the functionality of these complexes, given that complete conversion is still not taking place even under forcing conditions.

Given the tendency for DMSO to take on large quantities of water, low conversion could be due to the decomposition of catalyst via water during the course of the reaction. A prior reaction using **TA** (DMSO, 80 °C, 36 hours) with 1 equiv. of water added yielded no product. Similarly, using activated 4 Å molecular sieves in the standard catalytic procedure with **TP3** yielded no reaction (**Table 2.4**, entry 10), implying that water may play an active role in the catalytic cycle.

**Table 2.5.** Catalytic oxidation of new substrates using 10 mol% catalyst after 18 h in DMSO at 80 °C.

| Entry | Substrate | Cat. | Conv. (%)[a] | RCHO yield (%)[b] | RCOOH yield (%)[b] | S (%)[c] |
|---|---|---|---|---|---|---|
| 1 | 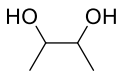 | **TP3** | 2.5 | 2 | 0 | 100 |
| 2 | | **TP4** | trace | trace | 0 | 100 |
| 3 | 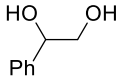 | **TP3** | 2 | 2 | 0 | 100 |
| 4 | | **TP4** | 8 | 1 | 0 | 100 |
| 5 | 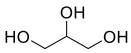 | **TP3** | 3 | 2 | 1 | 33 |
| 6 | | **TP4** | trace | trace | 0 | 100 |
| 7 | 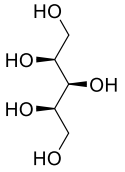 | **TP4** | 31 | 1[d] | 7[e] | −75 |
| 8 | 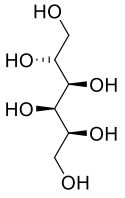 | **TP4** | 26 | 2[d] | 3[e] | −20 |

[a] $^1$H NMR integration against an internal standard; [b] Yields are based on the maximum theoretical amount of moles produced with respect to the substrate; [c] Selectivity for RCHO = (%RCHO − %RCOOH) / (%RCHO + %RCOOH) × 100; [d] Mixture of 4 products; [e] 1 product.

Considering the successful C–C bond cleavage of CHD, several previously unreactive substrates were examined using **TP3** and **TP4** (**Table 2.5**). Most gratifyingly, 1-phenyl-1,2-ethanediol was able to be converted into formaldehyde and benzaldehyde using both complexes, both with 100% selectivity and up to 8% conversion (**Table 2.5**, entries 3 and 4). 2,3-Butanediol, a far less sterically strained analogue of pinacol, was also selectively cleaved to acetaldehyde using either catalyst (**Table 2.5**, entries 1 and 2); however, conversion was limited to 2%. Glycerol was cleaved into a 67:33 mixture of aldehydes:carboxylic acids using **TP3** (**Table 2.5**, entry 5). **TP4**, however, was able to selectively yield aldehydes, albeit in trace quantities (**Table 2.5**, entry 6).

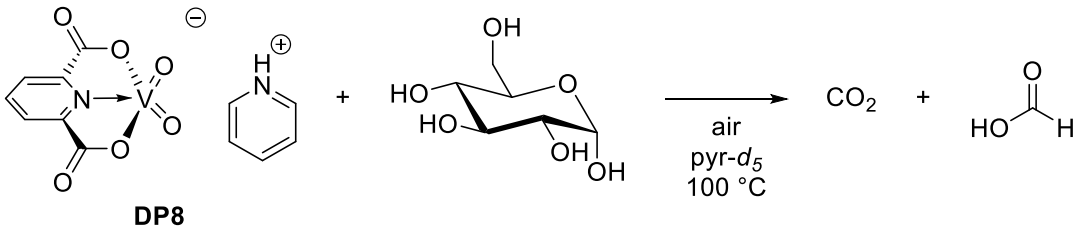


**Scheme 2.5.** Previously unpublished work by Hanson attempting C–C bond cleavage of glucose.[92]

In concert with the previously demonstrated ability to selectively oxidize to aldehydes at r.t. (**Table 2.3**, entry 5[d]) and the positive selectivity displayed under 1 atm of $O_2$ (**Table 2.4**, entry 12), **TP4** was selected to cleave more complex polyalcohols, as a model for cellulosic dissassembly. Xylitol was subjected to the standard reaction conditions and a 31 % conversion was achieved, albeit with poor selectivity (−75%, **Table 2.5**, entry 7). Encouragingly, a mixture of aldehydes was observed, indicating that the catalyst was cleaving all C–C bonds present in the sugar, not just the terminal bonds as the complex Hanson had previously observed when trying to cleave glucose with **DP8** (**Scheme 2.5**).[92] Similarly, xylitol gave 26 % conversion to a mixture of carboxylic acids and multiple aldehydes (−20% selectivity, **Table 2.5**, entry 8).

While the new generation of **TP** complexes gave access to new and exciting substrates, achieving high conversion and yield simultaneously was unable to be achieved. In order to understand how best to proceed with further ligand and catalyst design, the reactivity and oxidation mechanism of these complexes was investigated. **TA** and **TP1** were chosen as models to compare the trialkoxy- and triphenoxyamine catalysts.[84,94a]

*2.4 Mechanistic Investigations*

***2.4.1 Stoichiometric Reactions***

Previously reported oxovanadium catalysts **DP6** and **OQ** work synergistically with base to cleave the C–H bond of 1,2-diols, followed by cleavage of the C–C bond of the reduced hydroxyketone or dione intermediates. In the case of HBO, oxidation of these intermediates produces a mixture of aldehyde and carboxylic acid (**Scheme 2.6**). In contrast, the $^1$H NMR spectrum of the HBO oxidation reaction using complexes **TA** or **TP1** revealed no formation of mono- or diketone intermediates, even at short reaction times (**Scheme 3**), suggesting a direct C–

C bond cleavage. Although higher catalytic activity could be achieved with **OQ** (vs. **TA** or **TP1**) even in the absence of base (**Table 2.2**, entries 2,10,16-18), much lower selectivity of aldehydes (5% with **DP6** *vs.* 98% with **TA**) was observed.

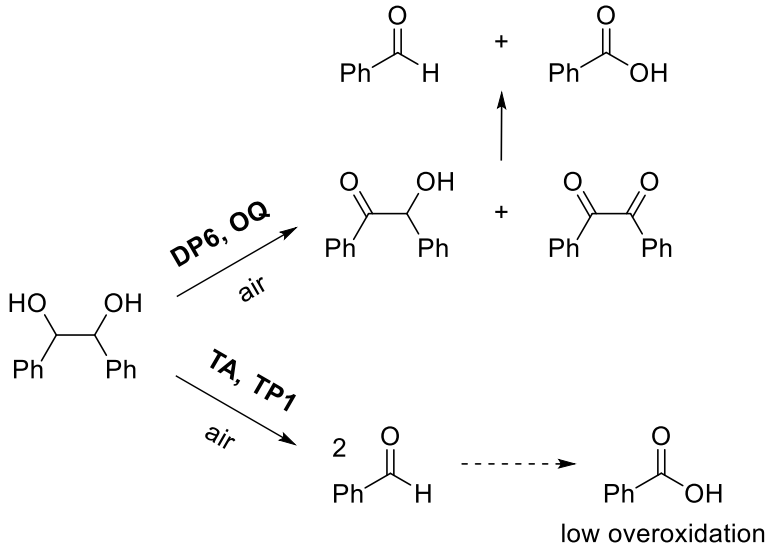


**Scheme 2.6.** Selectivity difference displayed by catalysts **DP6** and **OQ** vs. **TA** and **TP1**, respectively.

Further insight was gained from the stoichiometric reaction of complex **TP1** with HBO in the absence of air. The $^{1}$H NMR spectrum of the reaction between **TP1** and 3 equiv. of HBO-(CD)$_2$ in toluene-$d_8$ (**Scheme 2.7**) gave, after heating at 80 °C for 15 h, 2 equiv. of benzaldehyde-(CDO) along with characteristic broad resonances at δ 11.53 ($\Delta\nu_{1/2}$ = 85 Hz), 1.19 ($\Delta\nu_{1/2}$ = 36 Hz) and −1.18 (br, $\Delta\nu_{1/2}$ = 138 Hz) due to a paramagnetic V product. No evidence of a tetravalent V product was obtained by EPR, suggesting the reaction depicted in **Scheme 2.7**. In contrast, the stoichiometric reaction ($C_6D_6$, 80 ºC, 18 h) under nitrogen between complex **TA** and HBO gave 31% yield of benzaldehyde and an insoluble dark precipitate. The less bulky triethanolamine ligand in **TA** likely facilitates the intermolecular co-oligomerization of the resulting $V^{III}$ complex with **TA**.

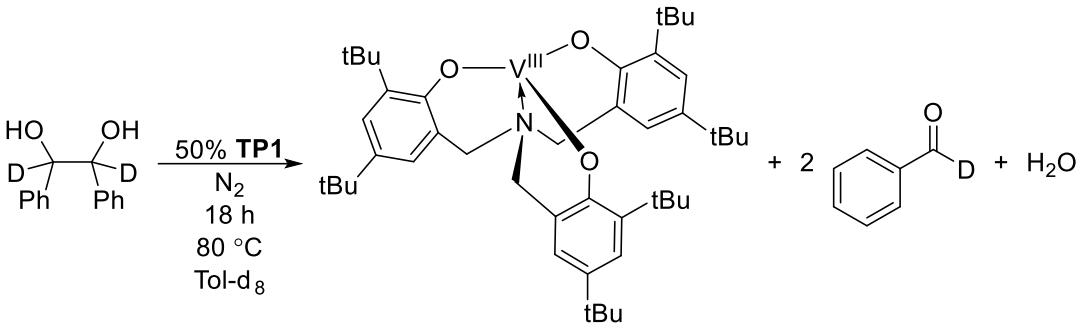


**Scheme 2.7.** Direct two-electron oxidative C–C bond cleavage of 1,2-(C–D)-HBO using catalyst **TP1**.

### *2.4.2 Kinetic Measurements*

A pseudo-first-order rate law was obtained for the disappearance of **TP1** and an excess of HBO under nitrogen (**Figure 2.3**). An Eyring plot in toluene-$d_8$ using kinetic data over a small temperature range (333 K - 348 K) provided the activation parameters; $\Delta H^{\neq}$ = 110 ± 5 kJ mol$^{-1}$ and $\Delta S^{\neq}$ = −5.24 ± 13 J K$^{-1}$ mol$^{-1}$ (**Table 2.6**, **Figure 2.4**), consistent with an associative transition state.

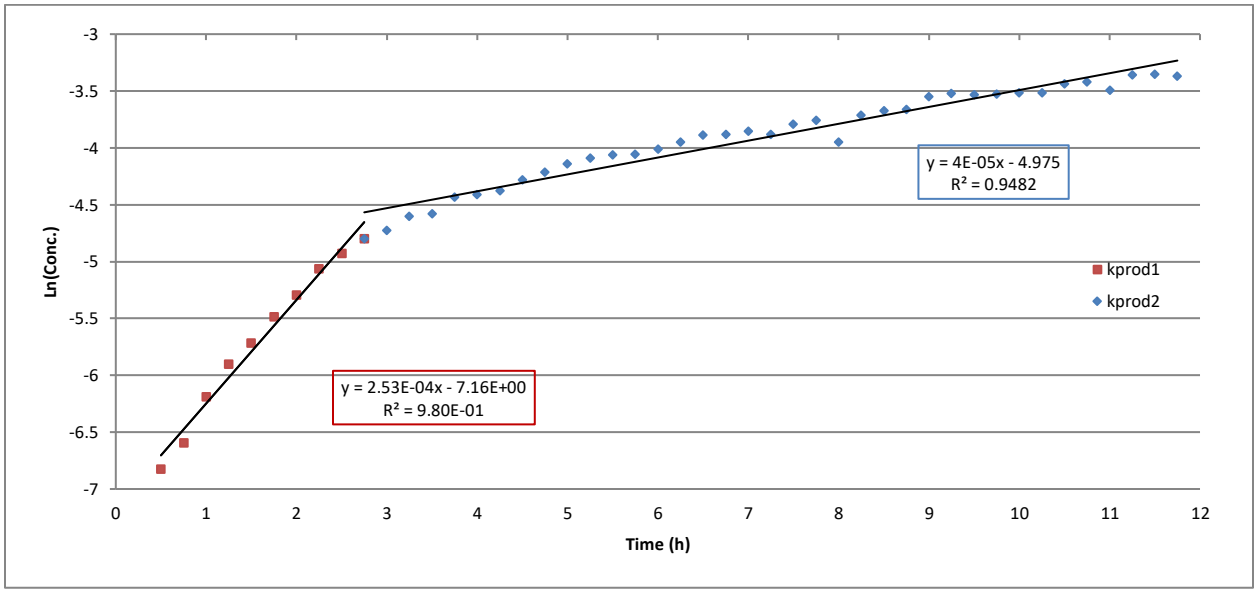


**Figure 2.3.** Kinetic data for the pseudo-first-order rate law approximation for the reaction of **TP1** with HBO at 353 K in toluene-$d_8$.

**Table 2.6.** Values of $k_{obs}$ for the reaction of **TP1** with HBO ($5.66 \times 10^{-2}$ M) in toluene-$d_8$.

| Temperature (K) | $10^{-5}$ $k_{obs}$ ($s^{-1}$)[a] |
|---|---|
| 333 | 2.2 ± 0.4 |
| 338 | 3.5 ± 0.9 |
| 343 | 6.9 ± 0.4 |
| 348 | 14 ± 4 |

[a]The uncertainty is the standard deviation of the average of two independent experiments.

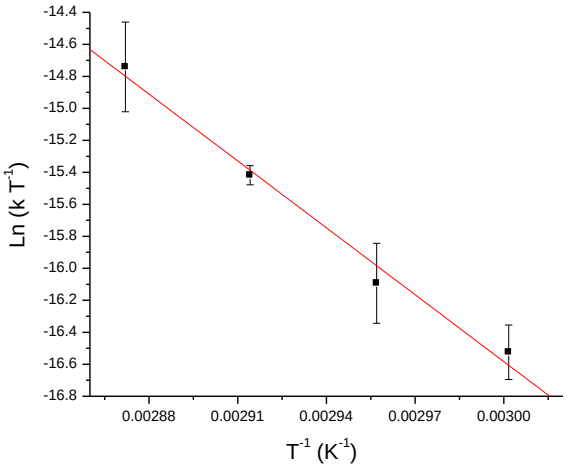


**Figure 2.4.** Eyring plot for the reaction of **TP1** with HBO ($5.66 \times 10^{-2}$ M) in toluene-$d_8$ at four temperatures ranging from 333 - 348 K.

The kinetic isotope effect (KIE) determined at 348 K in toluene-$d_8$ was 0.9 ± 0.1 for 1,2-$^2$HO and 1.0 ± 0.3 for 1,2-$^2$HC, suggesting that the C–C bond cleavage step may be rate-determining.

The reactions were approximated as first order in each substrate and second order overall. During the reaction there are two distinct catalytic regimes, the second of which has significantly slower rate. However, this shift in rate was much less dramatic in experiments performed in air; additionally, it was observed that less product appeared than expected during reactions under nitrogen. Catalyst decomposition was ruled out as a potential cause of the reduced rate over time

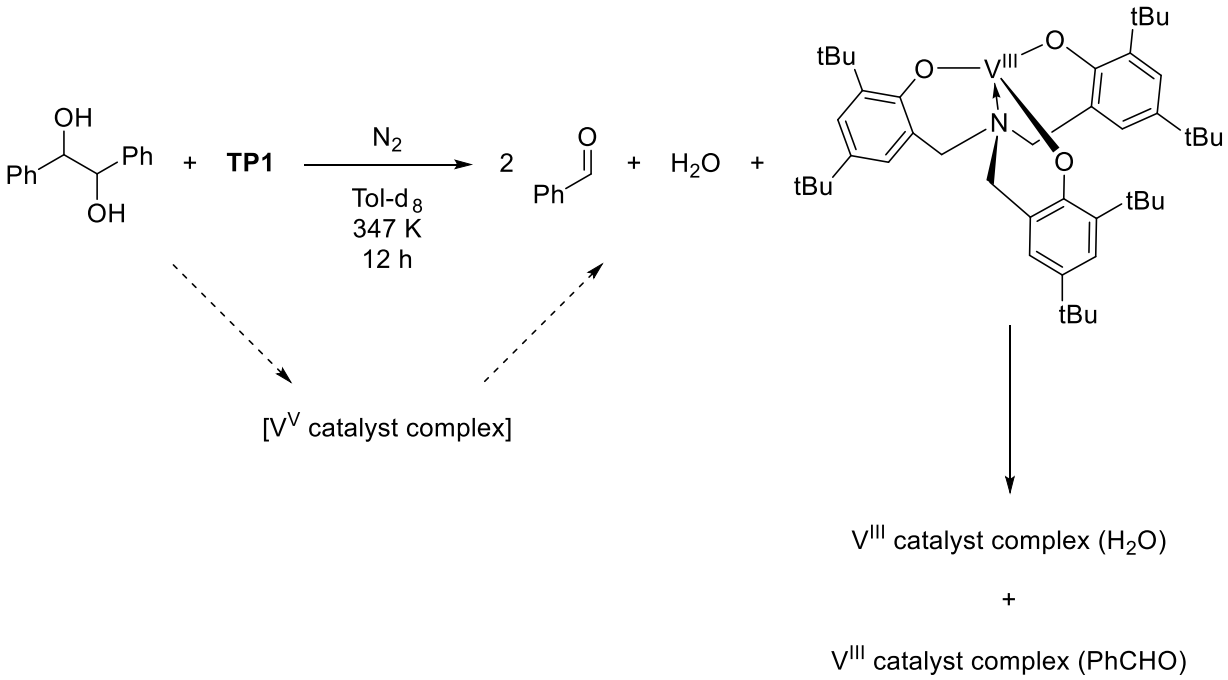


**Scheme 2.8.** Hypothesis for complexation of water and benzaldehyde during catalytic reaction between **TP1** and HBO under $N_2$.

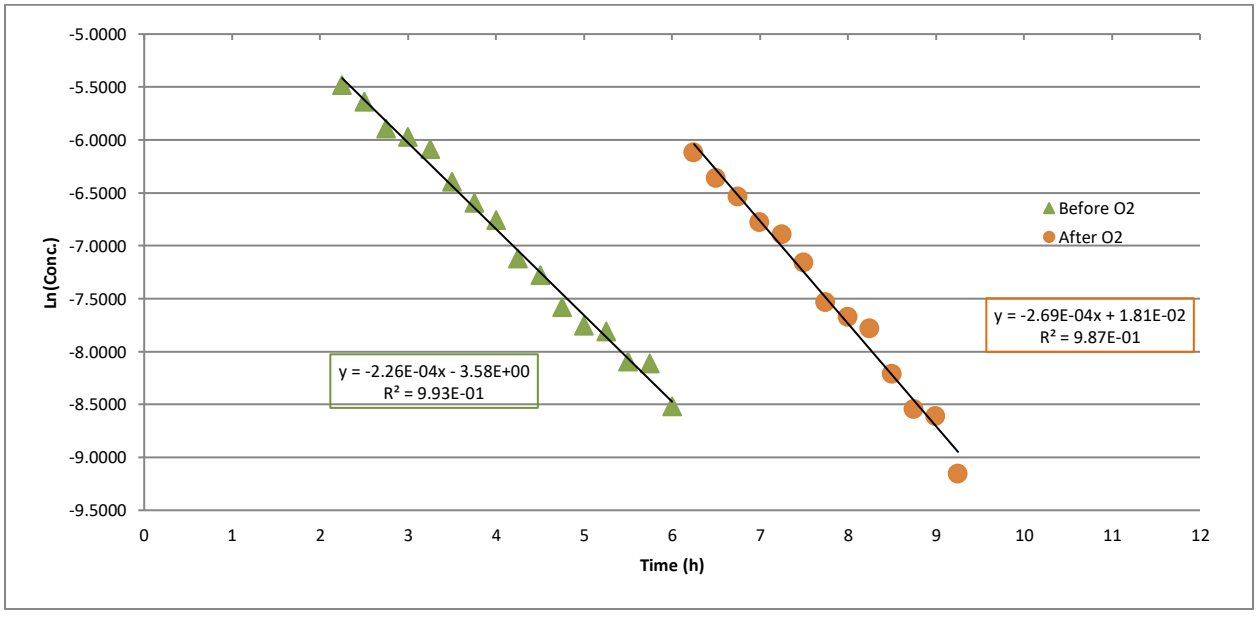


**Figure 2.5.** Introduction of air to anaerobic reaction with **TP1** before returning to anaerobic conditions.

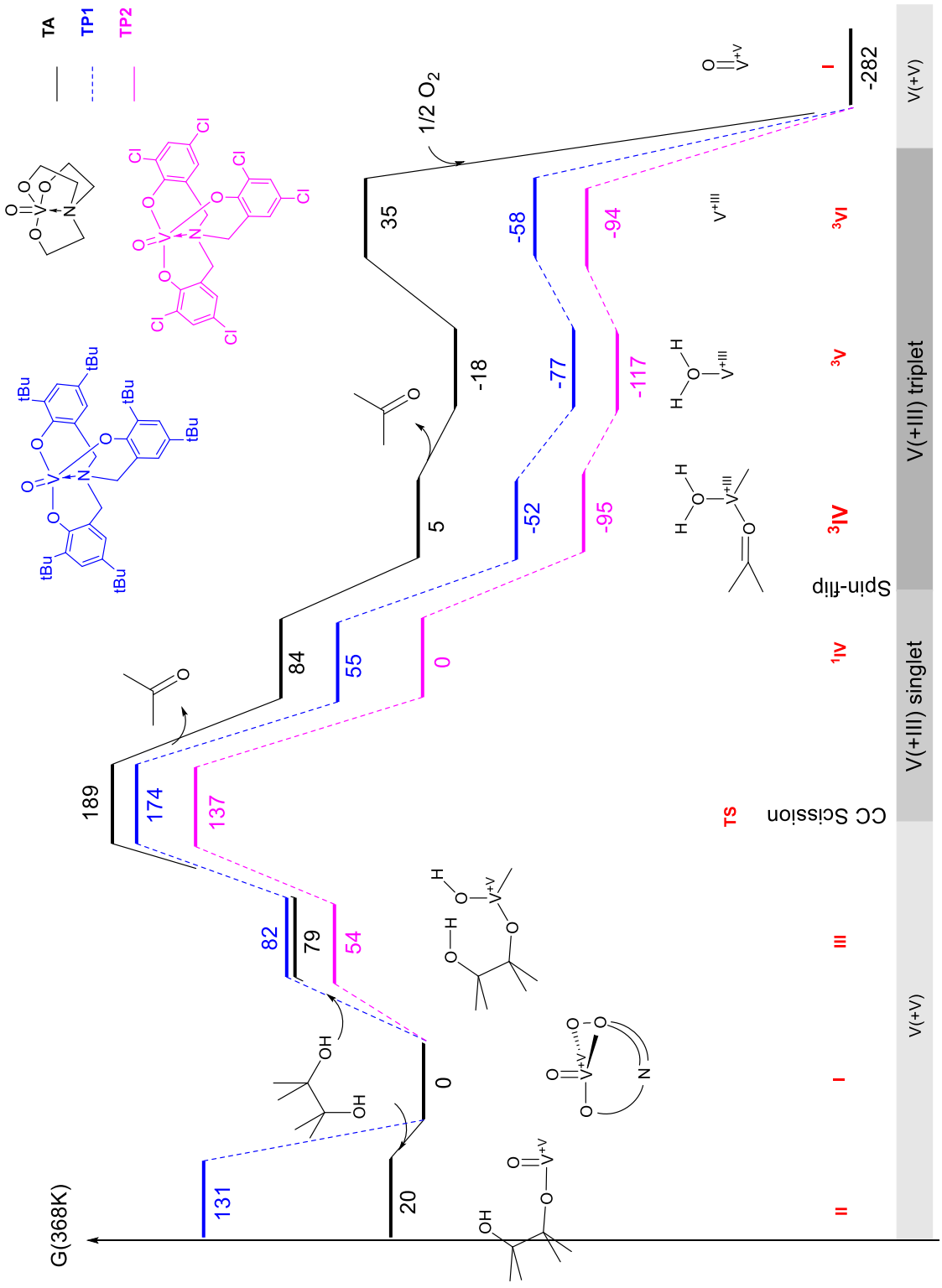


**Figure 2.6.** Free energy profile in kJ $mol^{-1}$, at 368 K and 1 bar, for the catalytic oxidation of pinacol with catalyst **TA** (plain black curve), **TP1** (dashed blue curve), and **TP2** (dashed pink curve).

as brief introduction of air showed that oxidation rates before and after the introduction of air were nearly identical (**Figure 2.6**). It was hypothesized that the $V^{III}$ complex could be strongly binding the aldehyde product (**Scheme 2.8**); calculations by Fleurat-Lessard, Michel, and coworkers suggested that a $V^{III}$-PhCHO complex is significantly higher energy than the $V^{III}$-$H_2O$ complex.

### *2.4.3 Computational Chemistry*

To provide a better understanding of the underlying processes governing the diol C–C bond cleavage, DFT calculations were employed to determine the reaction network for pinacol oxidation using catalysts **TA**, **TP1** and **TP2** in toluene.[102] In these calculations, the *tert*-butyl groups of **TP1** were replaced by methyl groups. The corresponding Gibbs energy profiles are shown in **Figure 2.6**. The overall reaction (**Scheme 2.9**) is exothermic (−247 kJ $mol^{-1}$). The first step is coordination of pinacol to the catalyst denoted by **I**; this produces either reaction intermediate **II,** in which a proton is transferred from the pinacol molecule to one arm of the catalyst, or **III,** in which the proton is transferred to the oxo moiety to give a hydroxy-vanadium moiety. This process is endothermic in both cases due to the entropic penalty and can yield a range of isomers, especially with the flexible catalyst **TA**. Focusing on the latter active route, one proton of the pinacol is transferred to the oxygen of the V=O moiety and the resulting alkoxy group coordinates to vanadium in the equatorial plane. The remaining alcohol group is H-bonded to the newly formed hydroxyl, stabilizing this active species; note that vanadium is still in the +5 oxidation state. Then, the C–C bond breaks, with a barrier of roughly 100-110 kJ $mol^{-1}$ and a C–C distance of 2.80 Å with **TP1** and 2.79 Å with **TA** in the transition state (**Figure 2.7**). This process is accompanied by proton transfer from the pinacol hydroxyl to the oxygen of V-OH, yielding one coordinated water, a coordinated acetone, and a free acetone in compound $^{1}$**III** (singlet state trivalent vanadium). The rate determining process is the C–C bond cleavage from the pinacol-catalyst complex **III**. As formation of **III** is faster than C–C bond cleavage, it can be assumed that **III** is in equilibrium with **I** and pinacol, so that the kinetic rate law is expected to be first order in pinacol and catalyst concentration in agreement with experiment (**Figure 2.4**).[23,103] The activation barrier of this rate determining step can be decomposed into its enthalpic and

entropic contributions. For **TP1**, the values for $\Delta H^{\ddagger}$= 98.7 kJ $mol^{-1}$ and $\Delta S^{\ddagger}$= −18.7 J $K^{-1}$ $mol^{-1}$ corroborate the experimental values obtained.


**Scheme 2.9.** Overall pinacol oxidative C–C bond cleavage reaction.

Along this reactive path, the two catalysts behave in a similar way. One difference lies in the slightly smaller activation energy endergonic for catalyst **TP1** than catalyst **TA** by around 15 kJ $mol^{-1}$. This partly explains the reduced activity of catalyst **TA** compared with **TP1**. Another source of deactivation is the multiple conformers of intermediate **II**; upon coordination, the pinacol may transfer one proton to the V(+V)=O as already described, but also to an oxygen atom of the ligand, yielding a protonated arm.

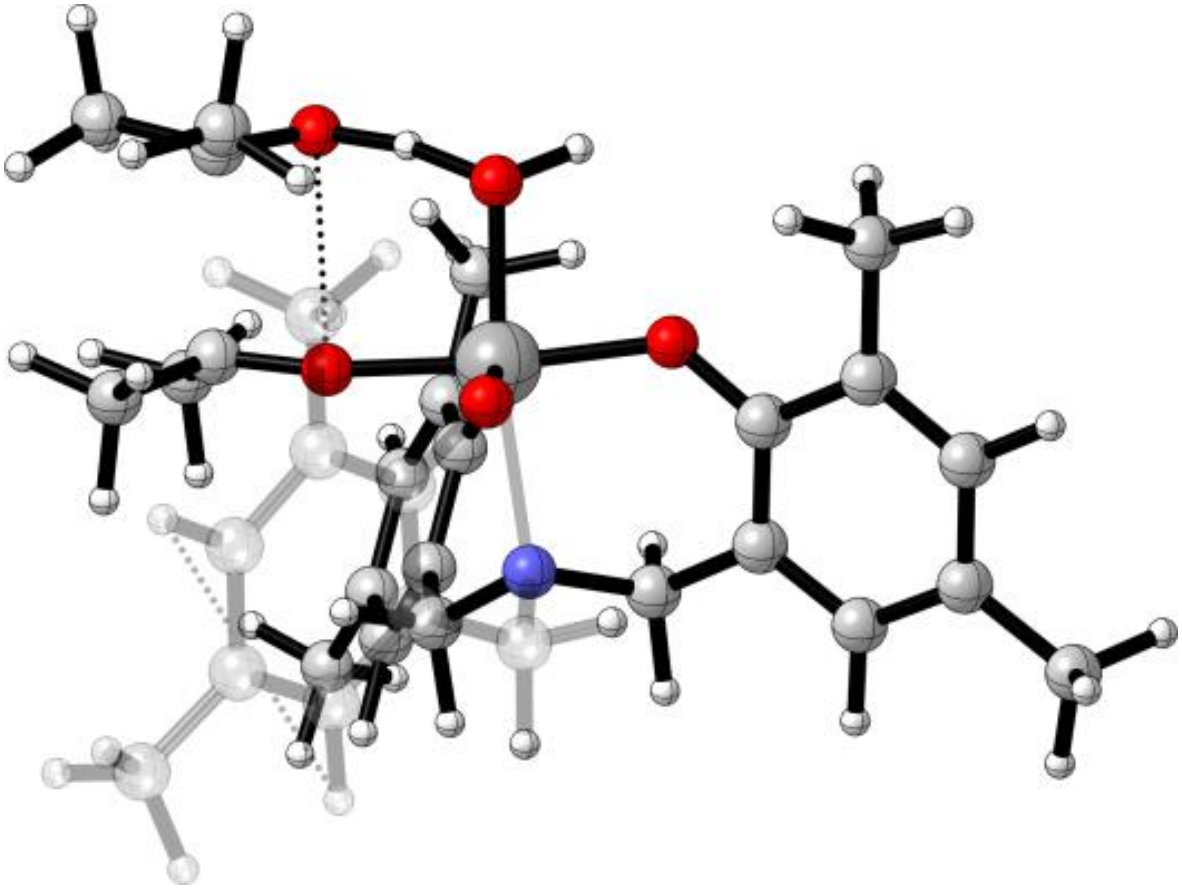

**Figure 2.7.** Transition state for the C−C bond breaking of pinacol with catalyst **TP1**.

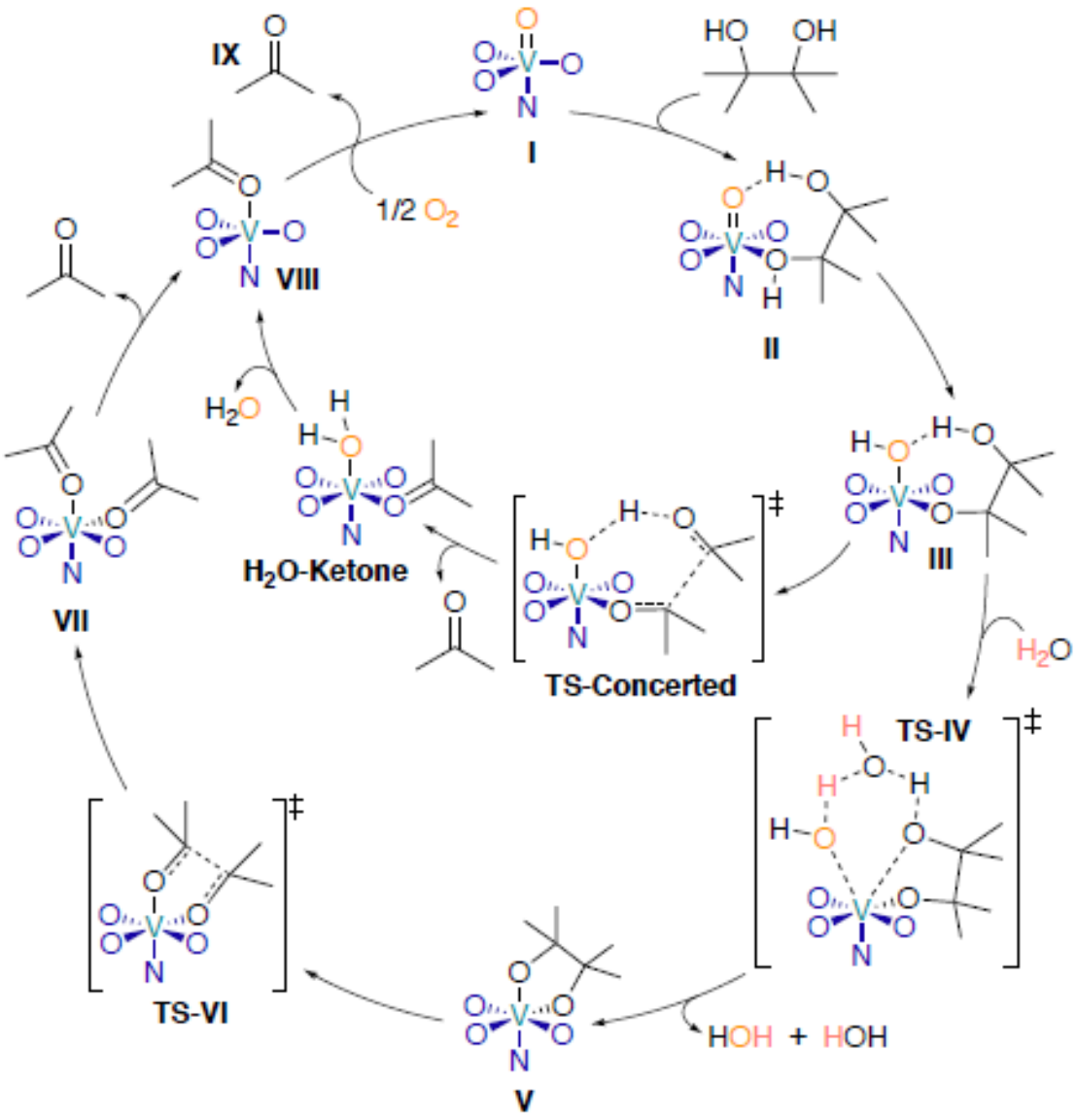


**Figure 2.8.** Proposed mechanisms for the oxidative C–C cleavage of pinacol. The outer mechanism is proposed by Bo, Licini, and coworkers while the inner mechanism is proposed by Fluerat-Lessard, Michel, and coworkers.[97]

This process is less favourable for **TP1** than for **TA** for two reasons. First, the rigid arms of **TP1** cannot easily move away from the vanadium center and rotation around the N−C−C bond is hampered compared to the flexible arms of **TA**; second, the phenoxide groups of **TP1** are much less basic than the alkoxides donors of catalyst **TA**. As a consequence, the alternative arm protonation is rather easy (+20 kJ $mol^{-1}$) for catalyst **TA** and will yield several conformers that are highly distorted. This is a source of deactivation of the catalyst since those stable conformers

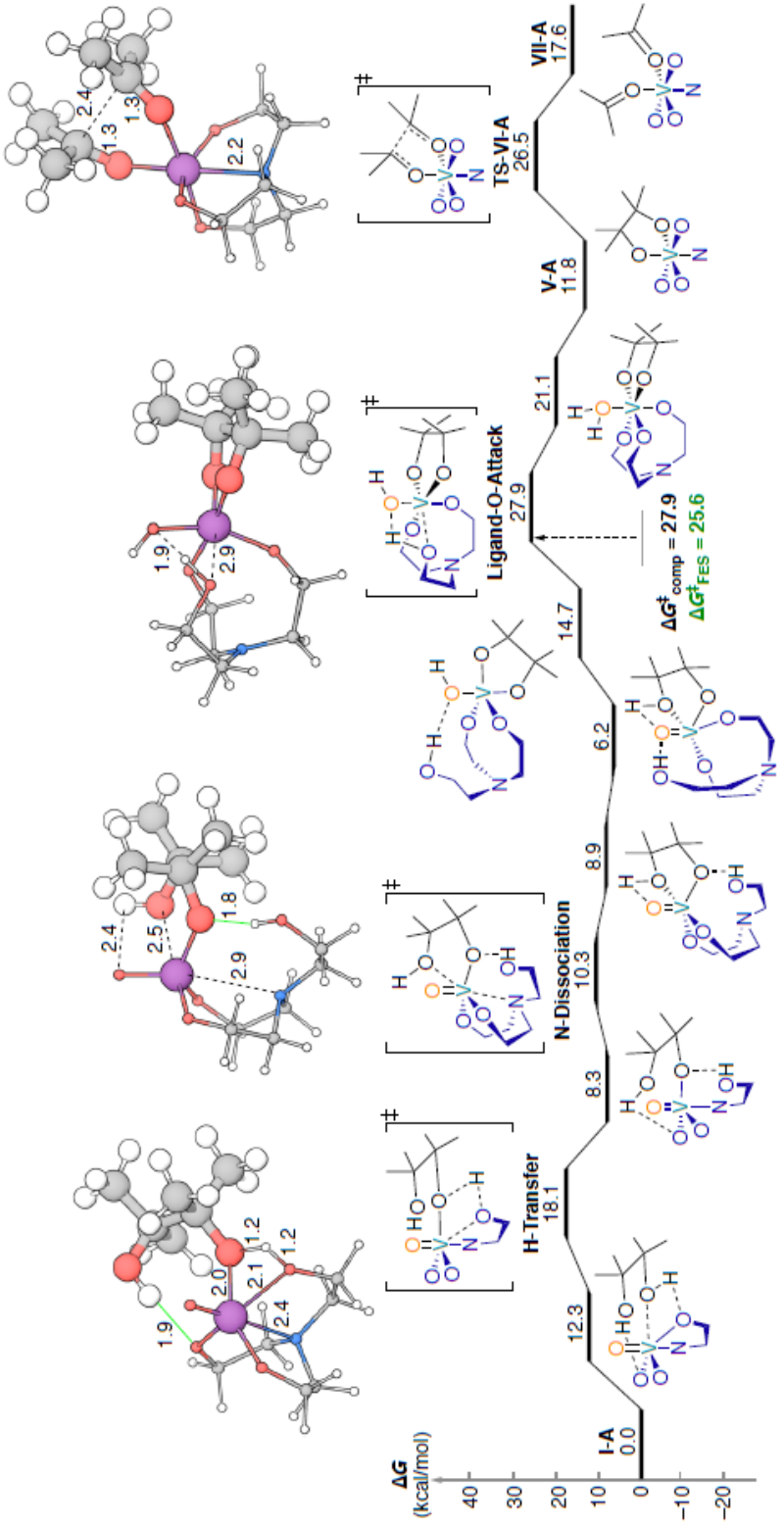


**Figure 2.9.** Alternative proposed mechanism for C–C cleavage of pinacol by **TA** by Fleurat-Lessard, Michel, and coworkers.

are not active for the C–C bond cleavage and would likely facilitate the oligomerization observed as an insoluble precipitate.

Bo, Licini, and coworkers suggested a mechanism which includes a proton transfer in the rate-determining step.[97] However, experimental results as well as theoretical calculations performed by collaborators at ENS de Lyon suggest that there is no KIE, implying that alternate mechanisms need to be considered (**Figure 2.8**). However, both Bo and Licini's proposed **TS-IV** and Fleurat-Lessard's proposed **TS-Concerted** involve the transfer of a proton. An alternative mechanism with lower energy barriers was proposed for **TA** (**Figure 2.9**). This mechanism involves numerous steps where the ligand hemilability can facilitate the removal of protons from pinacol to form water (**Figure 2.9**, steps **I-A** to **N-Dissociation**), with the rate-determining step being **Ligand-O-Attack**; crucially, this step does not involve the transfer of a proton and has a lower energy barrier than any previously proposed mechanism (25.6 kcal $mol^{-1}$). Additionally, this complex has been shown previously to react with alcohols via alkoxides arm protonation, even in some cases completely dissociating from the vanadium center.[93a] However, this still leaves the mechanism for **TP** complexes unsolved, as no currently proposed mechanism explains the lack of KIE observed experimentally.

*2.5 Conclusions*

Electron-rich trialkoxy-and triphenoxyamine oxovanadium(V) complexes, **TA** and **TP1**, shown previously to serve as functional mimics for vanadium hydroperoxidase enzymes, are demonstrated to be efficient catalysts for the selective aerobic oxidation of pinacol and HBO.[93] However, access to less activated substrates, such as 1,2-cyclohexanediol and sorbitol, requires the use of triphenoxyamine oxovanadium(V) complexes which have reduced electron density at the metal center and/or reduced steric bulk around the coordination sites. Highly polar, aprotic solvents such as DMSO are required to facilitate optimal reactivity and selectivity towards aldehydes in these reactions. Despite access to these new substrates, simultaneous high yield and conversions have yet to be achieved using these new complexes. Forcing conditions, such as increased heat and higher concentrations of $O_2$ can lead to higher conversions, but almost always cause overoxidation to carboxylic acids.

Experimentally, it has been determined that there is no KIE for either the **TA** or **TP** complexes; DFT calculations have been able to provide a reasonable mechanism for **TA**, but not

for **TP**. The slow appearance of aldehyde product when reacting **TP1** with hydrobenzoin anaerobically still remains unsolved, though a $V^{III}$ Lewis acid complex with the benzaldehyde product may explain the delay. Further study of this class of complex may reveal more effective methods to improve conversion of cellulose and hemicellulose models while maintaining aldehyde selectivity.

*2.6 References*


[77] Deuss, P. J.; Barta, K.; de Vries, J. G. *Catal. Sci. Technol.* **2014**, *4*, 1174-1196.
[78] Kusserow, B.; Schimpf, S.; Claus, P. *Adv. Synth. Catal.* **2003**, *345*, 289-299
[79] Román-Leshkov, Y.; Barrett, C. J.; Liu, Z. Y.; Dumesic, J. A. *Nature* **2007**, *447*, 982-985
[80] Castoldi, M. C. M.; Camara, L. D. T.; Aranda, D. A. G. *React. Kinet. Catal. Lett.* **2009**, *98*, 83-89.
[81] Lodish, H.; Berk, A.; Zipursky, S. L.; Matsudaira, P.; Baltimore, D.; Darnell, J. *Molecular Cell Biology*, 4th Ed., W. H. Freeman: New York, 2000.
[82] Huber, G. W.; Chheda, J. N.; Barrett, C. J.; Dumesic, J. A. *Science* **2005**, *308*, 1446-1450.
[83] Kamm, B.; Gruber, P. R.; Kamm, M. Eds. *Biorefineries - Industrial Processes and Products*, 2006, Vol. 2, p. 136.
[84] Sutton, A. D.; Waldie, F. D.; Wu, R.; Schlaf, M.; Silks, L. A.; Gordon, J. C. *Nature Chem.* **2013**, *5*, 428-432.
[85] a) Fieser, L. F.; Fieser, M. In *Reagents for Organic Synthesis*; Wiley-VCH: New York, 1967; p 815; (b) Shing, T. K. M. In *Comprehensive Organic Synthesis*; Trost, B. M., Eds.; Pergamon Press: Oxford, 1991; p 703; c) Knochel, P.; Molander, G. A. In *Comprehensive Organic Synthesis*; 2nd Ed.; Wong, A. W. H.; Shing, T. K. M., Eds.; Elsevier B.V: Amsterdam, 2014; p. 801.
[86] a) Okamoto, T.; Sasaki, K.; Oka, S. *J. Am. Chem. Soc.* **1988**, *110*, 1187-1196; b) Ishii, Y.; Yamawaki, K.; Ura, T.; Yamada, H.; Yoshida, T.; Ogawa, M. *J. Org. Chem.* **1988**, *53*, 3581-3593; c) Takezawa, E.; Sakaguchi, S.; Ishii, Y. *Org. Lett.* **1999**, *1*, 713-715; d) Du, G.; Woo, L. K. *Organometallics* **2003**, *22*, 450-455; e) Amadio, E.; Di Lorenzo, R.; Zonta, C.; Licini, G. *Coord. Chem. Rev.* **2015**, 301-302.
[87] More complex vanadium phosphomolybdate catalysts are effective aerobic diol oxidation catalysts: a) Brégault, J. M.; b) Neumann, R. *J. Am. Chem. Soc.* **2008**, *130*, 14474–14476.
[88] Escande, V.; Lam, C. H.; Coish, P.; Anastas, P. T. *Angew. Chem. Int. Ed.* **2017**, *56*, 9561-9565.
[89] Zhou, Z.-Z.; Liu, M.; Li, C.-J. *Angew. Chem. Int. Ed.* **2018**, *57*, 2616-2620.
[90] a) Sedai, B.; Díaz-Urrutia, C.; Baker, R. T.; Wu, R.; Silks, L. A. P.; Hanson, S. K. *ACS Catal.* **2011**, *1*, 794-804; b) Sedai, B.; Díaz-Urrutia, C.; Baker, R. T.; Wu, R.; Silks, L. A. P.; Hanson, S. K. *ACS Catal.* **2013**, *3*, 3111-3122; c) Díaz-Urrutia, C.; Chen, W. C.; Crites, C. O.; Daccache, J.; Korobkov, I.; Baker, R. T. *RSC Adv.* **2015**, *5*, 70502–70511; d) Díaz-Urrutia, C.; Sedai, B.; Leckett, K.; Baker, R. T.; Hanson, S. K. *ACS Sust. Chem. Eng.* **2016**, *4*, 6244-6251.
[91] a) Hanson, S. K.; Wu, R.; Silks, L. A. P. *Org. Lett.* **2011**, *13*, 1908-1911; b) Hanson, S. K.; Wu, R.; Silks, L. A. P. *Angew. Chem. Int. Ed.* **2012**, *51*, 3410-3413; c) Wigington, B. N.; Drummond, M. L.; Cundari, T. R.; Thorn, D. L.; Hanson, S. K.; Scott, S. L. *Chem. Eur. J.* **2012**, *18*, 14981-14988.
[92] S. K. Hanson, unpublished results.
[93] a) Crans, D. C.; Chen, H.; Anderson, O. P.; Miller, M. M. *J. Am. Chem. Soc.* **1993**, *115*, 6769-6779; b) Reis, P. M.; Armando, J.; Silva, L.; da Silva, J. J. R. F.; Pombeiro, A. J. L. *Chem. Comm.* **2000**, 1845-1846; c) Reis, P. M.; Silva, J. A. L.; Palavra, A. F.; Fraústo da Silva, J. J. R.; Kitamura, T.; Fujiwara, Y.; Pombeiro, A. J. L. *Angew. Chem. Int. Ed.* **2003**, *42*, 821-823; d) Reis, P. M.; Silva, J. A. L. da Silva, J. J. R. F.; Pombeiro, A. J. L.; *J. Mol. Catal. A. Chem.* **2004**, *224*, 189-195; e) Kirillova, M. V.; Kuznetsov, M. L.; Reis, P. M.; da Silva, J. A. L.; da Silva, J. J. R. F.; Pombeiro, A. J. L. *J. Am. Chem. Soc.* **2007**, *129*, 10531-10545; f) Kirillova, M. V.;

Kuznetsov, M. L.; da Silva, J. A. L.; Silva, M. F. C. G.; da Silva, J. J. R. F; Pombeiro, A. J. L. *Chem. Eur. J.* **2008**, *14*, 1828-1842.
[94] a) Groysman, S.; Goldberg, I.; Goldschmidt, Z.; Kol, M. *Inorg. Chem.* **2005**, *44*, 5073-5080; b) Mba, M.; Pontini, M.; Lovat, S.; Zonta, C.; Bernardinelli, G.; Kündig, P. E.; Licini, G. *Inorg. Chem.* **2008**, *47*, 8616-8618.
[95] a) Colpas, G. J.; Hamstra, B. J.; Kampf, J. W.; Pecoraro, V. L. *J. Am. Chem. Soc.* **1994**, *116*, 3627-3628; b) Messerschmidt, A.; Wever, R. *Proc. Natl. Acad. Sci. U*.S.A. **1996**, *93*, 392-396; c) Andersson, M.; Willetts, A.; Allenmark, S. *J. Org. Chem.* **1997**, *62*, 8455-8458; d) Pessoa, J. C; Garribba, E.; Santos, M. F. A.; Santos-Silva, T. *Coord. Chem. Rev.* **2015**, *301*, 49-86; e) Gupta, R.; Hou, G.; Renirie, R.; Wever, R.; Polenova, T. *J. Am. Chem. Soc.* **2015**, *137*, 5618-5628.
[96] Maeda, Y.; Kakiuchi, N.; Matsumura, S.; Nishimura, T.; Kawamura, T.; Uemura, S. *J. Org. Chem.* **2002**, *67*, 6718-6724. b) Weng, S. S.; Shen, M. W.; Kao, J. Q.; Munot, Y. S.; Chen, C. T. *Proc. Natl. Acad. Sci. U.S.A.* **2006**, *103*, 3522-3527; c) Son, S.; Toste, F. D. *Angew. Chem. Int. Ed.* **2010**, *49*, 3791-3794.
[97] Amadio,, E.; González-Fabra, J.; Carraro, D.; Denis,W.; Gjoka, B.; Zonta, C.; Bartik, K.; Cavani, F.; Solmi, S.; Bo, C.; Licini, G. *Adv. Synth. Catal.* **2018**, ***360*** , 3286-3296.
[98] Frye, C. L.; Vincent, G. A.; Hauschildt, G. L.; *J. Am. Chem. Soc.* **1966,** *88* 2727-2730
[99] Moriuchi, T.; Ikeuchi, K.; Hirao, T. *Dalton Trans.* **2013**,*42*, 11824-11830
[100] Wiberg, K. B. *J. Am. Chem. Soc.* **1954**, *76*, 5371-5375.
[101] Groysman, S.; Goldberg, I.; Kol, M.; Genizi, E.; Goldschmidt, Z. *Adv. Synth. Cat.* **2005**, *347*, 409-415.
[102] Evans, D. F. *J. Chem. Soc.* **1959**, 2003-2005.
[103] Cotton, A. F.; Wilkinson, G. *Advanced Inorganic Chemistry*; Wiley and Sons: New York, 1972; pp 538.

# Chapter 3: Mechanistic Studies of Oxovanadium Complex-Catalyzed C-C Bond Cleavage of Simple Lignin Models

*3.1 Introduction*

The efficient conversion of lignin into valuable chemicals has been a longstanding challenge within the scientific community. Several paths exist to convert isolated lignin into small molecules; examples include: oxidative depolymerization,[104] reductive depolymerization,[105] acid-catalyzed depolymerization,[106] depolymerization via oxidized lignin,[107] two-step processes,[108] and biochemical transformation.[109] Many of these require the use of expensive reagents (ILs,[104c-d] Pd,[105b] Au,[105d] Ru,[105h-i] Rh,[106c] Ir,[107c]), stoichiometric reagents,[104a-b,105d,105f,107b,108] high temperatures (100-300 °C),[104a,104d,105a-f,105h-i,106,107a,108] harsh/dangerous conditions ($O_2$ or $H_2$ atmosphere),[104c-d,105a-b,105d-f,105h-i,107a-b] or excessively long reaction times (up to 80 h).[109] Moreover, even successful methods for lignin depolymerization generally have low yields and require further time to separate the component mixtures.

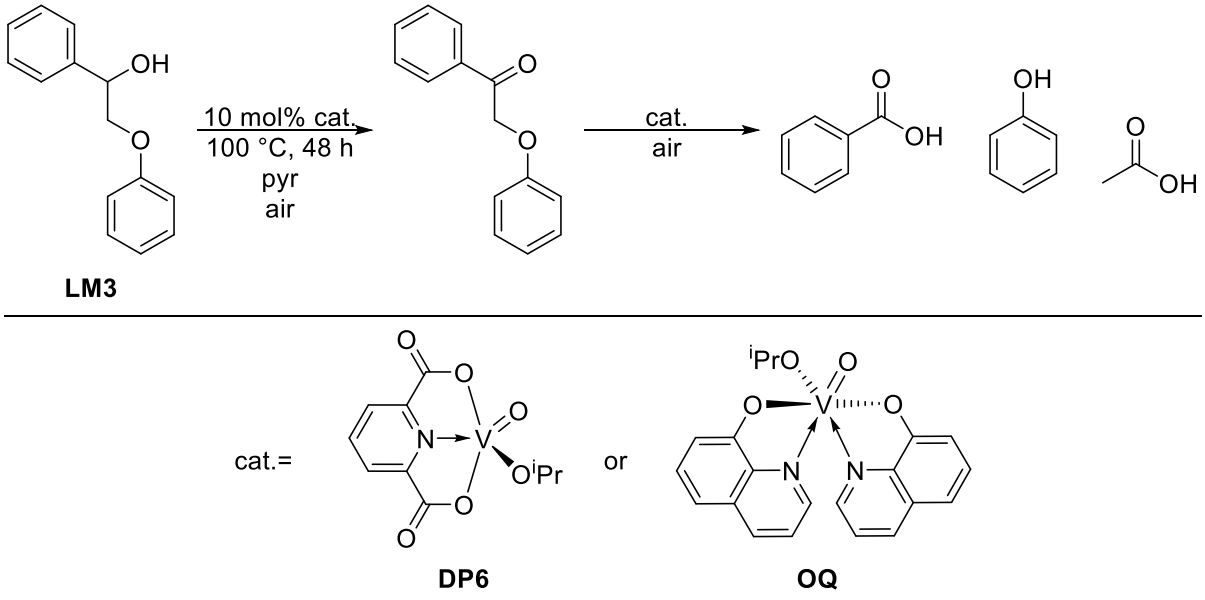


**Scheme 3.1.** Oxidative cleavage of **LM3** using **DP6** or **OQ** with base.

Within the field of oxidative lignin depolymerization, a great deal of effort has been made to selectively cleave C–O, C–H, and C–C bonds to afford specific products.[30] Of the methods currently being investigated, transition metal catalysis has been most thoroughly

examined. This includes methyltrioxorhenium, M-salen complexes, and various V and Mn based complexes.[29] However, of these methods, only oxovanadium(V) complexes have been shown capable of oxidatively cleaving lignin model compounds using air as an oxidant.

Previously, Baker and coworkers demonstrated the oxidative cleavage of **LM3** using **DP6** or **OQ** and added base; this first yielded a ketone product via C–H oxidative cleavage, followed by C–O and C–C cleavage to yield benzoic acid, phenol, and formic acid (**Scheme 3.1**).[90] However, base as an additive and overoxidation to carboxylic acids made this process undesirable. Further research by Baker and coworkers led to the creation of a new generation of bisphenoxy oxovanadium(V) complexes (**BP**), utilizing pendant arm bases integrated directly into the ligand of said complexes (**Figure 3.1**).[110] The **BP** complexes displayed significantly more reactivity than **DP6** or **OQ**, allowing them to be used in low catalyst loadings on lignin extracts, in addition to lignin models. **BP-pyr** was shown to have similar reactivity to **DP6** and **OQ** when cleaving **LM3**, favouring C–H cleavage, followed by C–O and C–C cleavage (**Scheme 3.1**). **BP1**, however, was observed to selectively favour C–O cleavage to afford ketone and aldehyde products. **BP2** was used to investigate the role of the pendant base in the reaction, and had similar reactivity to **BP1** with significantly less Cannizzaro- or Tishchenko-type chemistry (**Scheme 3.2**).[110]; however, as Tishchenko side reactions had not been observed with **DP6** or **OQ**, selectivity of the **BP** complexes remained a prevalent issue moving forward.

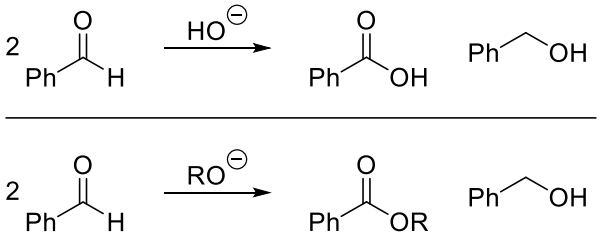


**Scheme 3.2.** Top: Cannizzaro reaction; bottom: Tishchenko reaction.

Chapter 2 established the effects that changing steric bulk and/or electron density at the metal center could have upon triphenoxyamine oxovanadium(V) complexes; utilizing what was learned, this design philosophy was incorporated into the bisphenoxy oxovanadium(V) catalyst complexes in an attempt to address the selectivity of **BP** complexes and to study the reactivity of these systems further. Additionally, the mechanism of oxidative cleavage was investigated using

substrate coordinated complexes **BP4** and **BP5** with the goal of better understanding why these complexes were far more active than **DP6 or OQ** (**Figure 3.1**).

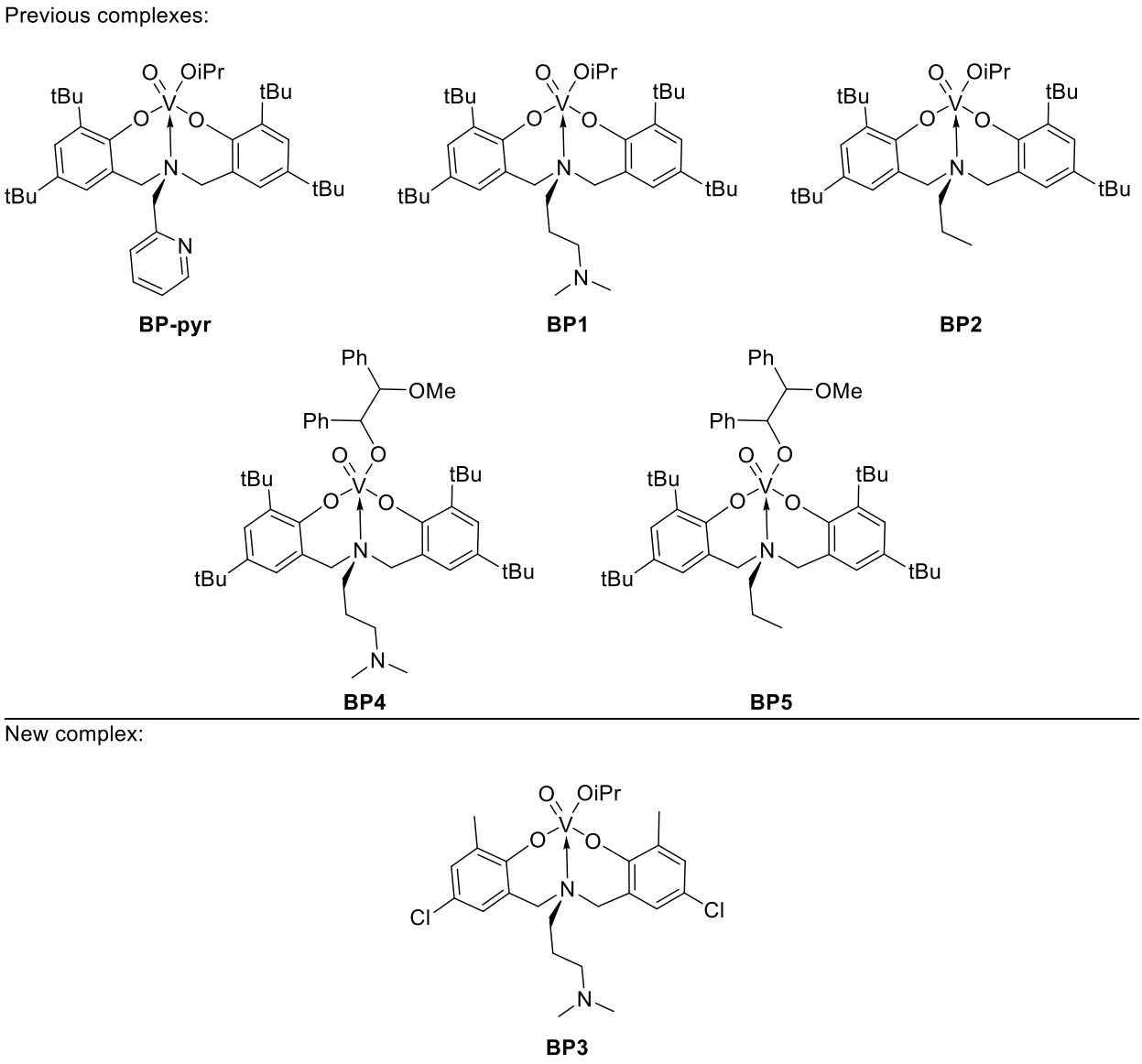


**Figure 3.1.** Second generation bisphenoxyamine oxovanadium(V) catalyst complexes.

*3.2 Materials and Methods*

### *3.2.1 General considerations*

Unless specified otherwise, all reactions were carried out under a dry nitrogen atmosphere using either glovebox or Schlenk techniques. Acetone, acetonitrile (MeCN), chloroform ($CHCl_3$), dichloromethane (DCM), diethyl ether ($Et_2O$), hexanes, methanol (MeOH), pentanes, tetrahydrofuran (THF), and toluene (Tol) were purchased from Alfa Aesar, Fisher Scientific, or Sigma-Aldrich. MeCN and DCM were dried via reflux over $CaH_2$. $Et_2O$, hexanes, THF, and Tol were dried on columns of activated alumina using a J. C. Meyer solvent purification system. All other solvents used in inert atmosphere were dried using activated 4 Å molecular sieves; all solvents used in air were used as obtained. Deuterated acetonitrile ($CD_3CN$), benzene ($C_6D_6$), chloroform ($CDCl_3$), dimethylsulfoxide (DMSO-$d_6$), and toluene (toluene-$d_8$) were purchased from Cambridge Isotope Laboratories and dried using activated 4 Å molecular sieves. Deuterated tetrahydrofuran (THF-$d_8$) was purchased from Sigma-Aldrich and used as obtained. All other reagents were used as obtained. $^1H$, $^{13}C\{^1H\}$, and $^{51}V$ NMR were obtained on Bruker AVANCE 300 MHz or 400 MHz spectrometers; chemical shifts were referenced to residual solvent signals ($^1H$ and $^{13}C\{^1H\}$) or externally to $VOCl_3$ (δ 0.00, $^{51}V$). The residual solvent peaks for $^1H$ NMR are: $CD_3CN$ (δ 1.94), $C_6D_6$ (δ 7.16), $CDCl_3$ (δ 7.26), DMSO-$d_6$ (δ 2.50), THF-$d_8$ (δ 3.58, 1.72), and toluene-$d_8$ (δ 7.09, 7.01, 6.97, and 2.08). The residual solvent peaks for $^{13}C\{^1H\}$ NMR are: $CD_3CN$ (δ 118.3, 1.3), $C_6D_6$ (δ 128.1), $CD_3Cl$ (δ 77.2), DMSO-$d_6$ (δ 39.5), THF-$d_8$ (δ 67.2, 25.3), and toluene-$d_8$ (δ 137.5, 128.9, 128.0, 125.1, and 20.4).

### *3.2.2 Synthesis of BL1 ligand*

**BL1** was synthesized according to a modified published procedure.[111] 2,4-Di-*tert*-butylphenol (6.2 g, 30 mmol), *N*,*N*-dimethyl-1,3-propanediamine (1.5 g, 15 mmol), and formaldehyde (3.5 mL, 42 mmol), were added to a 100 mL round bottom flask and dissolved in 7.5 mL of MeOH. The solution was stirred at reflux under air for 3 days. The solution was then cooled and the supernatant was removed. The resultant solid was recrystallized with boiling MeCN and kept at −35 °C for 3 days. Suction filtration and subsequent rinses with cold MeCN afforded 3.8 g of a white solid (47% yield). $^1H$ NMR (400 MHz, $CDCl_3$): δ 10.15 (s, 2H), 7.20

(d, 2H, *J*=2.4 Hz), 6.86 (d, 2H, *J*=2.8), 3.55 (s, 4H), 2.59 (t, 2H, *J*=6.0), 2.46 (m, 2H), 2.36 (s, 6H), 1.78 (pent, 2H, *J*=5.0), 1.40 (s, 18H), 1.27 (s, 18H). $^{13}C\{^{1}H\}$ NMR (100 MHz, $CDCl_3$): δ 153.3, 140.1, 135.8, 125.1, 123.2, 121.1, 58.6, 57.5, 55.2, 45.7, 35.0, 34.0, 31.7, 31.6, 29.5, 22.9.

### *3.2.3 Synthesis of BL2 ligand*

**BL2** was synthesized according to a modified published procedure.[104] 2,4-Di-*tert*-butylphenol (4.1 g, 20 mmol), *n*-propylamine (0.82 mL, 10 mmol), and formaldehyde (2.3 mL, 28 mmol), were added to a 100 mL round bottom flask and dissolved in 5 mL of MeOH. The solution was stirred at reflux under air for 3 days. The solution was then cooled and the supernatant was removed. The resultant solid was recrystallized with boiling MeOH and kept at 35 °C for 3 days. Suction filtration and subsequent rinses with cold MeOH afforded 1.2 g of a white solid (24% yield). $^{1}H$ NMR (400 MHz, $CDCl_3$): δ 7.22 (d, 2H, *J*=2.4 Hz), 6.92 (d, 2H, *J*=2.4 Hz), 3.68 (s, 4H), 2.51 (m, 2H), 1.64 (sext, 2H, *J*=7.4 Hz), 1.40 (s, 18H), 1.28 (s, 18H), 0.88 (t, 3H, *J*=7.5 Hz). $^{13}C\{^{1}H\}$ NMR (100 MHz, $CDCl_3$): δ 152.4, 141.5, 136.0, 125.0, 123.4, 121.7, 57.2, 55.5, 34.8, 34.2, 31.6, 29.7, 19.4, 11.7.

### *3.2.4 Synthesis of BL3 ligand*

4-Chloro-o-cresol (4.3 g, 30 mmol), *N*,*N*-dimethyl-1,3-propanediamine (1.5 g, 15 mmol), and formaldehyde (3.5 mL, 42 mmol), were added to a 100 mL round bottom flask and dissolved in 10 mL of MeOH. The solution was stirred at reflux under air for 3 days. The solution was then cooled and the supernatant was removed. The resultant solid was recrystallized with boiling MeOH and kept at −35 °C for 3 days. Suction filtration and subsequent rinses with cold MeOH afforded 1.9 g of a white solid (30% yield). $^{1}H$ NMR (400 MHz, $CDCl_3$): δ 7.05 (d, 2H, *J*=2.0 Hz), 7.01 (d, 2H, *J*=2.4 Hz), 3.65 (s, 4H), 2.44 (t, 2H, *J*=7.4 Hz), 2.10 (m, 9H), 2.03 (s, 6H), 1.63 (pent, 2H, *J*=7.0 Hz).$^{13}C\{^{1}H\}$ NMR (100 MHz, $CDCl_3$): δ 154.1, 129.5, 127.3, 127.1, 125.3, 122.4, 57.4, 54.7, 51.4, 45.4, 23.5.

### *3.2.5 Synthesis of BP1 complex*

**BP1** was synthesized according to a modified published procedure.[111] In a 20 mL scintillation vial, **BL1** (862 mg, 1.6 mmol) was dissolved in 4.5 mL of DCM. In a separate 20 mL scintillation vial, $V(O)(O^{i}Pr)_3$ (348 μL, 1.5 mmol) was dissolved in 4.5 mL of DCM. The

$V(O)(O^iPr)_3$ solution was added dropwise to the **BL1** solution over 5 minutes, yielding a dark brown and opaque solution. This was stirred for 18 hours before removing solvent *in vacuo*. The crude solid was then recrystallized with MeCN at −35 °C for 2 days. Suction filtration and subsequent rinses with cold benzene afforded 792 mg of a black solid (75% yield). $^1$H NMR (300 MHz, $C_6D_6$): δ 7.51 (d, 2H, *J* = 2.5 Hz), 6.95 (d, 2H, *J* = 2.5 Hz), 5.93 (sept, 1H, *J* = 6.0 Hz), 4.90 (d, 2H, *J* = 15 Hz), 3.46 (d, 2H, *J* = 15 Hz), 2.90 (m, 2H), 1.65 (s, 6H), 1.63 (d, 6H, *J* = 6.0 Hz), 1.60 (s, 18H), 1.51 (t, 2H, *J* = 6.5 Hz), 1.37 (s, 18H), 1.29 (m, 2H). $^{51}$V NMR (79 MHz, $C_6D_6$): δ −514.7, −566.8.

### *3.2.6 Synthesis of BP2 complex*

**BP2** was synthesized according to a modified published procedure.[105] In a 20 mL scintillation vial, **BL2** (1.2 g, 2.4 mmol) was dissolved in 5 mL of DCM. In a separate 20 mL scintillation vial, $V(O)(O^iPr)_3$ (628 μL, 2.6 mmol) was dissolved in 3 mL of DCM. The $V(O)(O^iPr)_3$ solution was added dropwise to the **BL2** solution over 5 minutes, yielding a dark brown and opaque solution. This was stirred for 18 hours before removing solvent *in vacuo*. The crude solid was then recrystallized with pentanes at −35 °C for 2 days. Suction filtration and subsequent rinses with cold benzene afforded 687 mg of a red-brown solid (46% yield). $^1$H NMR (300 MHz, $C_6D_6$): δ 7.53 (d, 2H, *J*=2.4), 6.95 (d, 2H, *J*=2.4), 5.93 (quint, 1H, *J*=6.2), 4.90 (d, 2H, *J*=14.7), 3.47 (d, 2H, *J*=14.7), 2.75 (m, 2H), 1.62 (m, 24H), 1.36 (s, 18H), 1.14 (m, 2H), 0.36 (t, 3H, *J*=7.2). $^{13}$C{$^1$H} NMR (75 MHz, $C_6D_6$): 142.4, 123.5, 123.3, 121.5, 59.8, 35.0, 35.0, 34.1, 31.5, 31.5, 29.8, 29.8, 25.4, 25.1, 13.3, 10.8.

### *3.2.7 Synthesis of BP3 complex*

In a 20 mL scintillation vial, **BL3** (130 mg, 0.31 mmol) was dissolved in 3 mL of DCM. In a separate 20 mL scintillation vial, $V(O)(O^iPr)_3$ (89 μL, 0.38 mmol) was dissolved in 3 mL of DCM. The $V(O)(O^iPr)_3$ solution was added dropwise to the **BL3** solution over 5 minutes, yielding a dark brown and opaque solution. This was stirred for 18 hours before removing solvent *in vacuo*. The crude solid was then recrystallized with MeCN and kept at −35 °C for 2 days. Suction filtration and subsequent rinses with cold benzene afforded 77 mg of a black solid (46% yield). $^1$H NMR (300 MHz, $CDCl_3$): δ 7.00 (s, 4H), 3.64 (s, 4H), 2.42 (m, 7H), 3.24 (m, 9H), 1.51 (m, 2H).

### *3.2.8 Synthesis of 1,2-$^{13}$C-LM2*

1,2-$^{13}$C-LM2 was synthesized according to modified published procedures.[112,113] In a 20 mL scintillation vial, NaCN (500 mg, 2.1 mmol) was partially dissolved in 0.65 mL EtOH and 0.5 mL of $H_2O$. The solution was stirred and heated to 95 °C. 1-$^{13}$C-Benzaldehyde (0.49 mL, 4.7 mmol) was added to the solution, which was capped and stirred for 30 minutes. The reaction was cooled to r.t., then to 0 °C in an ice bath. Suction filtration and subsequent drying *in vacuo* for 12 hours afforded 1,2-$^{13}$C-benzoin. In a 25 mL round bottom flask, 1,2-$^{13}$C-benzoin (365 mg, 1.7 mmol), $Ag_2O$ (738 mg, 3.2 mmol), MeI (0.71 mL, 11.5 mmol), and 8.4 mL of $CH_3Cl$ were combined and stirred at reflux for 20 hours. Additional portions of $Ag_2O$ (246 mg, 1.1 mmol) and MeI (0.24 mL, 3.8 mmol) were added and the mixture was heated at reflux for an additional 4 hours. The reaction was cooled to r.t., then decolorized with activated charcoal. The mixture was filtered through a bed of $MgSO_4$ and solvent was removed *in vacuo* to afford 1,2-$^{13}$C-benzoin methyl ether. In a 100 mL round bottom flask, $NaBH_4$ (334 mg, 8.8 mmol) was dissolved in 10.2 mL of MeOH and 10.2 mL of $H_2O$ and cooled to 0 °C. In a 20 mL scintillation vial, 1,2-$^{13}$C-benzoin methyl ether (384 mg, 1.7 mmol) was dissolved in 10.2 mL of MeOH. The 1,2-$^{13}$C-benzoin methyl ether solution was added dropwise to the $NaBH_4$ solution over 5 minutes. The solution was warmed to r.t. and stirred for 1 hour. The solution was then quenched with 2.0 mL of a 10% NaOH solution. The reaction mixture was diluted with 120 mL of $Et_2O$, washed with 3 × 60 mL of water, 2 × 60 mL of 1 M HCl, and 1 × 60 mL of brine. The solution was dried with $MgSO_4$, filtered, and solvent was removed *in vacuo* to afford 270 mg of a light yellow solid (50% yield). $^1$H NMR (300 MHz, $CDCl_3$): δ 7.16 (m, 10H), 4.89 (ddd, 1H, *J*=3.9, 9.3, 145.5), 4.34 (dddd, 1H, *J*=2.7, 3.9, 5.4, 141.9), 3.24 (d, 3H, *J*=4.5), 2.33 (ddd, 1H, *J*=2.7, 3.9, 5.4). $^{13}$C{$^1$H} NMR (100 MHz, $CDCl_3$): δ 128.1, 128.1, 128.0, 128.0, 128.0, 128.0, 127.0 (Ph), 89.2 (d, ×, minor diasteromer), 87.6 (d, 40.5, major diasteromer), 78.7 (d, 39.5, minor diasteroemer), 78.1 (s, OMe), 76.9 (d, 40.5, major diasteromer).

### *3.2.9 Synthesis of BP4 complex*

**BP4** was synthesized according to a modified published procedure.[111] In a 20 mL scintillation vial, **BP1** (128 mg, 0.19 mmol) was dissolved in 1.5 mL of DCM. In a separate 20 mL scintillation vial, **LM2** (209 mg, 0.92 mmol) was dissolved in 1.5 mL of DCM. The **BP1** solution was added dropwise to the **LM2** solution over 5 minutes. The mixture was stirred for 18

hours. Solvent was removed *in vacuo* and the crude product was recrystallized with a 3:1 mixture of MeCN:DCM. This solution was capped and left at −35 °C for 4 days. Suction filtration and subsequent rinses with cold benzene afforded 101 mg of a brown solid (63% yield). This procedure was also used to couple **BP1** and 1,2-$^{13}$C-**LM2**. $^{1}$H NMR (300 MHz, Tol-$d_8$): δ 7.73 (d, 1H, *J* = 2.3 Hz), 7.64 (d, 1H, *J* = 2.3 Hz), 7.42 (m, 2H), 7.22 (d, 1H, *J* = 2.3 Hz), 7.12 (m, 4H), 7.05 (m, 1H), 6.97 (m, 4H), 6.69 (s, 1H), 4.79 (d, 1H, *J* = 145 Hz), 4.08 (d, 1H, *J* = 142 Hz), 3.92 (d, 1H, *J* = 12 Hz), 3.32 (d, 1H, *J* = 12 Hz), 3.22 (s, 3H) 3.18 (d, 1H, *J* = 12 Hz), 1.96 (s, 9H), 1.89 (s, 6H), 1.70 (s, 9H), 1.63 (m, 2H), 1.57 (m, 2H), 1.43 (s, 9H), 1.42 (s, 9H) 1.37 (m, 2H). $^{13}$C{$^{1}$H} NMR (Tol-$d_8$, 75 MHz): δ 165.9, 164.5, 142.3, 141.8, 141.3, 138.2, 137.4, 136.3, 135.4, 124.5, 124.3, 124.2, 123.8, 122.8, 122.7, 94.2, 91.3, 57.7, 57.6, 57.4, 56.7, 53.3, 52.4, 45.4, 35.7, 35.2, 34.5, 32.0, 31.9, 30.8, 30.5, 18.8. $^{51}$V NMR (79 MHz, Tol-$d_8$): δ −562.3.

### *3.2.10 Synthesis of BP5-1,2-$^{13}$C-LM2 complex*

**BP5** was synthesized according to a modified published procedure.[111] In a 20 mL scintillation vial, **BP2** (82 mg, 0.13 mmol) was dissolved in 1.5 mL of DCM. In a separate 20 mL scintillation vial, 1,2-$^{13}$C-**LM2** (138 mg, 0.6 mmol) was dissolved in 1.5 mL of DCM. The **BP2** solution was added dropwise to the 1,2-$^{13}$C-**LM2** solution over 5 minutes. The mixture was stirred for 18 hours. Solvent was removed *in vacuo* and the crude product was recrystallized with a 3:1 mixture of MeCN:DCM. This solution was capped and left at −35 °C for 2 days. Suction filtration and subsequent rinses with cold benzene afforded 18 mg of a brown solid (16% yield). $^{1}$H NMR (300 MHz, Tol-$d_8$): δ 7.73 (d, 1H, *J* = 2.4 Hz), 7.64 (d, 1H, *J* = 2.4 Hz), 7.43 (m, 3H), 7.19 (d, 2H, *J* = 2.4 Hz), 7.13 (d, 2H, *J* = 7.5 Hz), 7.08 (d, 1H, *J* = 2.4 Hz), 6.98 (m, 2H), 6.97 (d, 1H, *J* = 2.4 Hz), 6.70 (d, 1H, *J* =9.2 Hz), 4.81 (d, 1H, *J* = 144 Hz), 4.08 (d, 1H, *J* = 147 Hz), 3.91 (d, 1H, *J* = 12 Hz), 3.29 (d, 1H, *J* = 12 Hz), 3.23 (s, 3H), 3.17 (d,1H, J = 12 Hz), 1.97 (s, 9H,), 1.71 (s, 9H), 1.42 (s, 18H), 1.36 (d,1H, *J* = 5.4 Hz), 0.58 (s, 2H), 0.35 (t, 3H, *J* = 7.4 Hz), 0.29 (s, 1H). $^{51}$V NMR (79 MHz, Tol-$d_8$): δ −561.4

### *3.2.11 General procedure for catalysis of LM2 with BP complexes*

In a 4 mL scintillation vial, **LM2** (25 mg) was dissolved in 0.5 mL of the desired solvent. In a separate 4 mL scintillation vial, the desired amount of oxovanadium catalyst was dissolved in 0.5 mL of the desired solvent. The **LM2** solution was then added to the oxovanadium solution.

5 μL of 1,3,5-trimethoxy benzene or mesitylene were added as an internal standard. A small sample was taken for an initial $^{1}H$ NMR spectrum and a Teflon stir bar was added before sealing the vial and heating at the desired temperature for the desired reaction time. After completion of the allotted reaction time, another sample was taken to obtain $^{1}H$, $^{13}C$, and/or $^{51}V$ NMR spectra.

### *3.2.12 General procedure for pre-complexed thermolysis reactions*

In a 4 mL scintillation vial, 10 mg of the desired pre-complexed oxovanadium compound was dissolved in 1 mL of the desired deuterated solvent. 5 μL of 1,3,5-trimethoxy benzene or mesitylene were added as an internal standard. The solution was then transferred to an NMR tube and sealed. The reaction was monitored over 2 hours via NMR spectroscopy at the desired temperature, with an initial and final spectrum being taken at 25 °C.

## *3.3 Results and Discussion*

Upon synthesis of new complex **BP3**, it was subjected to the optimal conditions that had been ascertained via previously established complexes **BP-pyr**, **BP1**, and **BP2**: 18 hours at 105 °C open to air in toluene (**Scheme 3.3**). However, a much larger catalyst loading was used for the initial reaction (**Table 3.1**). A total conversion was observed via $^{1}H$ NMR, similar to what had been seen with prior **BP** complexes (**Table 3.1**, entries 1-4). **BP3** was observed to have a 51:49 ratio of CHO:COOH and a 55:45 ester:BzOH ratio; this was significantly higher than the respective ratios for previously established catalysts (**Table 3.1**, entries 1-3). Additionally, no BME was observed, suggesting that **BP3** favors C–O and C–C cleavage as **BP-pyr** and **BP2** do; this is especially curious as **BP3** has more in common structurally with **BP2**, the complex which favors C–H cleavage significantly more. However, this could also mean that C–C cleavage with **BP3** is so fast that any BME produced is quickly broken down further.

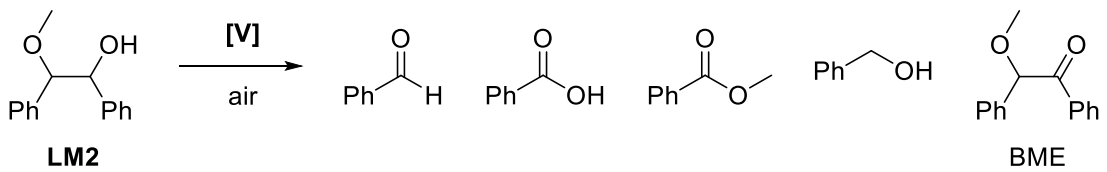


**Scheme 3.3.** Aerobic oxidative cleavage of **LM2** by **BP** complexes (**Table 3.1**).

**Table 3.1.** Comparison of **BP** complex ability to oxidatively cleave **LM2** after 18 hours at 105 °C (**Scheme 3.2**).

| Entry | Cat. (mol%) | Solvent | Conv. (%)[a] | CHO (%)[b] | COOH (%)[b] | Ester (%)[b] | BzOH (%)[b] | BME (%)[b] |
|---|---|---|---|---|---|---|---|---|
| 1 | **BP-pyr** (0.1) | Tol | 100 | 35 | 51 | 25 | 58 | 7 |
| 2 | **BP1** (0.1) | Tol | 100 | 27 | 120 | 7 | 63 | 27 |
| 3 | **BP2** (0.1) | Tol | 98 | 27 | 67 | 18 | 76 | 9 |
| 4 | **BP3** (10) | Tol | 100 | 38 | 37 | 12 | 10 | 0 |
| 5 | **BP3** (10) | DMSO | 99 | 9 | 12 | 1 | trace | trace |
| 6[c] | **BP3** (10) | Pyr | 100 | 32 | 30 | 0 | 5 | 0 |

[a] $^1$H NMR integration against an internal standard. [b] Yields are based on the maximum theoretical amount of moles produced with respect to the substrate. [c] Run at 85 °C.

Despite the nearly equimolar ratios of each pair of products and no BME detected, mass balance was poor in Tol (~50%, entry 4). Suspecting this could be due to poor solvation of the relatively more polar complex, DMSO was chosen as a substitute due to its successful usage for **TP** complexes and high boiling point. Unfortunately, this exacerbated the issue and the mass balance was even lower (~14%, entry 5). Reactivity was also less than ideal, with BME appearing for the first time with **BP3**. Additionally, the reaction did not reach completion (99%, entry 5), suggesting that DMSO had a negative effect on reaction rate. Pyridine was then examined as a solvent; it was hypothesized that despite its lower boiling point, its ability to act as a base could increase reaction speed by enough to offset the reduced thermal energy (**Table 3.1**, entry 6). Similar reactivity to entry 4 was observed, with a 52:48 CHO:COOH ratio and no BME observed. Curiously, no ester was observed as a product, suggesting that Tishchenko-type chemistry may have been inhibited in some way; this seems counterintuitive, as a more basic solution should produce more methoxide, which should facilitate more Tishchenko-type chemistry (**Scheme 3.2**). Once again the mass balance was poor (~35%), suggesting solubility may still be an issue.

While **BP3** displayed encouraging C–C and C–O cleavage selectivity**,** the results observed called further into question the role of the pendant base on the **BL** ligands. With this in mind, a closer examination of the mechanism of **BP** complexes with **LM2** was undertaken.

*3.4 Mechanistic Investigations*

In order to investigate the mechanism, **BP4** was anaerobically heated at 100 °C for 2 hours, as per a similar procedure performed by Baker and coworkers (**Scheme 3.4**).[111] The reaction was monitored by $^{1}$H NMR, with spectra taken every 15 minutes. After the first 15 minutes, approximately 20% of the **BP4** complex was converted to BME; presumably, this oxidation also formed a $V^{III}$ complex and 1 equiv. of water, similar to what was observed with **TP1** (Chapter 2, **Scheme 2.8**). At 30 minutes, approximately 55% of the **BP4** complex had been converted, despite only 25% of the reaction time having elapsed. The final conversion by $^{1}$H NMR at 2 hours was only 80%, implying two disparate rates within the reaction; this is similar to the KIE results observed with **TP1**, which suggests this may be common to these two classes of oxovanadium(V) complexes. $^{51}$V NMR showed that by 1 hour, 60% of the **BP4** had been consumed, and over 95% had been consumed by 2 hours. Two new signals at −476 and −527 ppm (compared to −516 and −567 ppm for **BP1**) appeared and grew through the reaction, likely the major and minor isomers of a **BP1** $V^{V}$ complex. It is possible this complex was ligated with water, as no evidence of water was seen by $^{1}$H NMR despite the reaction producing 1 equiv. of water;

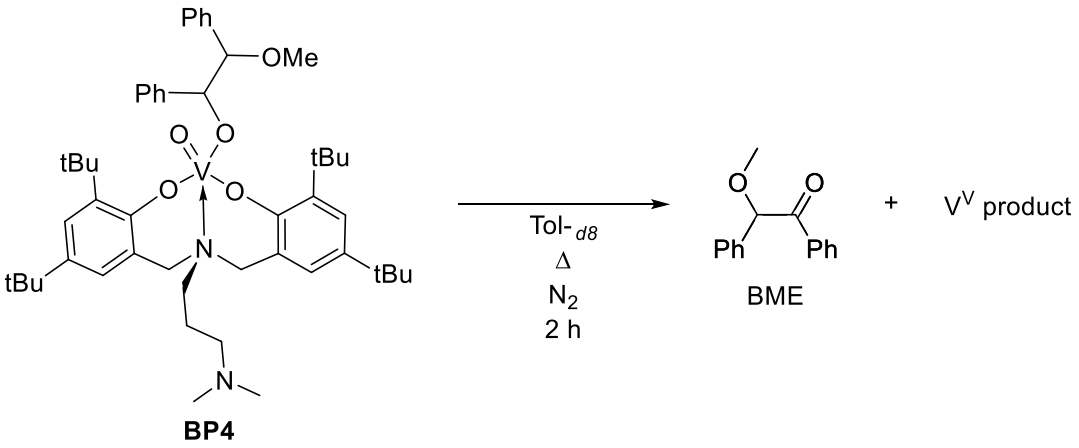


**Scheme 3.4.** Anaerobic thermolysis of **BP4** substrate complex.

this would be plausible assuming that the energies for coordinated $V^V$-**TP1** (discussed in Chapter 2) are representative of this complex.

The only oxidation product observed was BME, indicating that only C–H cleavage takes place during the course of the reaction. While **BP1** has the highest selectivity towards BME out of the four **BP** complexes, it is not normally the highest yielding product. This suggests that C–H cleavage may be faster than C–C and C–O cleavage for this substrate. Also observed in the reaction is evidence for free **BL1** ligand; a very broad (~0.5 ppm wide) signal, which suggests a very deshielded alcohol proton, and a signal correlating to the reported $^1$H NMR shift for **BL1** *tert*-butyl (1.63 and 1.35 ppm to 1.58 and 1.31 ppm). Despite this, no evidence of catalyst decomposition was seen via $^{51}$V NMR. At present, no other hypotheses have been formed for the apparent appearance of **BL1** by $^1$H NMR.

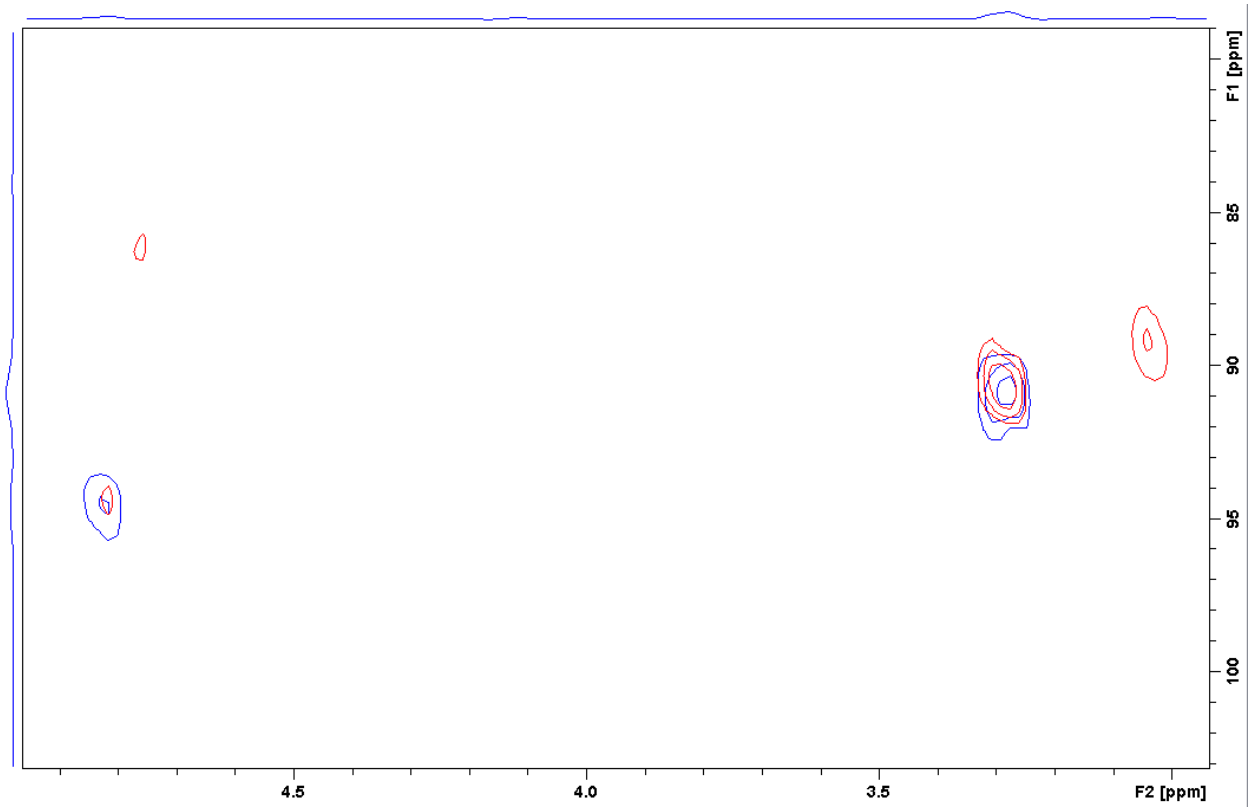


**Figure 3.2.** HMBC of **BP4** thermolysis at 60 °C. Initial spectrum in blue and final spectrum in red. Zoomed in to highlight the upfield shift of the methyl ether.

HSQC and HMBC experiments were utilized to further study the reactivity of the **BP4** complex, in an attempt to identify potential intermediates forming during the reaction. Given the

speed of the thermolysis and concerns about possible catalyst decomposition at 100 °C, a much milder 60 °C was chosen as the target temperature for these reactions. HSQC was not diagnostic of any reactivity. HMBC, however, displayed surprising reactivity given the lower temperature (**Figure 3.2**). An estimated conversion of 90% was obtained, as evidenced by the conversion from the coordinated methyl ether signal ($^{1}$H NMR: 4.82 ppm, $^{13}$C NMR: 94.5 ppm) to the BME methyl ether signal ($^{1}$H NMR: 3.04 ppm, $^{13}$C NMR: 89.5 ppm). No evidence for uncoordinated ligand was observed, indicating that the lower temperature prevented the possible catalyst decomposition observed at 100 °C. Additionally, a signal likely corresponding to benzoic acid was observed ($^{1}$H NMR: 11.9 ppm, $^{13}$C NMR: 214 ppm) in the final spectrum, indicating that C–C bond cleavage was occurring at 60 °C, despite not being observed at 100 °C. Currently, there is no hypothesis for this unexpected reactivity.

In order to explain this inconsistent reactivity, carbon labelled substrate 1,2-$^{13}$C-**LM2** was synthesized and complexed with **BP1** to form **BP4**-1,2-$^{13}$C-**LM2**. Additionally, this was used as an opportunity to more fully explore the role of the pendant base in this reaction, and an analogous **BP2** complex, **BP5**-1,2-$^{13}$C-**LM2**, was synthesized. The thermolysis of **BP4**-1,2-$^{13}$C-**LM2** had a 20% conversion compared to the 33% of **BP5**-1,2-$^{13}$C-**LM2**. This is contrary to previous results of these catalysts in air (**Table 3.1**, entries 2 and 3). However, while BME was produced by **BP4**-1,2-$^{13}$C-**LM2**, **BP5**-1,2-$^{13}$C-**LM2** had evidence of aldehyde by $^{1}$H and $^{13}$C NMR (9.59 and 190.9 ppm, respectively). This implies that in the course of thermolysis, the *N'-N''*-dimethylamine pendant arm on **BP2** and **BP4** somehow impedes C–C bond cleavage.

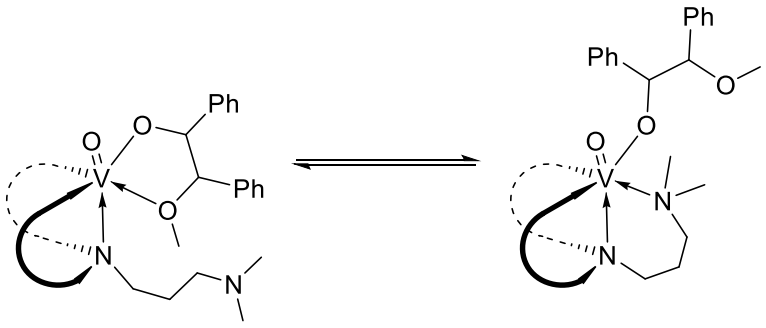


**Figure 3.3.** Hypothesized competition between amine and ether lone pairs for open coordination site on **BP4** oxovanadium(V) catalyst center. Aryl rings on **BP4** have been abbreviated for clarity.

This could be due to a competition for the Lewis acidic $V^V$ center between the methyl ether lone pair of **LM2** and the amine lone pair of the pendant arm (**Figure 3.3**). Despite the unfavourable nature of the 6-membered amine metallacycle vs. the 5-membered ether metallacycle, the more available lone pair of the amine may force the ether away from the metal center; **BP-pyr** and a methanol analogue of **BP1** have been previously shown via X-ray crystallography to form 5- and 6-membered amine metallacycles, respectively.[94] As C–C bond cleavage necessitates both oxygens of the substrate to be coordinated to V, this could explain the exclusive C–H cleavage of **BP4**-1,2-$^{13}$C-**LM2**; as no re-oxidation of the $V^{III}$-**BP1** can occur, BME cannot undergo C–C bond cleavage. Additionally, it has been shown previously that alcohols directly bound to $V^V$ complexes will undergo oxidative bond C–H cleavage (Chapter 1, section 1.5).

### *3.5 Conclusions*

New bisphenoxyamine complex **BP3**, synthesized based on previous work in Chapter 2, demonstrated higher selectivity towards aldehydes and esters relative to previous second generation oxovanadium(V) **BP** complexes. No evidence of BME was observed with the use of this complex, which either indicates that C–H cleavage of **LM2** does not take place with **BP3** or that C–C cleavage occurs quickly enough after C–H cleavage that no BME is observed. Solvent was observed to have a major effect on reactivity, with Tol leading to the highest selectivity and conversion.

Mechanistic investigations via substrate pre-coordinated oxovanadium(V) complex **BP4** revealed that C–H cleavage is faster than C–O or C–C bond cleavage, as neither were observed anaerobically at 100 °C. Catalyst decomposition may be taking place at this temperature, impacting reactivity and selectivity, as evidenced by $^1$H NMR. However, this was contrary to $^{51}$V NMR data, implying unknown reactivity taking place during the anaerobic thermolysis. HMBC strongly correlated that C–H bond cleavage takes place quickly during thermolysis of **BP4**. Evidence of benzoic acid was seen at 60 °C, but not at 100 °C, once again implying that further experiments are required to understand the chemistry taking place during these reactions. Finally, thermolysis of **BP4**-1,2-$^{13}$C-**LM2** and **BP5**-1,2-$^{13}$C-**LM2** demonstrated apparent inhibition of C–

C bond cleavage. This discrepancy in reactivity is likely caused by the *N'-N''*-dimethylamine pendant arm competing for the open coordination site on the metal center.

[104] a) Deng, H.; Lin, L.; Sun, Y.; Pang, C.; Zhuang, J.; Ouyang, P.; Li, J.; Liu, S. *Energy Fuels*, **2009**, *23*, 19-24; b) Gu, X.; Kanghua, C.; Ming, H.; Shi, Y.; Li, Z. *Maderas. Cienc. y Tecnol.* **2012**, *14*, 31-41; c) Stark, K.; Taccardi, N.; Bosmann, A.; Wasserscheid, P. *ChemSusChem* **2010**, *3*, 719-723; d) Liu, S.; Shi, Z.; Li, L.; Yu, S.; Xie, C.; Song, Z. *RSC Adv.* **2013**, *3*, 5789-5793; e) Yamamoto, K.; Hosoya, T.; Yoshioka, K.; Miyafuji, H.; Ohno, H.; Yamada, T. *ACS Sustainable Chem. Eng.* **2017**, *5*, 10111-10115.
[105] a) Barta, K.; Warner, G. R.; Beach, E. S.; Anastas, P. T. *Green Chem.* **2014**, *16*, 191-196; b) Gao, F.; Webb, J. D.; Sorek, H.; Wemmer, D. E.; Hartwig, J. F. *ACS Catal.* **2016**, *6*, 7385-7392; c) Jiang, Y.; Li, Z.; Tang, X.; Sun, Y.; Zeng, X.; Liu, S.; Lin, L. *Energy Fuels* **2015**, *29*, 1662-1668; d) Konnerth, H.; Zhang, J.; Ma, D.; Prechtl, M. H. G.; Yan, N. *Chem. Eng. Sci.* **2015**, *123*, 155-163; e) Si, X.; Lu, F.; Chen, J.; Lu, R.; Huang, Q.; Jiang, H.; Taarning, E.; Xu, J. *Green Chem.* **2017**, *19*, 4849-4857; f) Xiao, L.-P.; Wang, S.; Li, H.; Li, Z.; Shi, Z.-J.; Xiao, L.; Sun, R.-C.; Fang, Y.; Song, G. *ACS Catal.* **2017**, *7*, 7535-7542; g) Feghali, E.; Carrot, G.; Thuéry, P.; Genre, C.; Cantat, T. *Energy Environ. Sci.* **2015**, *8*, 2734-2743; h) Shuai, L.; Amiri, M. T.; Questell-Santiago, Y. M.; Héroguel, F.;Li, Y.; Kim, H.; Meilan, R.; Chapple, C.; Ralph, J.; Luterbacher, J. S. *Science* **2016**, *354*, 329-333; i) Shao, Y.; Xia, Q.; Dong, L.; Liu, X.; Han, X.; Parker, S. F.; Cheng, Y.; Daemen, L. L.; Ramirez-Cuesta, A. J.; Yang, S.; et al. *Nat. Commun.* **2017**, *8*, 16104.
[106] a) Deuss, P. J.; Lancefield, C. S.; Narani, A.; de Vries, J. G.; Westwood, N. J.; Barta, K. *Green Chem.* **2017**, *19*, 2774−2782; b) Deuss, P. J.; Lahive, C. W.; Lancefield, C. S.; Westwood, N. J.; Kamer, P. C. J.; Barta, K.; de Vries, J. G. *ChemSusChem* **2016**, *9*, 2974-2981; c) Jastrzebski, R.; Constant, S.; Lancefield, C. S.; Westwood, N. J.; Weckhuysen, B. M.; Bruijnincx, P. C. A. *ChemSusChem* **2016**, *9*, 2074−2079.
[107] a) Rahimi, A.; Ulbrich, A.; Coon, J. J.; Stahl, S. S. *Nature* **2014**, *515*, 249-252; b) Lancefield, C. S.; Ojo, O. S.; Tran, F.; Westwood, N. J *Angew. Chem. Int. Ed.* **2015**, *54*, 258-262; c) Bosque, I.; Magallanes, G.; Rigoulet, M.; Kärkäs, M. D.; Stephenson, C. R. J. *ACS Cent. Sci.* **2017**, *3*, 621-628.
[108] Jiang, Z.; He, T.; Li, J.; Hu, C. *Green Chem.* **2014**, *16*, 4257-4265.
[109] a) Linger, J. G.; Vardon, D. R.; Guarnieri, M. T.; Karp, E. M.; Hunsinger, G. B.; Franden, M. a.; Johnson, C. W.; Chupka, G.; Strathmann, T. J.; Pienkos, P. T.; et al. *Proc. Natl. Acad. Sci. U. S. A.* **2014**, *111*, 12013-12018; b) Vardon, D. R.; Franden, M. A.; Johnson, C. W.; Karp, E. M.; Guarnieri, M. T.; Linger, J. G.; Salm, M. J.; Strathmann, T. J.; Beckham, G. T. *Energy Environ. Sci.* **2015**, *8*, 617-628.
[110] Diaz-Urrutia, C. *Vanadium Catalyzed Aerobic Oxidation of Diols and Lignin Models/Extracts*, **2016**.
[111] Tshuva, E. Y.; Goldberg, I.; Kol, M.; Goldschmidt, Z. *Organometallics* **2001**, *20*, 3017-3028.
[112] Kang, P.; Foote, C. S. *J. Am. Chem. Soc.* **2002**, *124*, 9629-9638.
[113] Davis, F. A.; Haque, M. S. ; Przeslawski, R. M. *J. Org. Chem.* **1989**, *54*, 2021-2024.

## Chapter 4: Conclusions and Future Work

### *4.1 Conclusions*

The use of oxovanadium(V) complexes to oxidatively depolymerize lignocellulosic model complexes has been expanded. Chapter 2 introduced several new triphenoxyamine oxovanadium(V) complexes and their corresponding ligands (**TP3-4**, **TL3-4**). These complexes, along with **TP2** and **TP5**, were able to successfully cleave a variety of previously inaccessible substrates, albeit in low conversion: 1,2-cyclohexanediol, 2,3-butanediol, 1-phenyl-1,2-ethanediol, glycerol, xylitol, and sorbitol. Higher conversion was achievable with forcing conditions, but selectivity suffered as a result. Additionally, these complexes were shown to be just as effective as previously reported **TP** complexes when reacted with previous substrates hydrobenzoin and pinacol. Mechanistic studies of previously established oxovanadium(V) complexes **TA** and **TP1** were performed, indicating that no KIE exists within either mechanism. A proposed mechanism for **TA** involving ligand arm dissociation and reassociation was supported by previous research,[93a] DFT calculations, and experimental observations, as the rate determining step did not contain any proton transfer. However, postulated mechanisms for **TP** complexes both by collaborators and other researchers indicated that the rate determining step would contain a proton transfer, which is in contrast with the lack of KIE determined experimentally.[97]

Chapter 3 attempted to utilize similar ligand design from Chapter 2, which resulted in the synthesis of **BP3**. This complex was found to have similar reactivity to previously established complexes **BP-pyr**, **BP1**, and **BP2**; however, C–H bond cleavage was less favored, indicating that one or more of steric bulk around the metal center, electron density at the metal center, or solvation play a significant role in the selectivity of oxidative bond cleavage. The mechanism of this reaction was studied via thermolysis of the substrate pre-complexed **BP4**. The anaerobic thermolysis showed a strong preference for C–H bond cleavage, with little to no C–C or C–O cleavage observed. NMR spectroscopy suggested there may be catalyst decomposition during thermolysis of **BP4** at 100 °C, potentially causing unexpected reactivity. At 60 °C, evidence for both C–C and C–H cleavage was observed, suggesting further unexpected reactivity. Comparison of **BP4** vs. **BP5** anaerobic thermolysis revealed that the **BP1** complex produced no

aldehyde while BP2 could. It is possible this is due to a competition between the **LM2** methyl ether lone pair and the *N*-appended base on **BP1** inhibiting C–C bond cleavage.

### *4.2 Future Work*

In order to fully understand the role that substituents on triphenoxyamine ligands play, further efforts must be put into designing and testing new ligands; specifically, identifying the effect that steric bulk around the metal center has vs. the effect that reduced electron density has in C–C bond cleavage of cellulosic and hemicellulosic model compounds. Ligands with varying degrees of both should be studied further to understand how substrate selectivity and reaction rate are affected. Additionally, further efforts must be put towards understanding the mechanism at play with **TP** complexes, as all current mechanisms point to a rate determining step that contains a proton transfer, which does not corroborate with experimental results indicating no KIE. Finally, using this information, conversion and selectivity must be improved significantly if these complexes are to see use industrially.

To optimize the use of **BP** complexes, a much greater understanding of the factors which influence oxidative bond cleavage selectivity (C–H vs. C–C vs. C–O) must be elucidated. Much like **TP** complexes, this means that the degree to which steric bulk around the metal center and electron density at the metal center affect catalyst activity must be determined with far greater certainty; additionally, the effect of the pendant groups on the ligand must be fully understood; while they seem to have an effect on reactivity, the exact mechanism is still unknown. Temperature also seems to play a greater role on selectivity than previously thought, as evidenced by the disparate reactivity observed with **BP4** thermolysis. Further studies of the effect of temperature must be undertaken to understand the stability of the catalyst in relation to the reactivity. DFT calculations and more in-depth mechanistic studies similar to what was done for **TA** and **TP** complexes in Chapter 2 could aid in understanding this process.

Overall, these catalyst complexes show promise for mild aerobic cleavage of lignocellulosic biomass. However, further expansion of substrate scope to include more complex models with a variety of bonds must be attempted. For **TP** complexes, this includes monosaccharides such as glucose, and polysaccharides such as lactose and cellulose. More

complex substrates which include 5–5, β– β, β–O–4, β–5, β–1, α–O–4, and 4–O–5 bonds should be explored with **BP3** and any future analogues. This could enable access to selective lignin depolymerization, if successful.

# Appendix: Supplemental Information

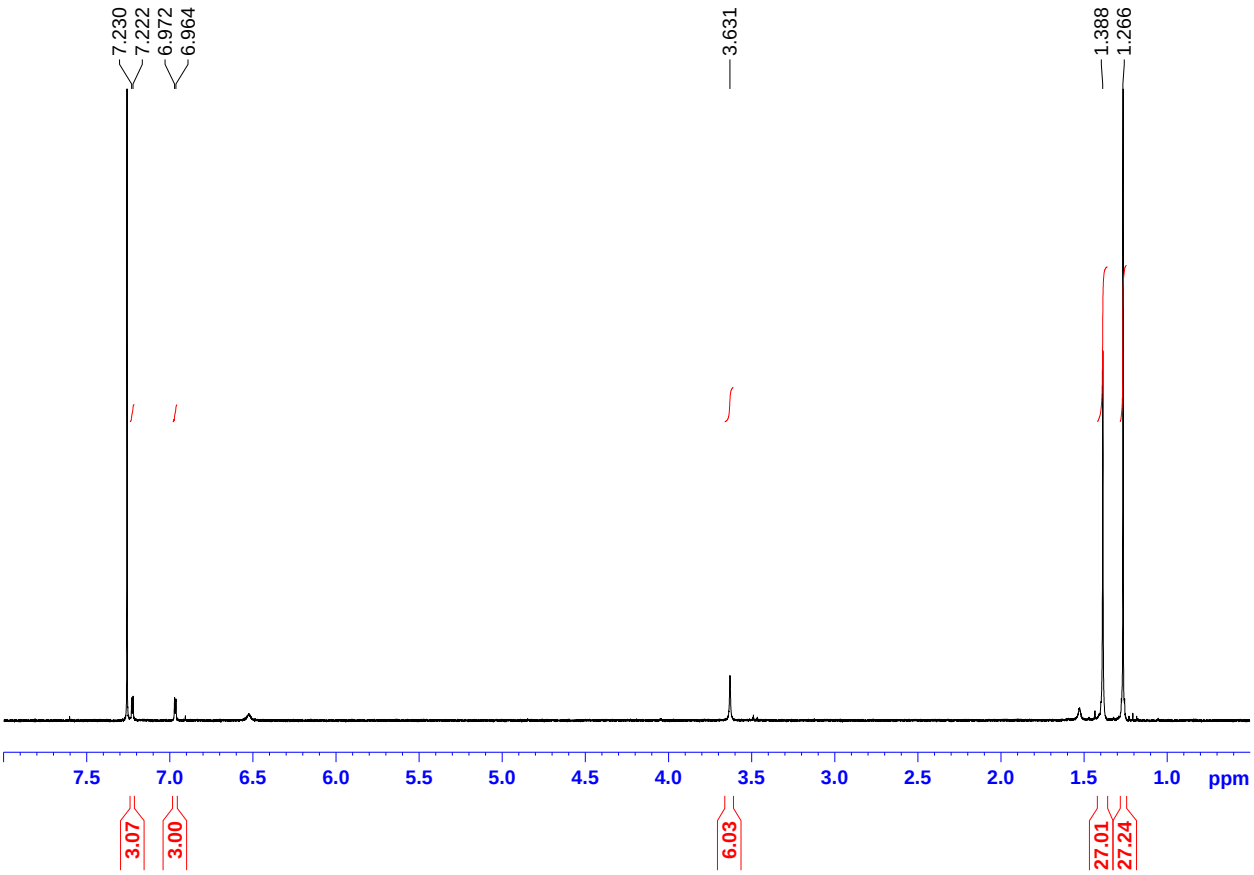


**Figure A. $^{1}$H NMR spectrum of TL1 ligand in $CDCl_3$, 300 MHz.**

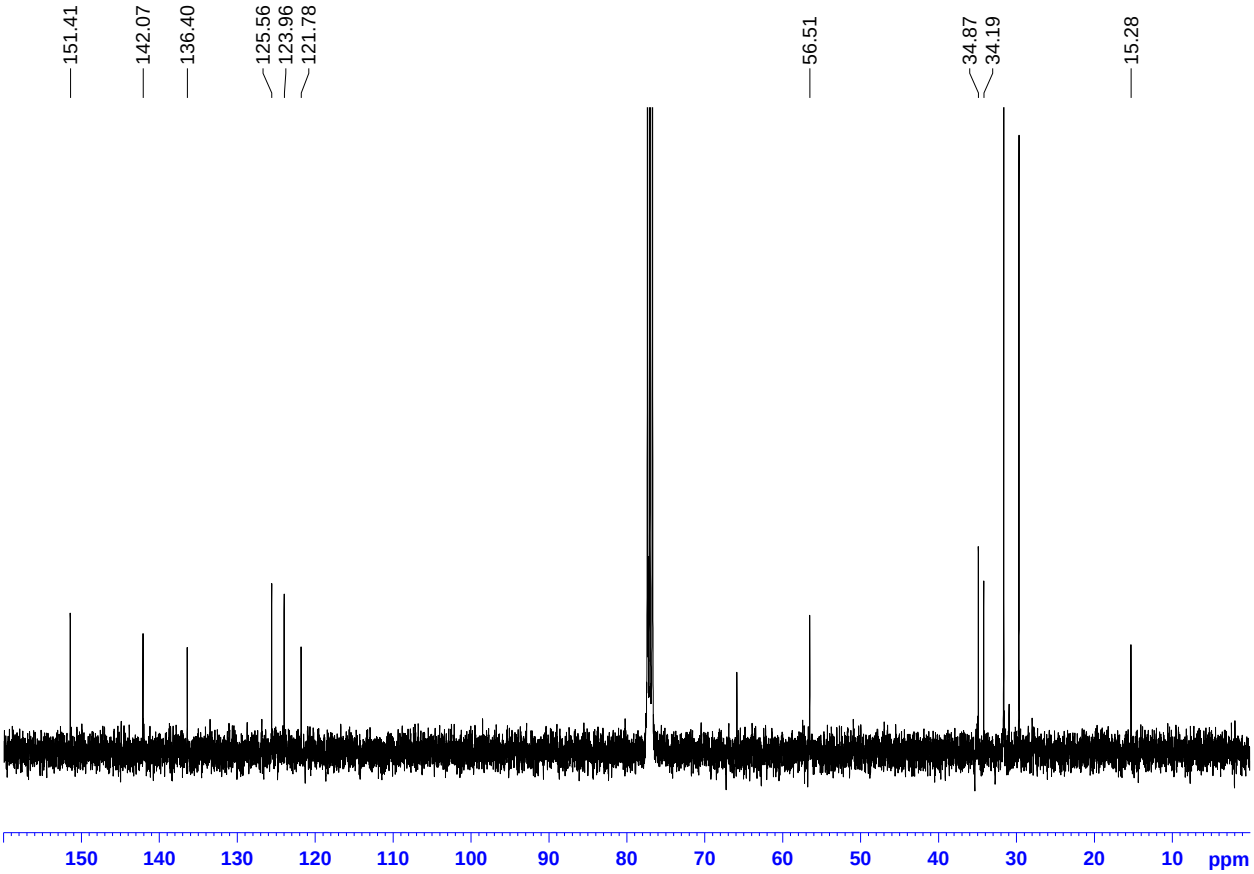


**Figure B. $^{13}C\{^{1}H\}$ NMR spectrum of TL1 ligand in $CDCl_3$, 100 MHz.**

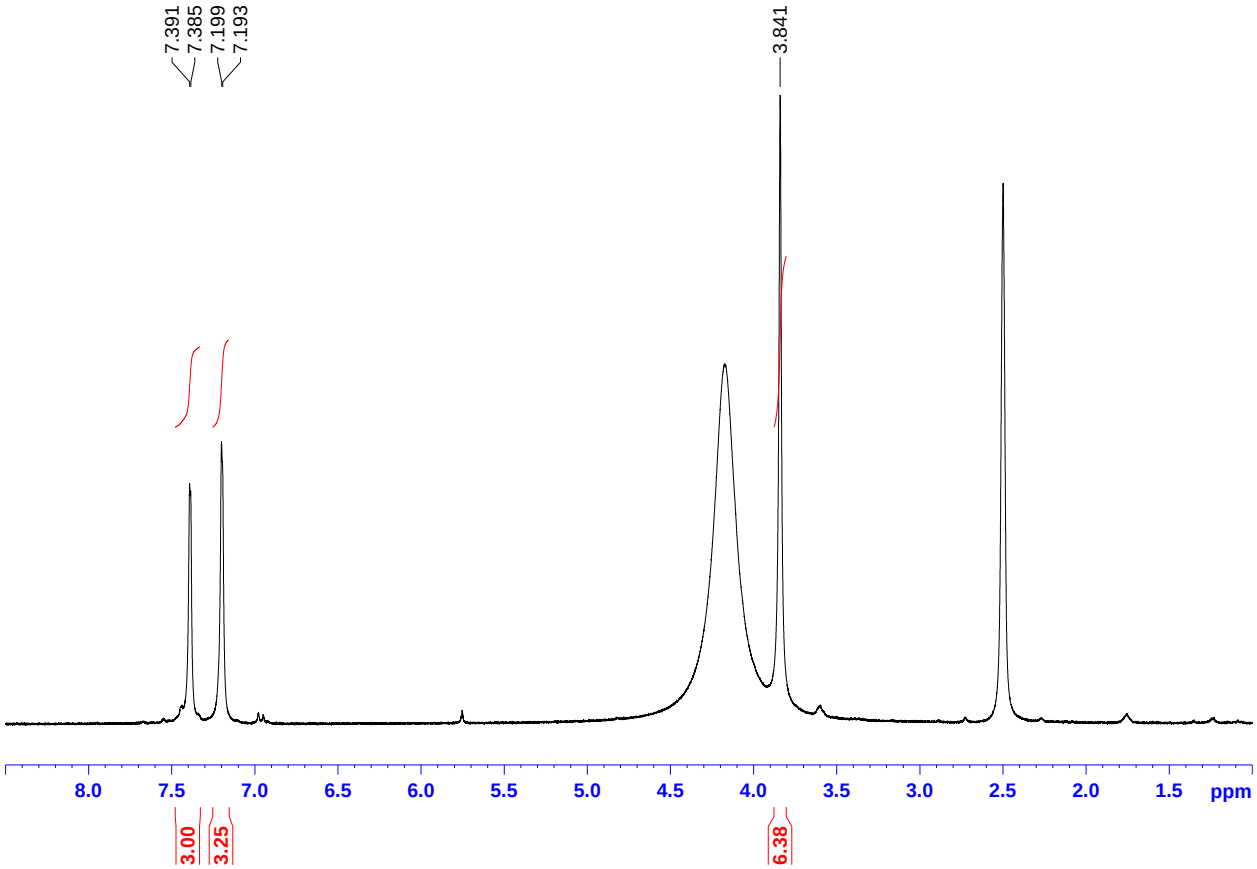


**Figure C. $^{1}$H NMR spectrum of TL2 ligand in DMSO-$d_6$, 300 MHz.**

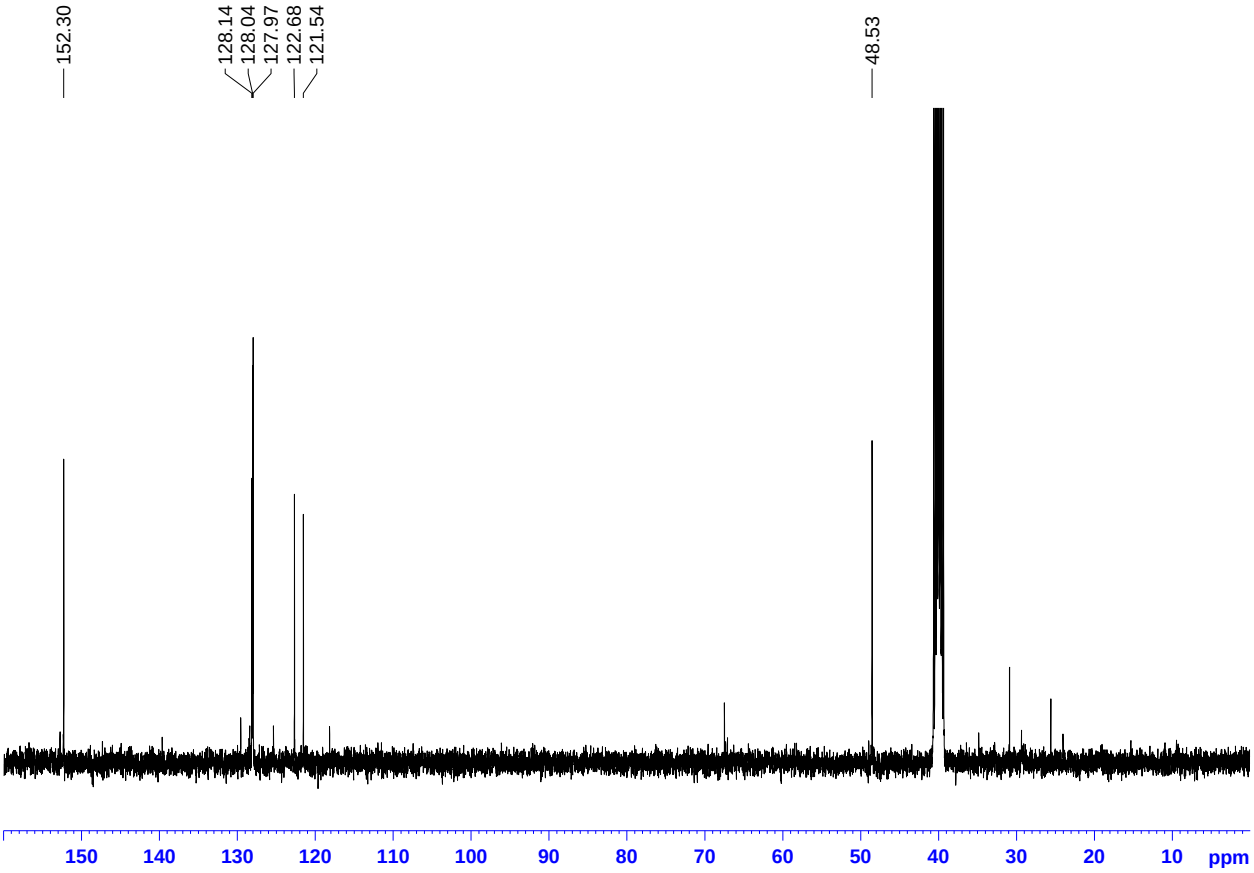


**Figure D. $^{13}C\{^{1}H\}$ NMR spectrum of TL2 ligand in DMSO-$d_6$, 100 MHz.**

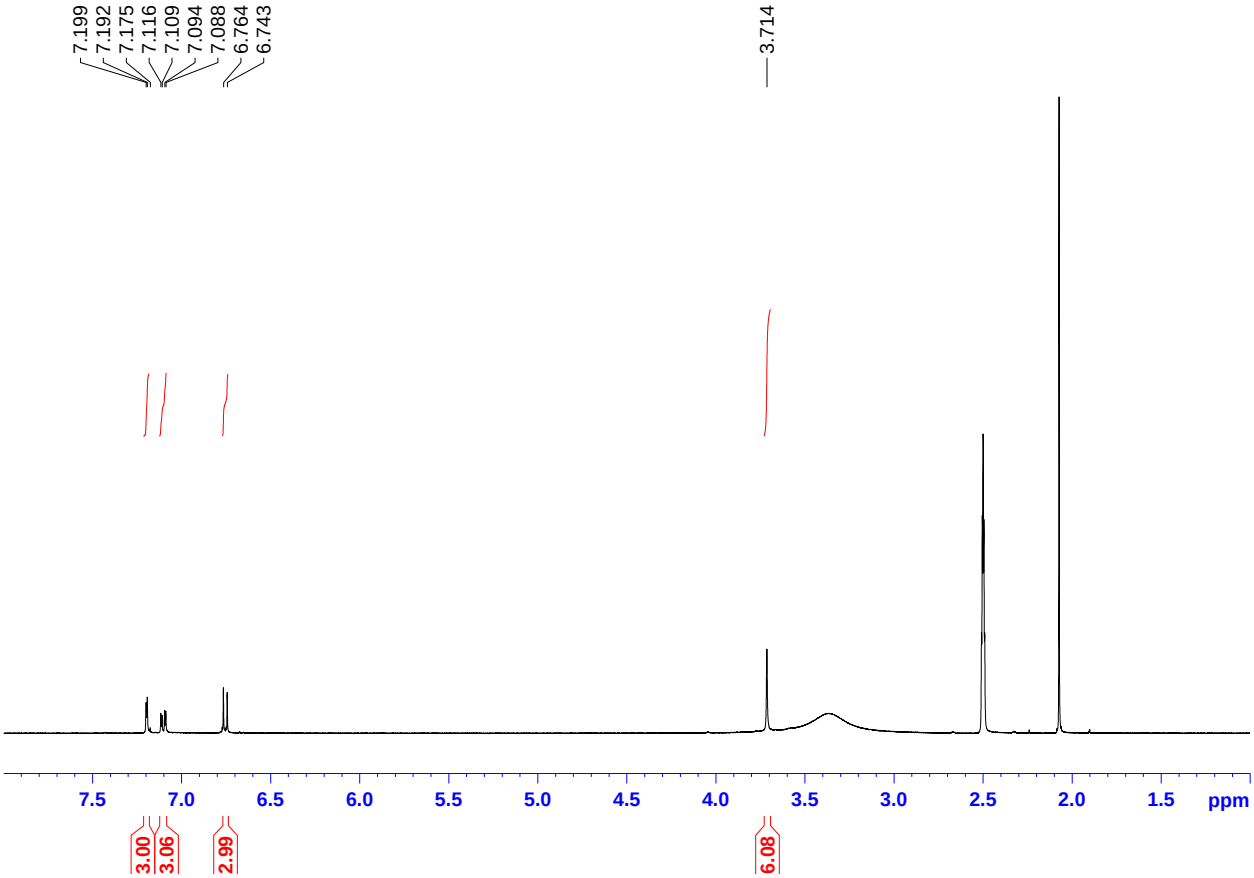


**Figure E. $^{1}$H NMR spectrum of TL3 ligand in DMSO-$d_6$, 400 MHz.**

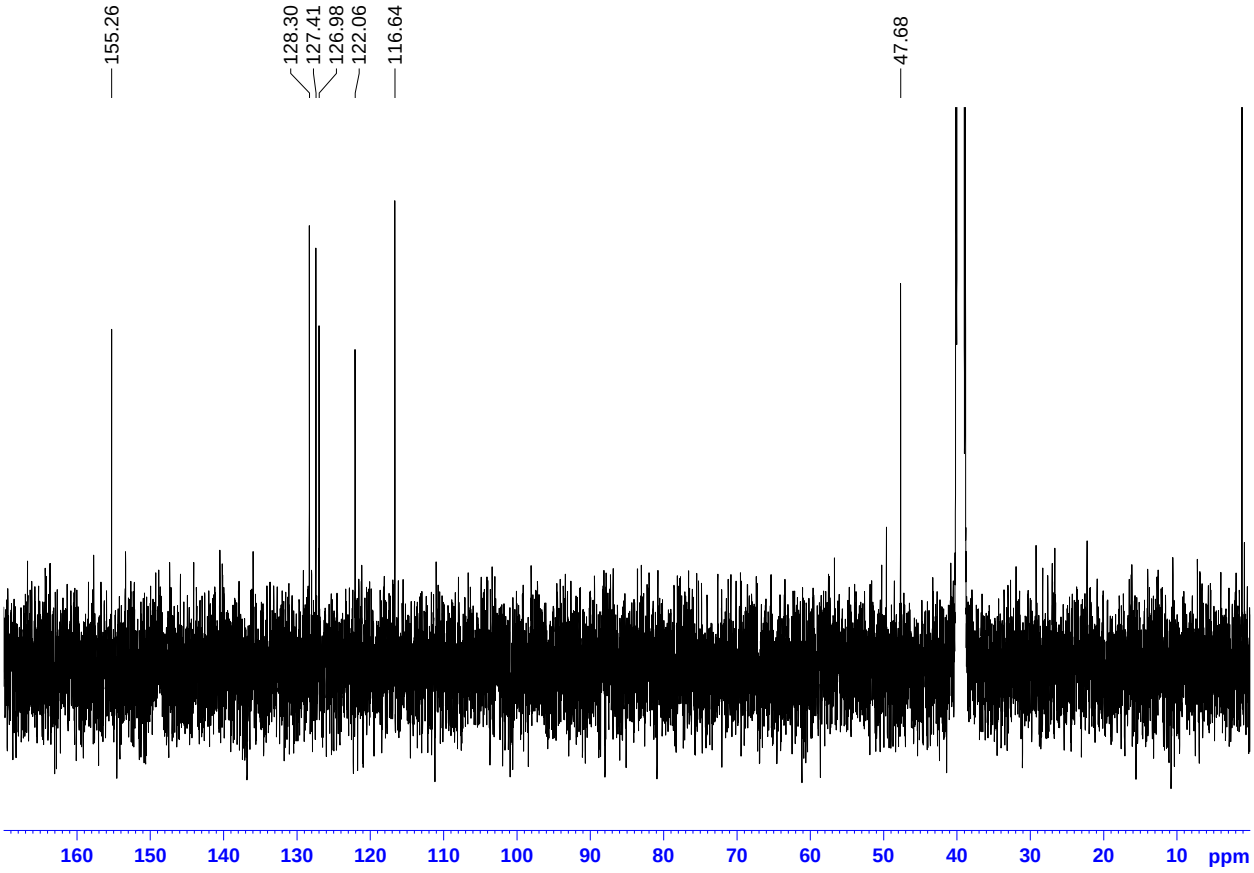


**Figure F. $^{13}C\{^{1}H\}$ NMR spectrum of TL3 ligand in DMSO-$d_6$, 100 MHz.**

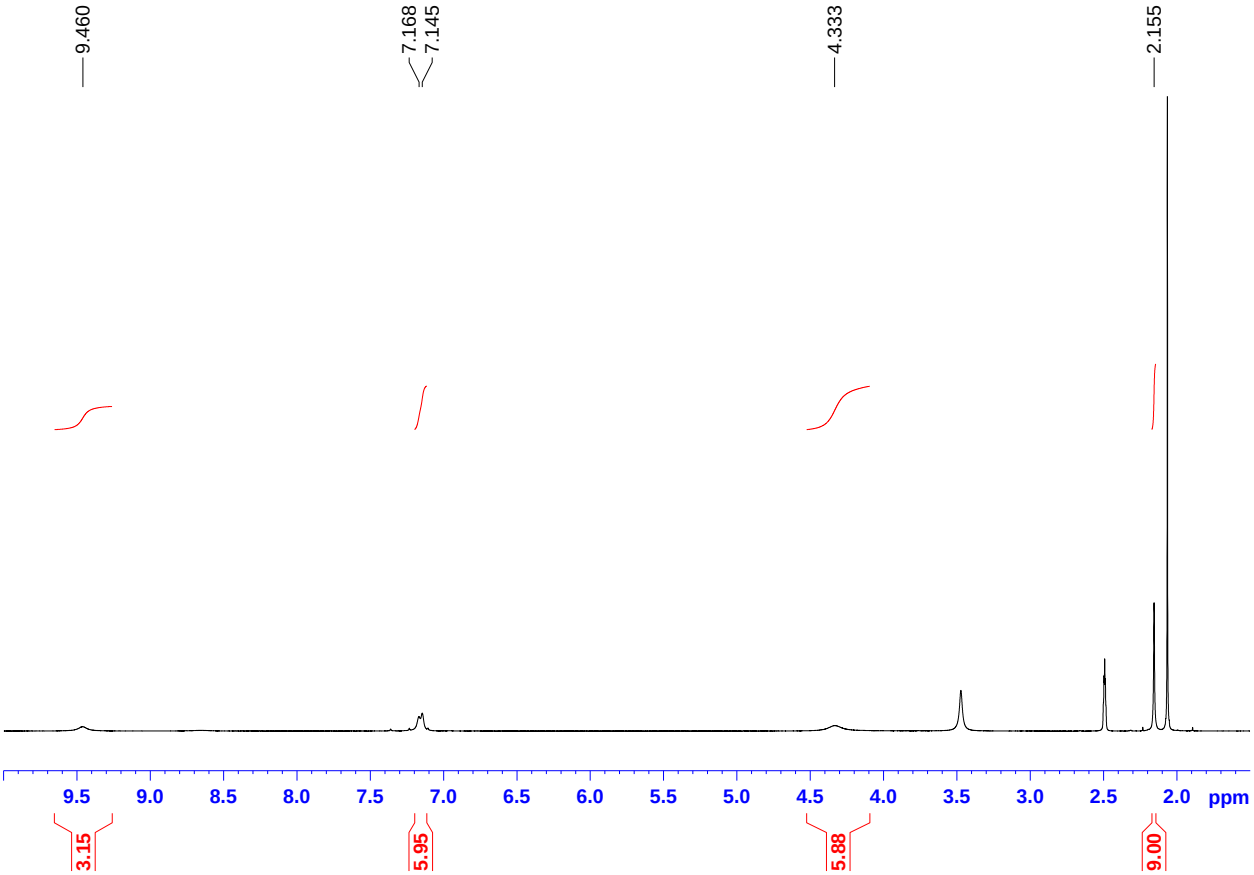


**Figure G. $^{1}$H NMR spectrum of TL4 ligand in DMSO-$d_6$, 400 MHz.**

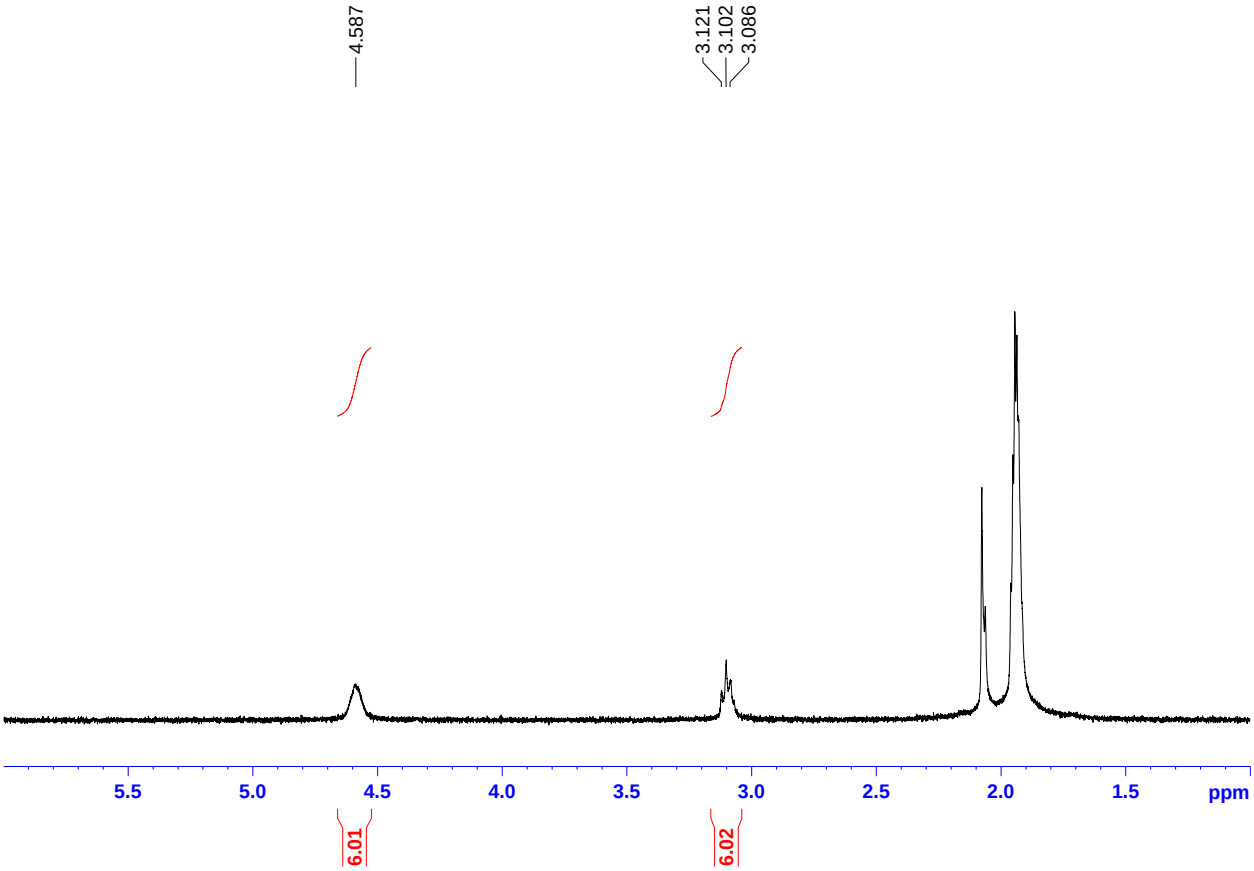


**Figure H. $^{1}$H NMR spectrum of TA complex in $CD_3CN$, 300 MHz.**

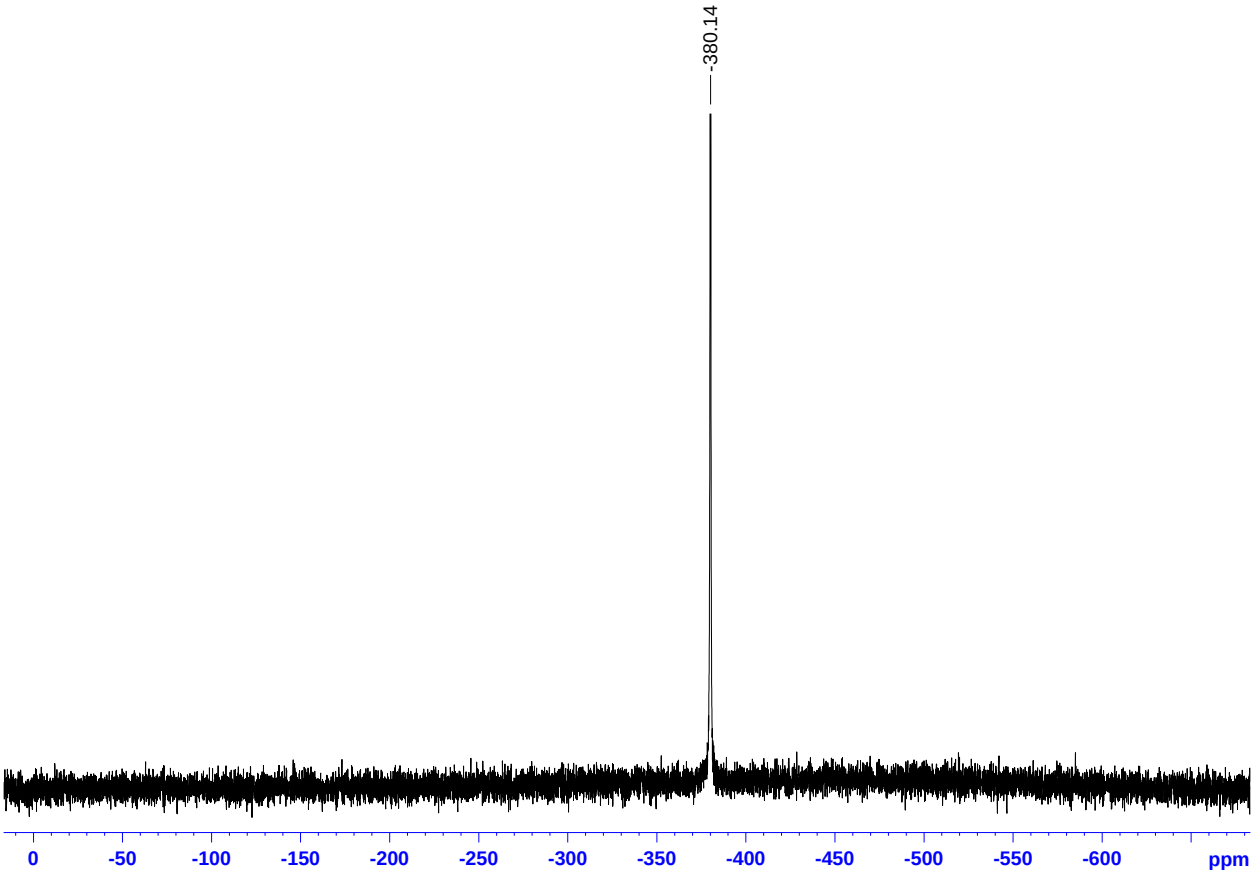


**Figure I. $^{13}$V NMR spectrum of TA complex in $CD_3CN$, 79 MHz.**

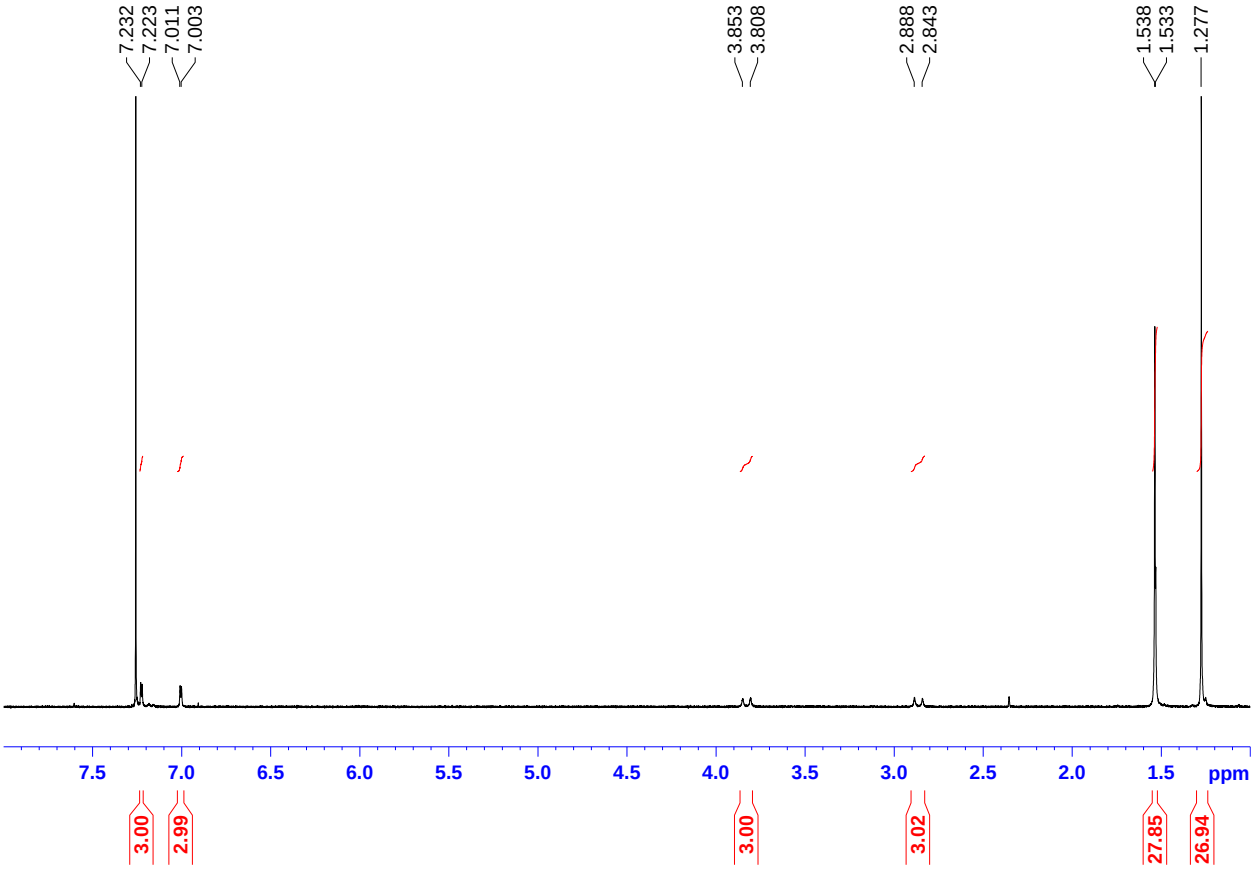


**Figure J. $^{1}$H NMR spectrum of TP1 complex in $CDCl_3$, 300 MHz.**

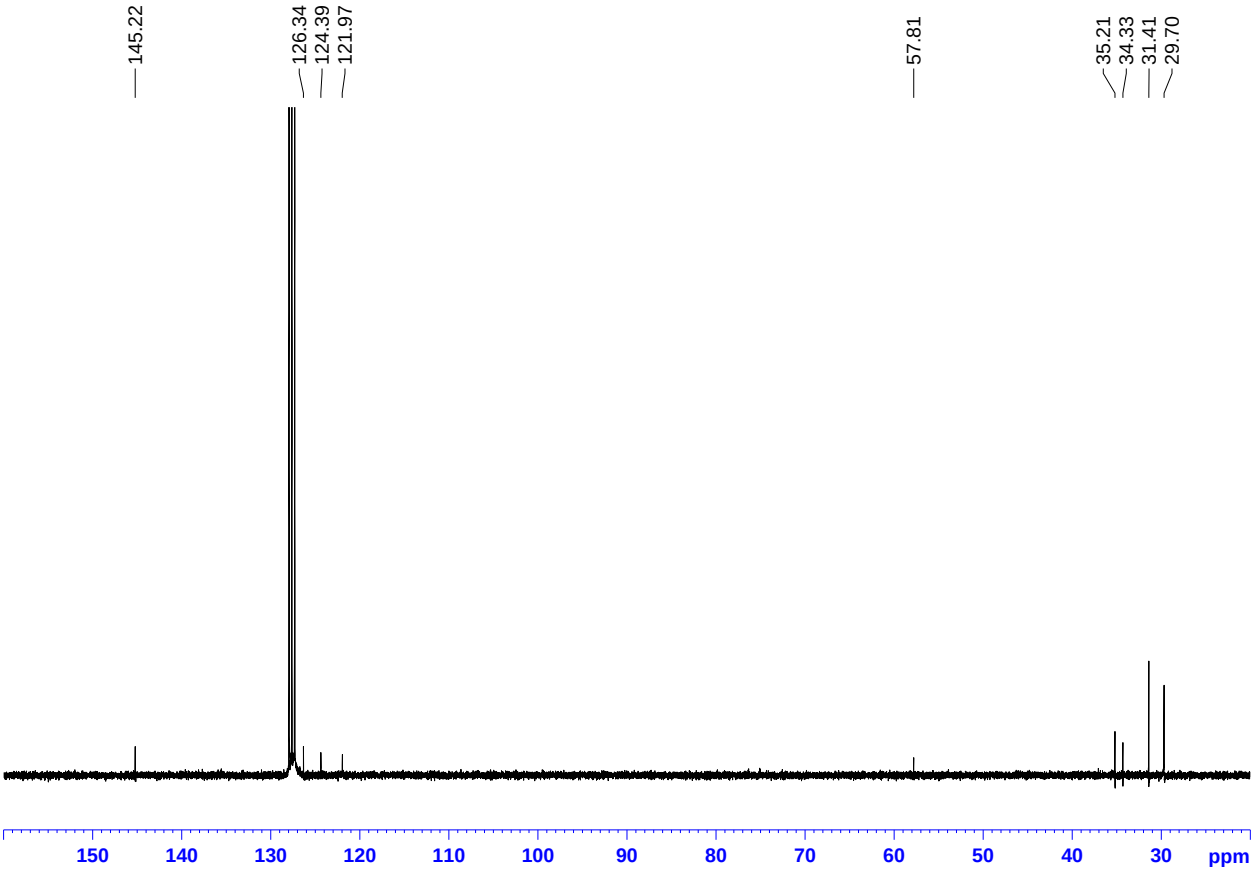


**Figure K. $^{13}C\{^{1}H\}$ NMR spectrum of TP1 complex in $C_6D_6$, 75 MHz.**

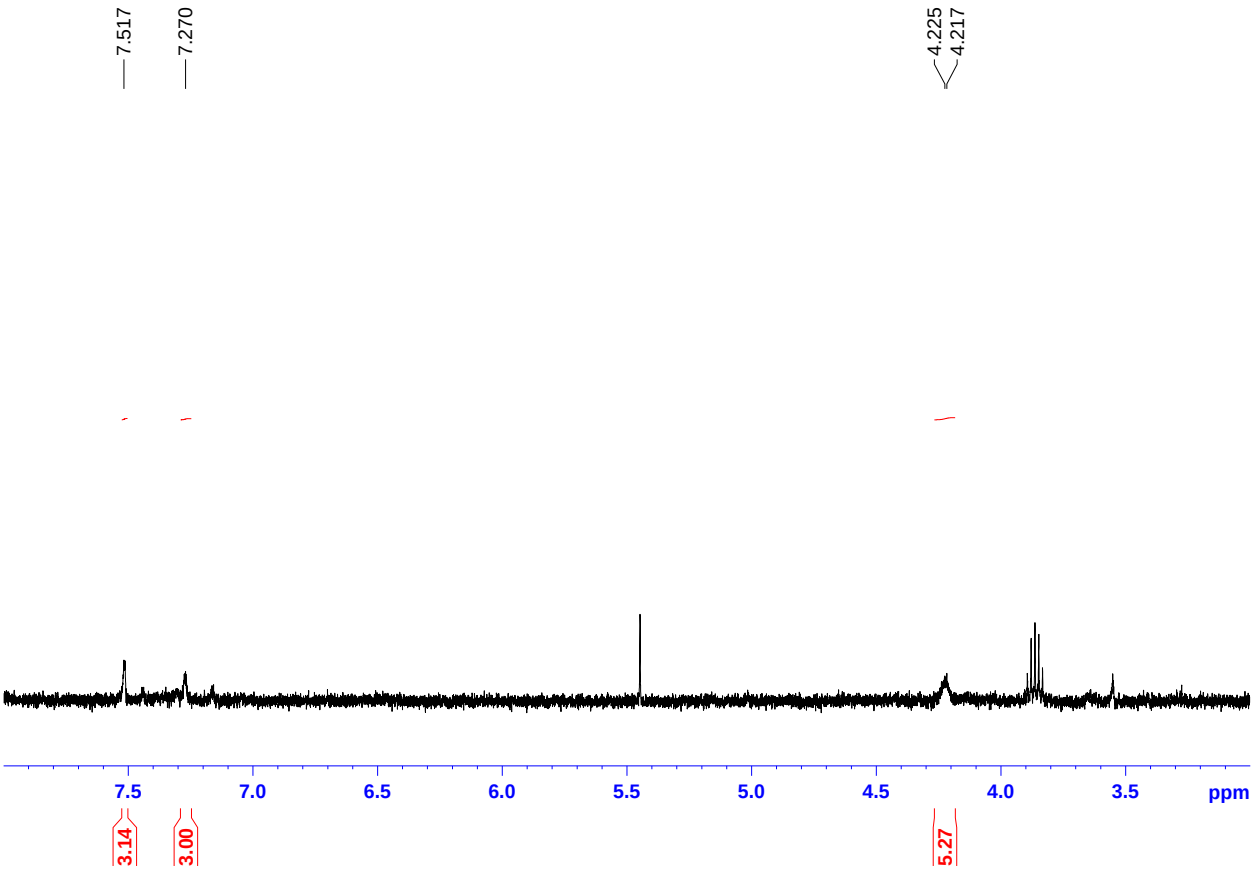


**Figure L. $^{1}$H NMR spectrum of TP2 complex in $CD_3CN$, 400 MHz.**

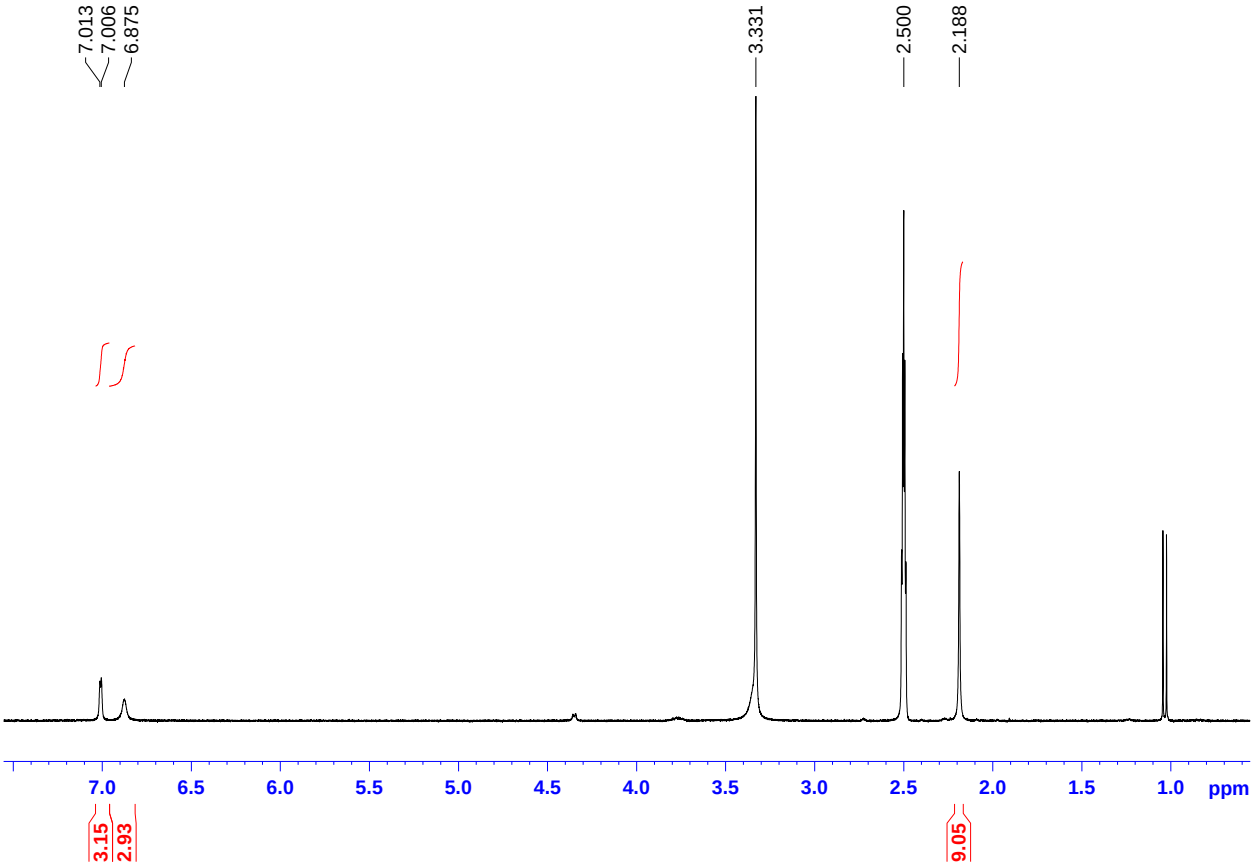


**Figure M. $^{1}$H NMR spectrum of TP4 complex in DMSO-$d_6$, 300 MHz.**

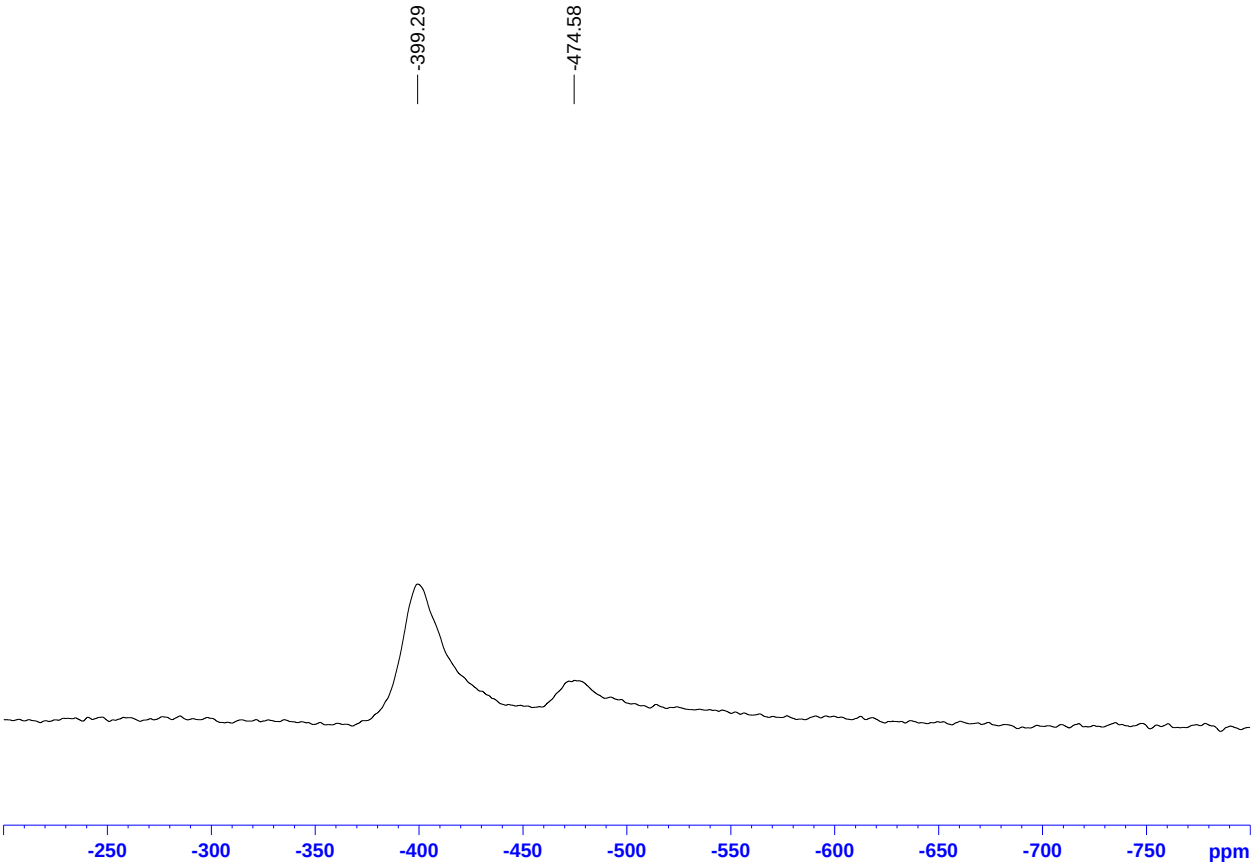


**Figure N. $^{51}$V NMR spectrum of TP4 complex in DMSO-$d_6$, 79 MHz.**

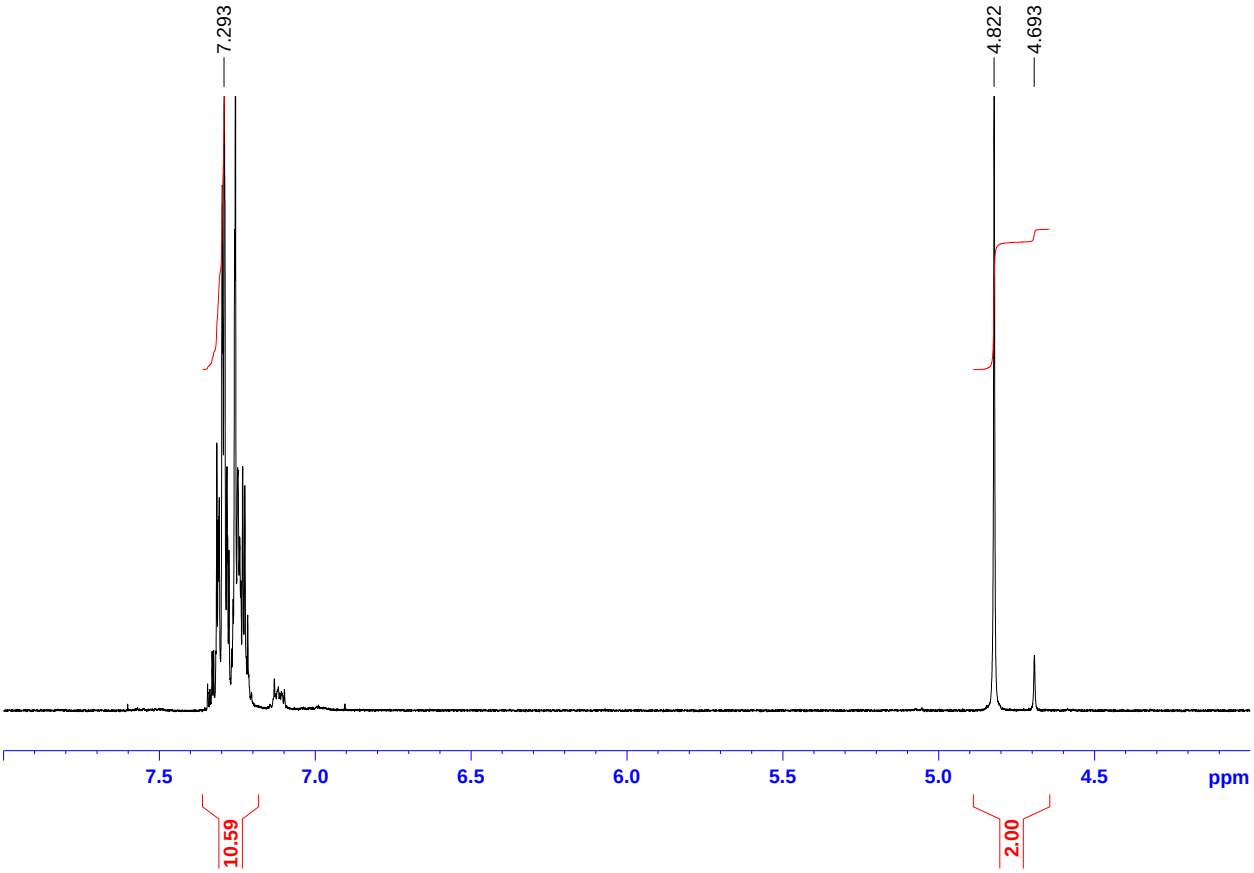


**Figure O. $^{1}$H NMR spectrum of Hydrobenzoin-($OD_2$) in $CDCl_3$, 300 MHz.**

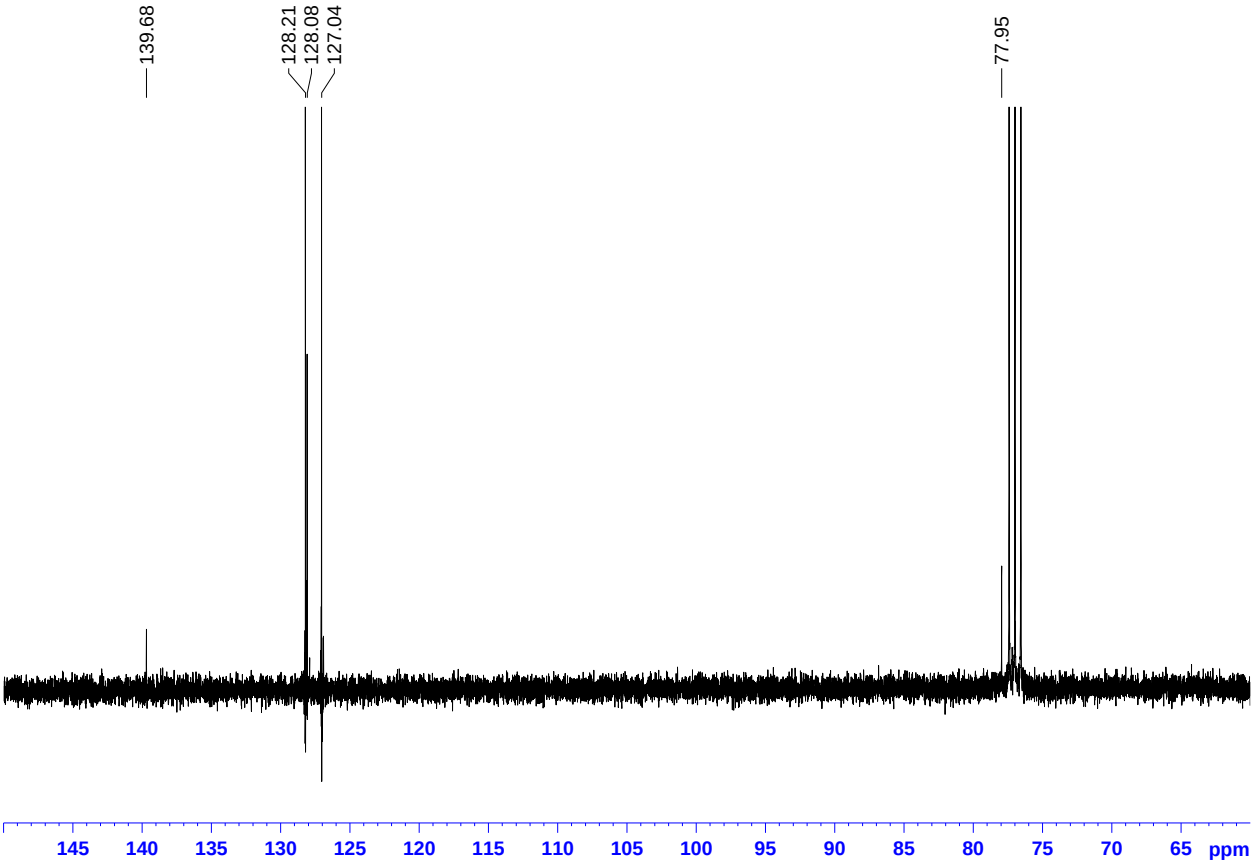


**Figure P. $^{13}C\{^{1}H\}$ NMR spectrum of Hydrobenzoin-($OD_2$) in $CDCl_3$, 75 MHz.**

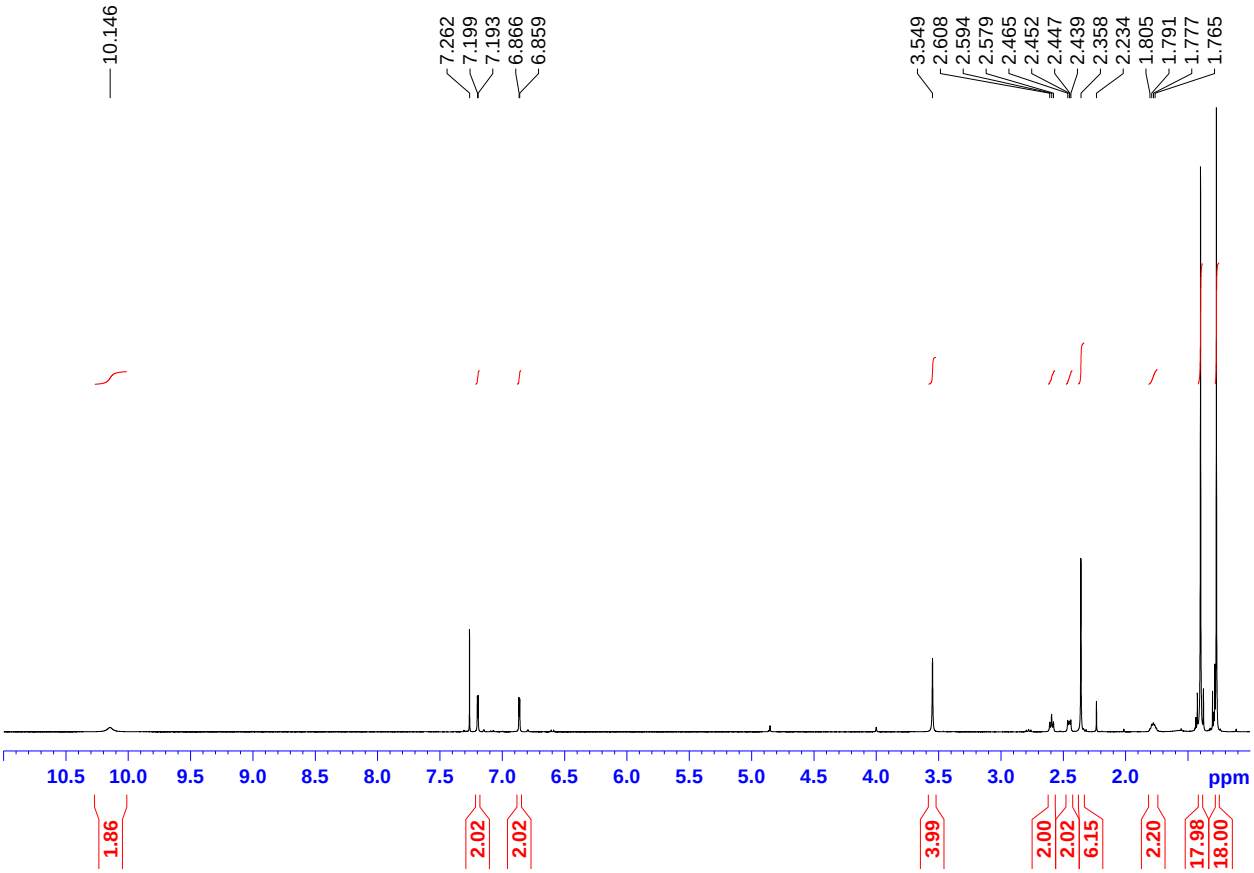


**Figure Q. $^{1}H$ NMR spectrum of BL1 ligand in $CDCl_3$, 300 MHz.**

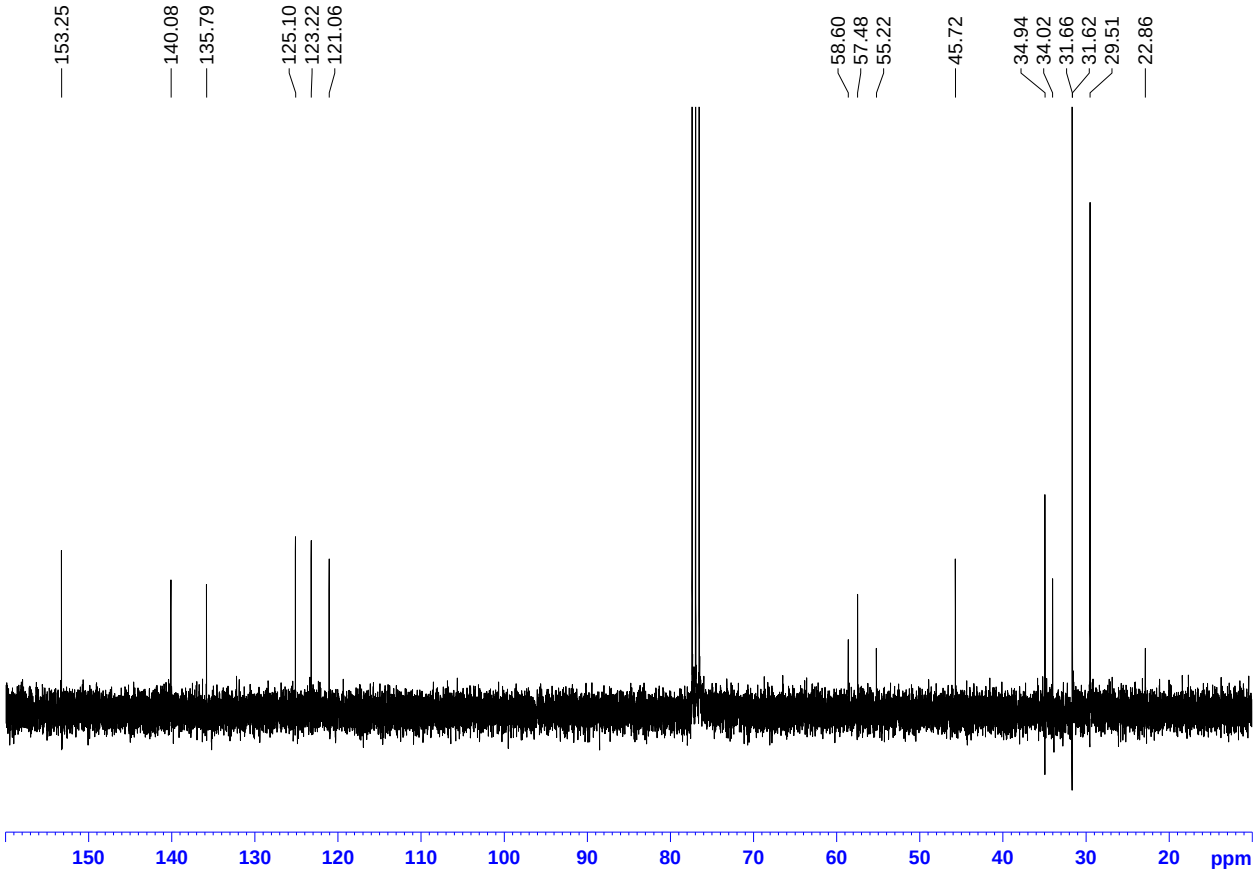


**Figure R. $^{13}C\{^{1}H\}$ NMR spectrum of BL1 ligand in $CDCl_3$, 75 MHz.**

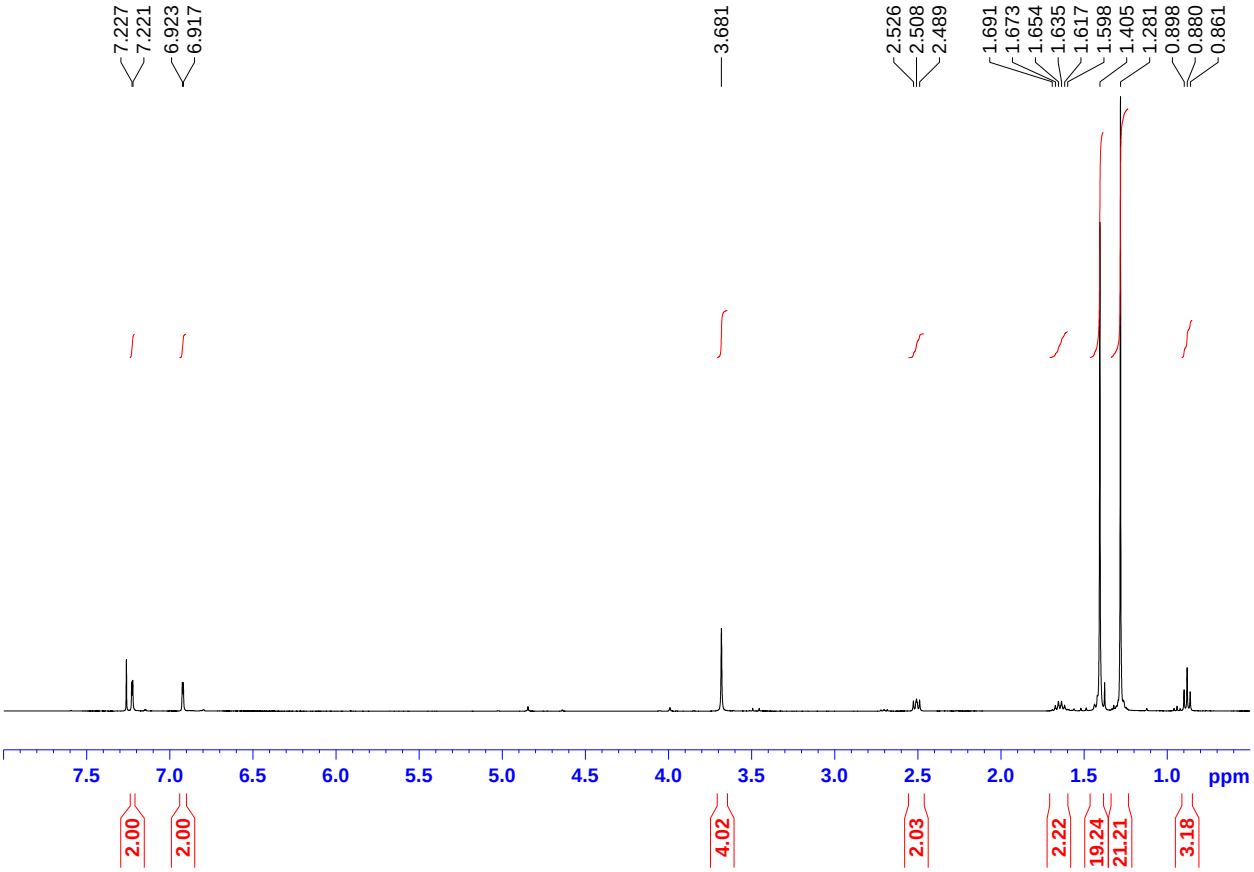


**Figure S. $^{1}H$ NMR spectrum of BL2 ligand in $CDCl_3$, 400 MHz.**

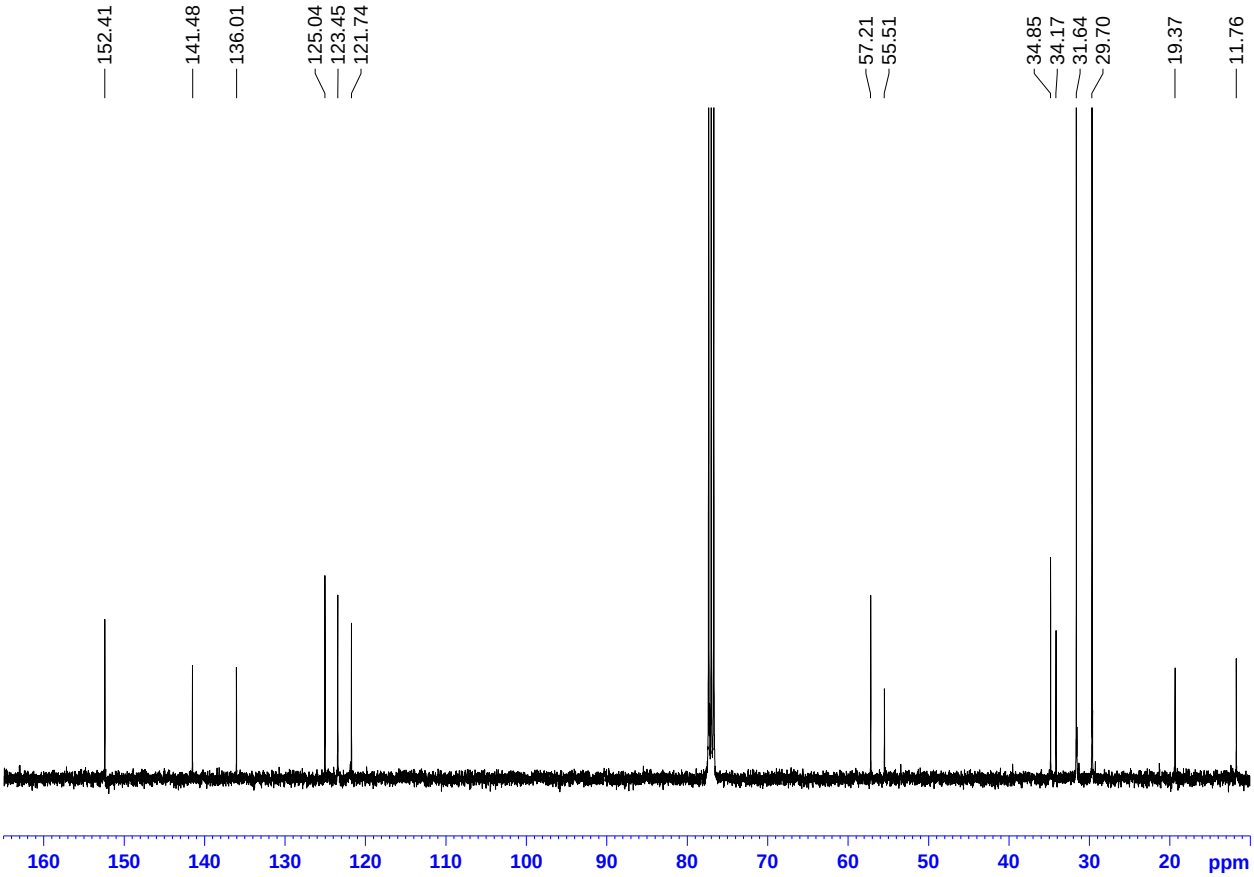


**Figure T. $^{13}C\{^{1}H\}$ NMR spectrum of BL2 ligand in $CDCl_3$, 100 MHz.**

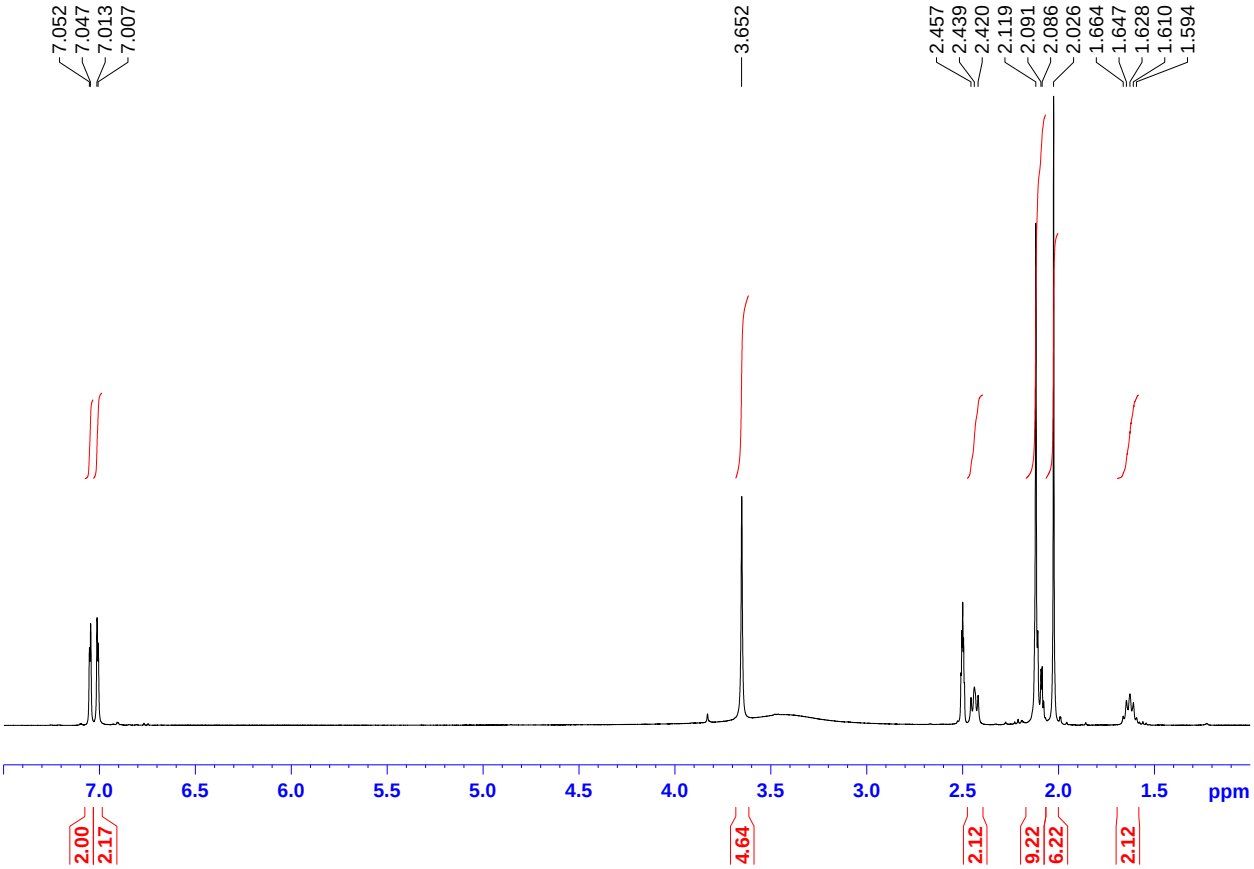


**Figure U. $^{1}$H NMR spectrum of BL3 ligand in DMSO-$d_6$, 400 MHz.**

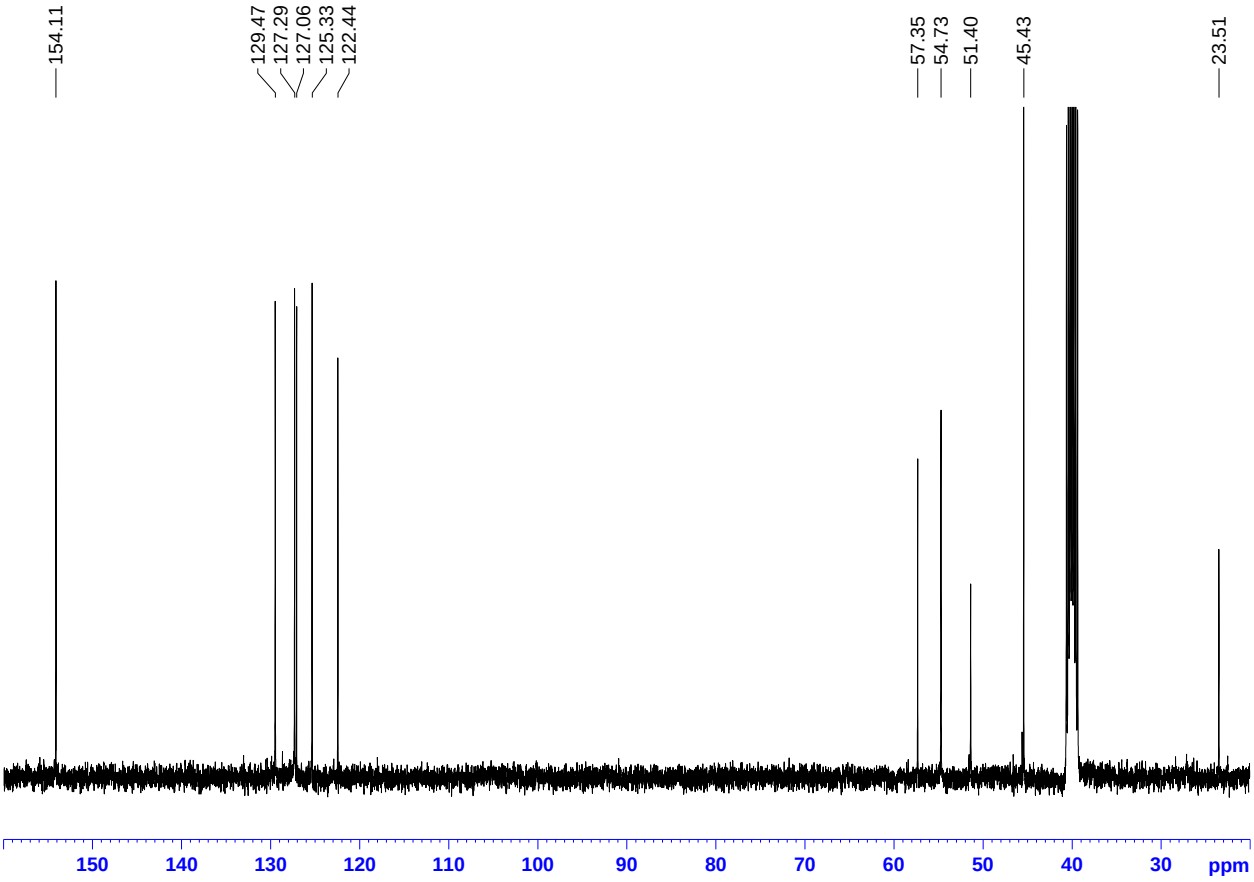


**Figure V. $^{13}C\{^{1}H\}$ NMR spectrum of BL3 ligand in DMSO-$d_6$, 100 MHz.**

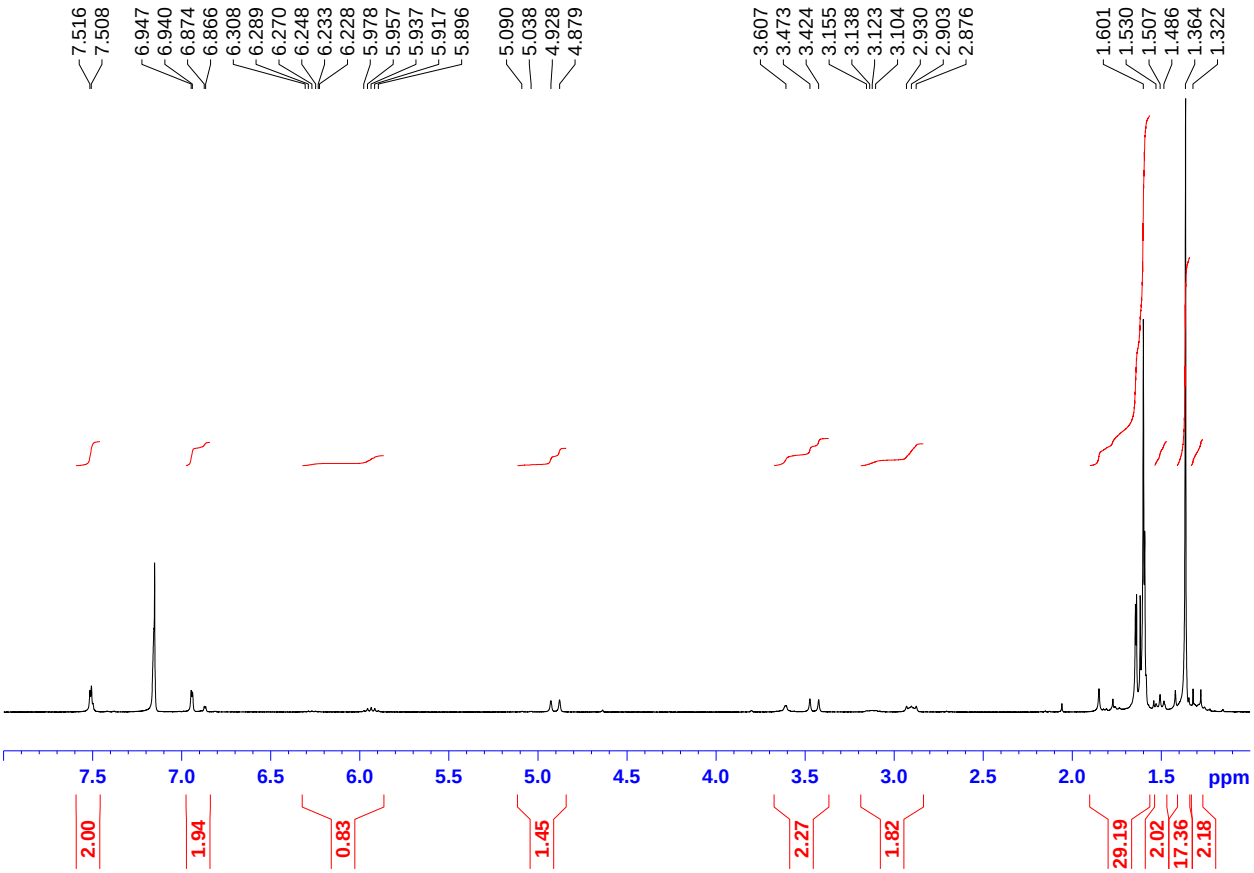


**Figure W. $^{1}H$ NMR spectrum of BP1 complex in $C_6D_6$, 300 MHz.**

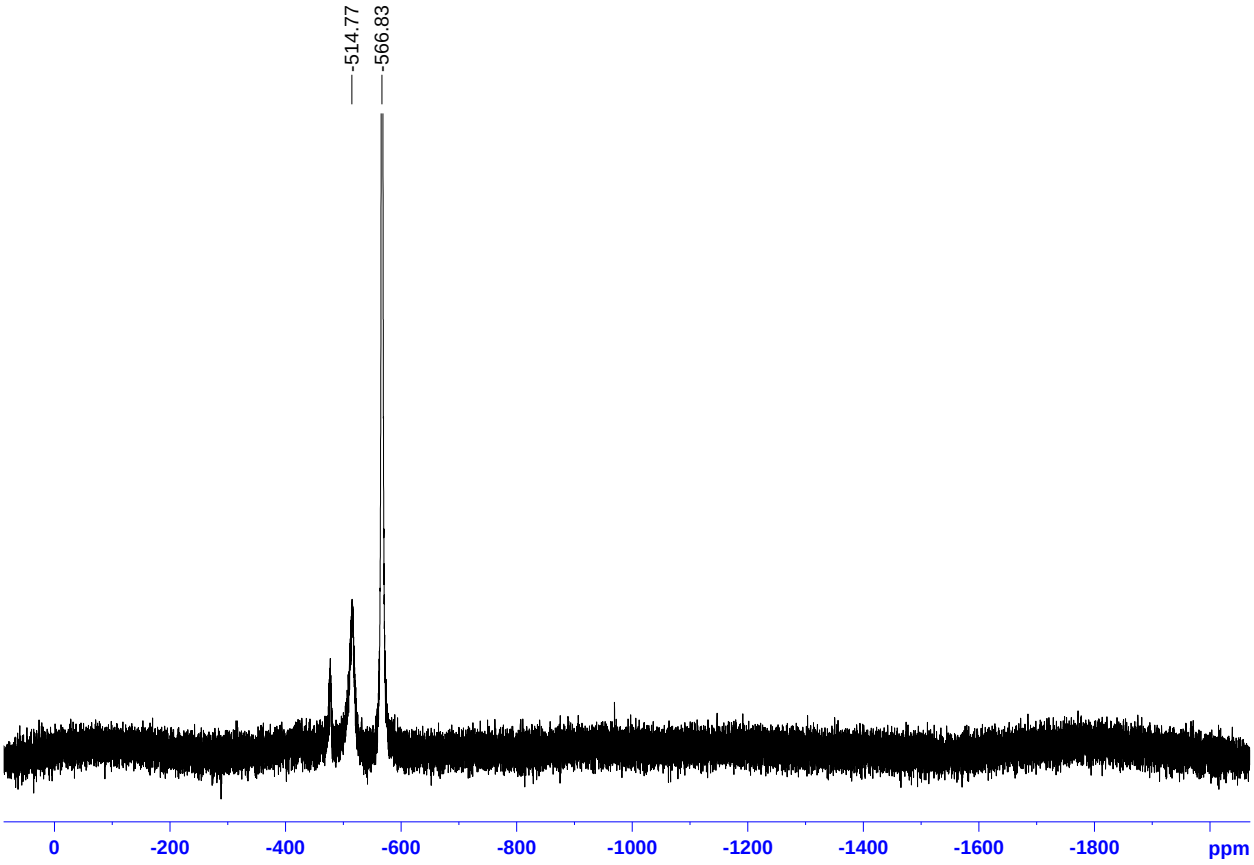


**Figure X. $^{51}V$ NMR spectrum of BP1 complex in $C_6D_6$, 79 MHz.**

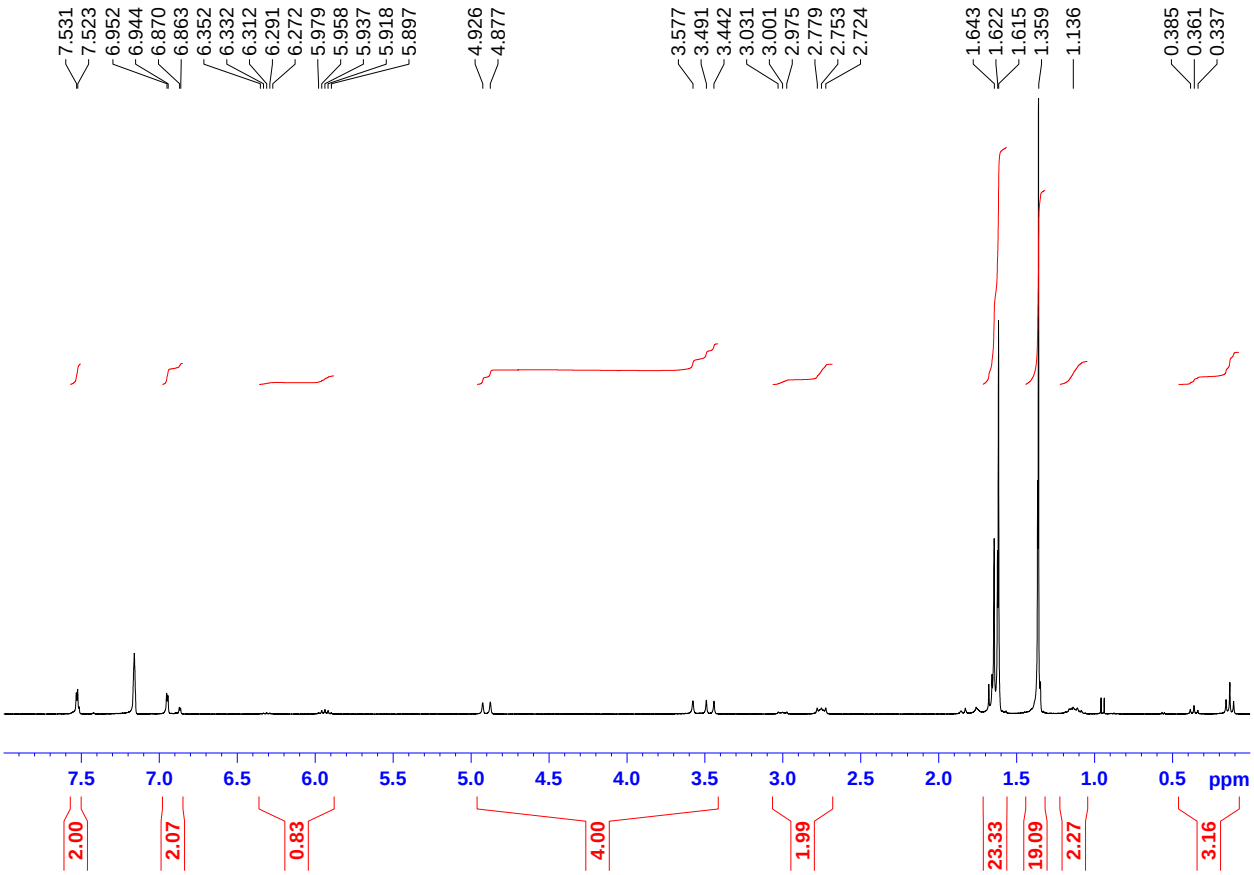


**Figure Y. $^{1}H$ NMR spectrum of BP2 complex in $C_6D_6$, 300 MHz.**

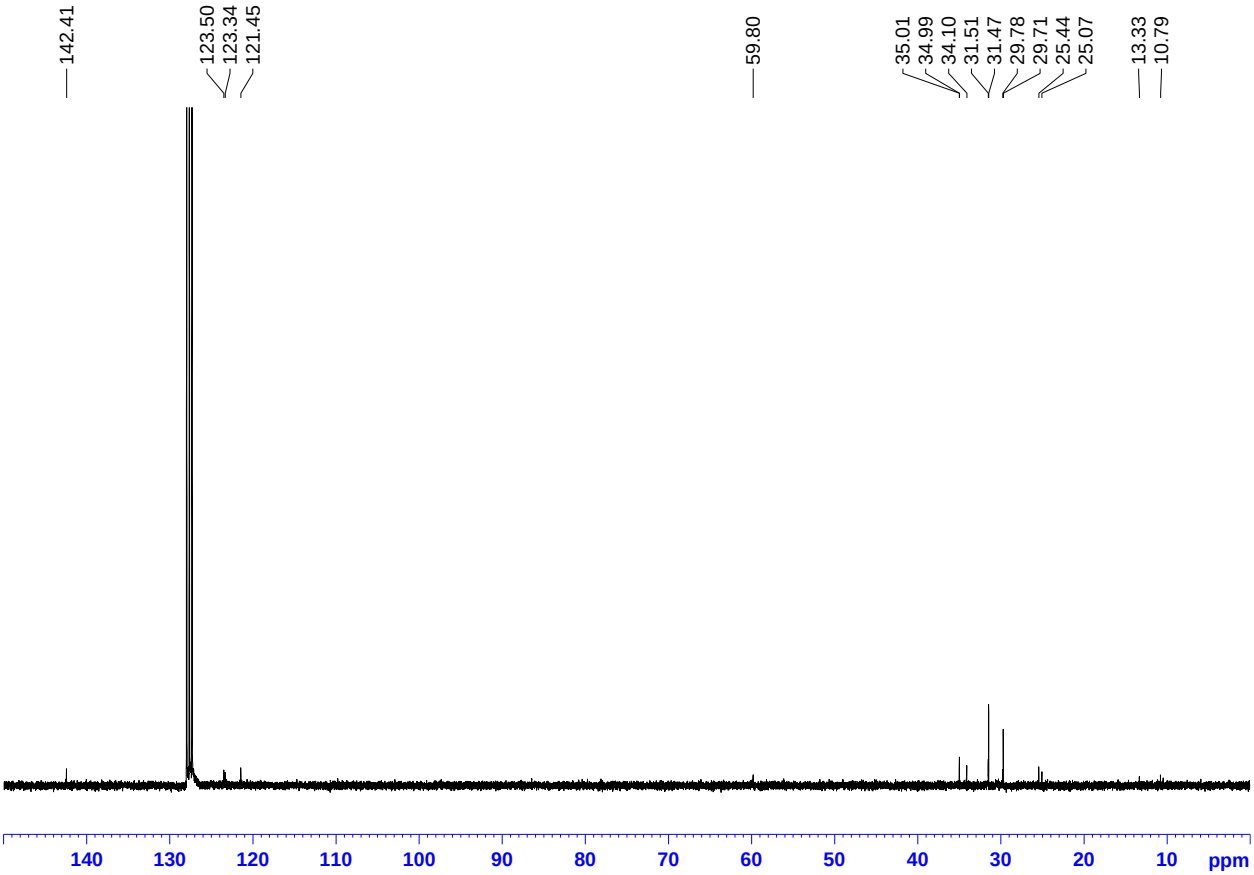


**Figure Z. $^{13}C\{^{1}H\}$ NMR spectrum of BP2 complex in $C_6D_6$, 75 MHz.**

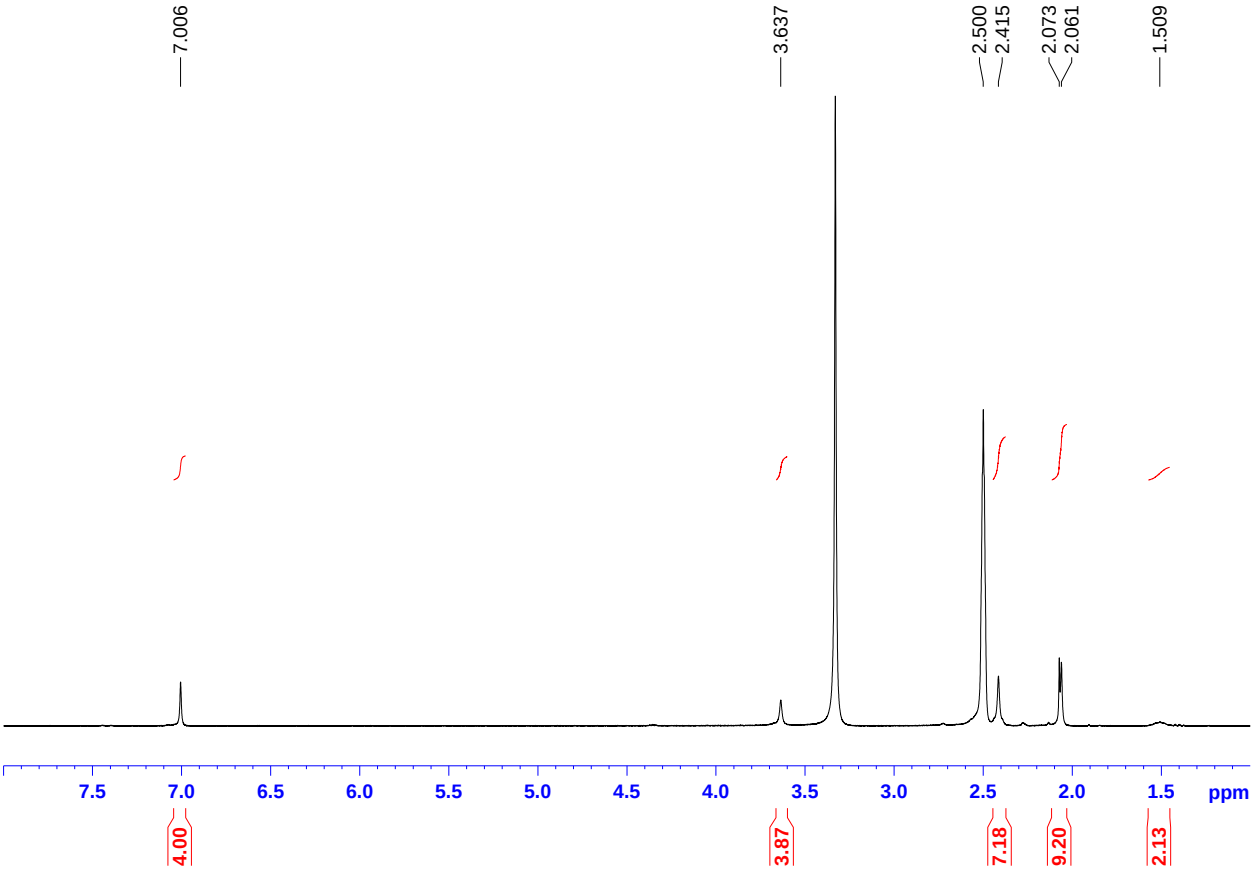


**Figure AA. $^{1}$H NMR spectrum of BP3 complex in DMSO-$d_6$, 300 MHz.**

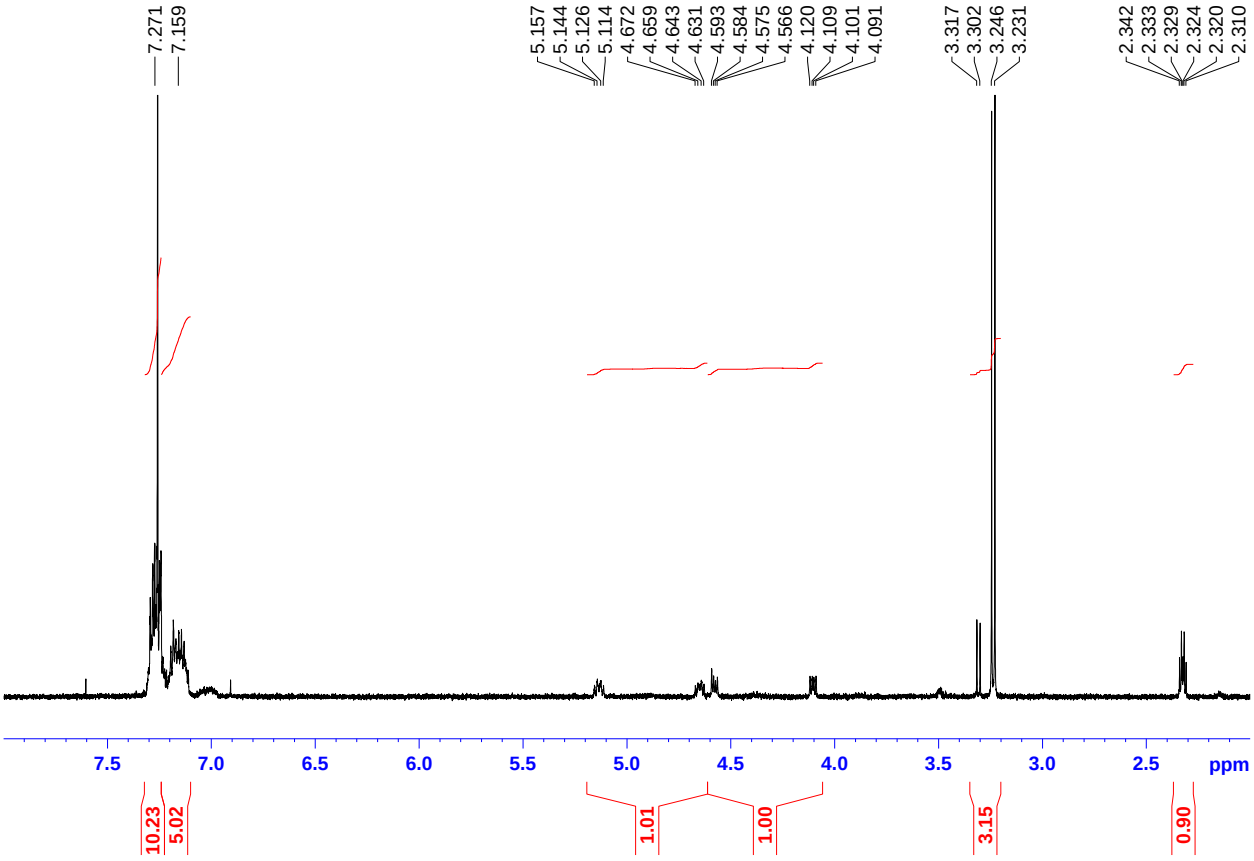


**Figure AB. $^{1}H$ NMR spectrum of 1,2-$^{13}C$-LM2 in $CDCl_3$, 300 MHz.**

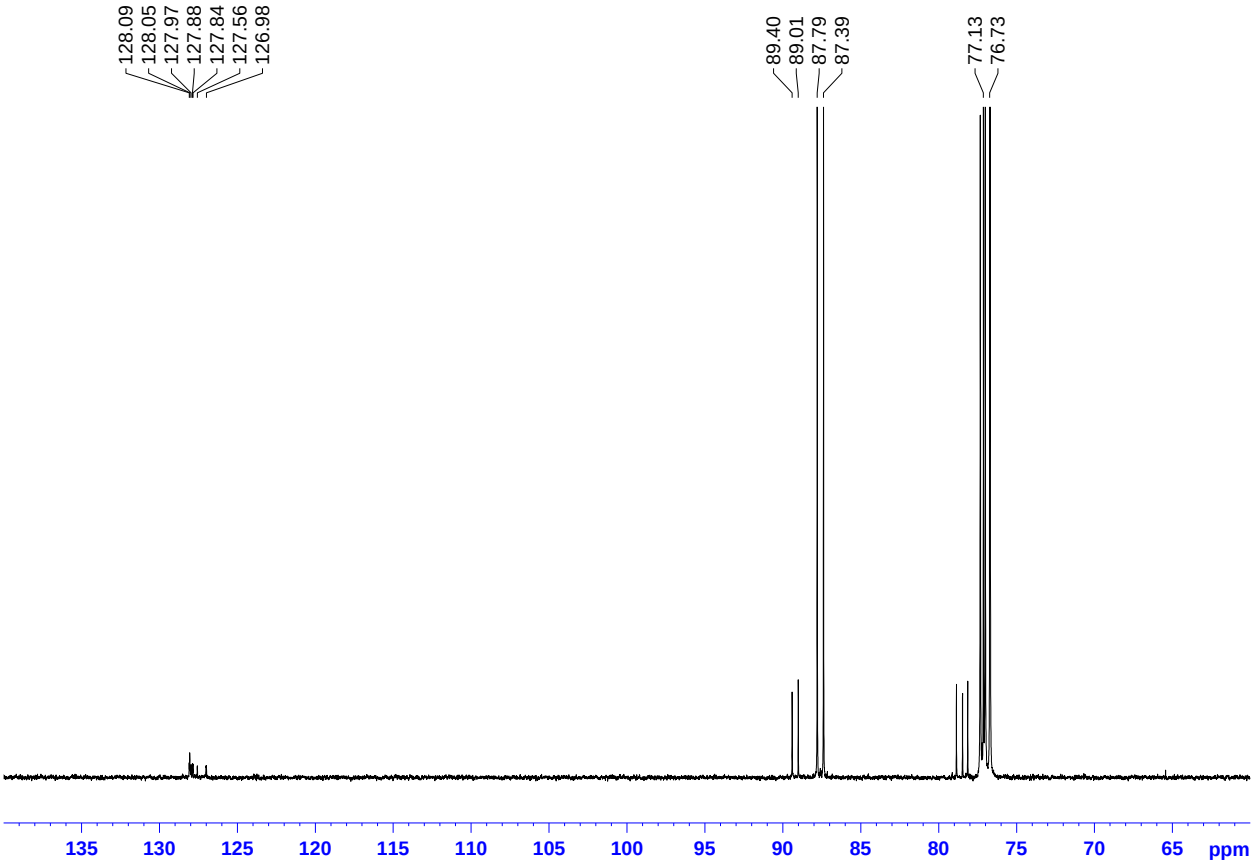


**Figure AC. $^{13}C\{^{1}H\}$ NMR spectrum of 1,2-$^{13}C$-LM2 in $CDCl_3$, 100 MHz.**